



**TRIBHUVAN UNIVERSITY
INSTITUTE OF ENGINEERING
PULCHOWK CAMPUS**

Thesis No-

Climate Change Impact on Streamflow in the Chilime River Basin under CMIP6

by

Kabita Bhattarai

A THESIS

**SUBMITTED TO THE DEPARTMENT OF APPLIED SCIENCES AND CHEMICAL
ENGINEERING IN PARTIAL FULFILLMENT OF THE REQUIREMENTS FOR THE
DEGREE OF MASTER OF SCIENCE IN
CLIMATE CHANGE AND DEVELOPMENT**

DEPARTMENT OF APPLIED SCIENCE AND CHEMICAL ENGINEERING

LALITPUR, NEPAL

May, 2025

COPYRIGHT

The author has agreed that the library, Department of Applied Sciences and Chemical Engineering, Pulchowk Campus, Institute of Engineering may make this thesis freely available for inspection. Moreover, the author has agreed that permission for extensive copying of this thesis for scholarly purpose may be granted by the professors who supervised the work recorded herein or, in their absence, by the Head of the Department wherein the thesis was done. It is understood that the recognition will be given to the author of this thesis and to the Department of Applied Sciences and Chemical Engineering, Pulchowk Campus, Institute of Engineering in any use of material of this thesis. Copying and publication or the other use of this thesis for financial gain without approval of the Department of Civil Engineering, Pulchowk Campus, Institute of Engineering and author's written permission is prohibited. Request for permission to copy or make any other use of the material in this thesis in whole or in part should be addressed to:

Sahin

Head Department of Applied Sciences and Chemical Engineering

Institute of Engineering

Pulchowk, Lalitpur

Nepal



TRIBHUVAN UNIVERSITY
INSTITUTE OF ENGINEERING
CENTRAL CAMPUS, PULCHOWK

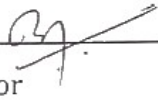
DEPARTMENT OF APPLIED SCIENCES AND CHEMICAL ENGINEERING

The undersigned certify that they have read, and recommended to the institute of engineering for Final defense of a thesis entitled “**Climate Change Impact on Streamflow in the Chilime River Basin under CMIP6**” submitted by Ms. Kabita Bhattarai in partial fulfillment of the requirement for the degree of Master of Science in Climate change and Development.



Supervisor

Prof. Dr. Bhola Nath Sharma Ghimire, Department
of Civil Engineering, IOE Pulchowk Campus



Supervisor

Dr. Babu Ram Tiwari, Department of
Applied Sciences and Chemical
Engineering, IOE Pulchowk Campus



Program Coordinator

Prof. Dr. Rinita Raj Bhandari

Department of Applied Sciences and Chemical
Engineering, IOE, Pulchowk Campus



External Examiner

Prof. Er. Devi Prasad Bhattarai

Department of Civil Engineering, IOE Pulchowk
Campus

DECLARATION

I hereby declare that this study titled “Climate Change Impact on Streamflow in the Chilime River Basin under CMIP6 “is based on my original research work. Related works on the topic by other researchers have been duly acknowledged. I owe all the liabilities relating to the accuracy and authenticity of the data and any other information included hereunder.

Name of student: Kabita Bhattarai

Roll number of the student: 079MSCCD007

MSc in Climate Change and Development

Date: April 2025

ACKNOWLEDGEMENT

First and foremost, I would like to express my heartfelt gratitude to my supervisor, Dr. Bhola Nath Sharma Ghimire, Department of Civil Engineering, and my co-supervisor, Dr. Babu Ram Tiwari, Department of Applied Sciences and Chemical Engineering, Pulchowk Campus, for their valuable guidance, constructive feedback, and continuous encouragement throughout the course of this research. Their academic mentorship has played a crucial role in shaping the quality and direction of this thesis.

I am sincerely thankful to Prof. Dr. Rinita RajBhandari Joshi, Program Coordinator of MSc in Climate Change and Development, for her consistent support, timely suggestions, and encouragement during my academic journey.

My special thanks go to Mr. Saroj Mainali for his kind assistance in formatting, reviewing, and refining this report. His cooperation and guidance greatly enhanced the final presentation of the work.

Most importantly, I express my deepest appreciation to my husband, Mr. Mukunda Agaasti, for his unwavering support, patience, and motivation throughout this endeavor. His understanding and sacrifices have been the foundation of my academic progress. I am equally grateful to my family members, friends and well-wishers, whose encouragement and belief in me have been a constant source of strength.

Kabita Bhattarai

079MSCCD007

ABSTRACT

High-altitude, snow-fed river basins in the Himalayas are exceptionally sensitive to climate variability, posing challenges for long-term water resource planning and hydropower sustainability. This study assesses the potential impacts of climate change on streamflow dynamics in the Chilime River Basin, Nepal, by coupling bias-corrected projections from thirteen CMIP6 Global Climate Models (GCMs) with the process-based Soil and Water Assessment Tool Plus (SWAT⁺). Simulations were conducted under two Shared Socioeconomic Pathways—SSP2-4.5 and SSP5-8.5—for mid-century (2025–2050) and end-century (2051–2100) periods.

Bias correction was implemented using Quantile Mapping for precipitation and Linear Scaling with lapse rate adjustments for temperature, enhancing the spatial fidelity of climate inputs in the basin's complex terrain. The SWAT⁺ model, configured with snowmelt routines and elevation-sensitive parameters, demonstrated good agreement with observed streamflow patterns during calibration and validation, effectively capturing seasonal flow variability and monsoon peaks.

Future climate projections indicate pronounced warming and intensified precipitation, resulting in substantial hydrological shifts. Under SSP2-4.5, monsoon season streamflow is projected to increase by approximately 8–12%, while SSP5-8.5 yields higher increases exceeding 20–25% by the end of the century. Winter baseflows also exhibit moderate improvements, driven by earlier snowmelt and increased cold-season rainfall. These findings point to heightened risks of late-monsoon flooding and persistent concerns over dry-season water availability.

The study underscores the vulnerability of snow-dependent Himalayan catchments to climatic perturbations and affirms the utility of integrating ensemble climate projections with physically-based hydrological modeling. The results provide critical insights to support climate-resilient hydropower planning, seasonal water allocation, and adaptive watershed governance in the context of a rapidly changing cryosphere.

Contents

COPYRIGHT	II
DECLARATION	III
ACKNOWLEDGEMENT	V
ABSTRACT	VI
LIST OF FIGURS	IX
LIST OF TABLES	XII
LIST OF SYMBOLS AND ABBREVIATIONS	XIII
CHAPTER I INTRODUCTION	1
1.1 Background	1
1.2 Problem Statement	2
1.3 Research Questions.....	3
1.4 Objectives	4
1.4.1 <i>General Objective</i>	4
1.4.2 <i>Specific Objectives</i>	4
1.5 Need of the Study.....	4
CHAPTER II LITERATURE REVIEW	6
2.1 Global Climate Change and Water Resources	6
2.2 Hydrological Impacts in Mountainous Regions.....	6
2.3 Climate Scenarios and the CMIP6 Framework.....	7
2.4 Hydrological Modeling Approaches (e.g., SWAT+)	7
2.5 Studies in Nepal and the Chilime Basin	8
2.6 Research Gap	9
CHAPTER III DATA AND METHODOLOGY	10
3.1 Study Area	12
3.1.1 <i>Spatial Characteristics</i>	12
3.1.2 <i>Temporal Scope</i>	13
3.2 Data Sources and Collection.....	14
3.3 Climate Scenario Bias Correction	16
3.4 SWAT+ Model Setup and Configuration.....	17
3.5 Snowmelt Representation.....	20
3.6 Model Calibration and Validation	21

3.6.1 Calibration and Validation Periods.....	21
3.6.2 Calibration Procedure and Parameter Selection	21
3.6.3 Performance Evaluation Metrics	22
3.7 Climate Scenario Streamflow Simulation	22
CHAPTER IV RESULTS AND DISCUSSIONS.....	24
4.1 Historical Climate and Streamflow Trends	24
4.1.1 Observed Temperature Trends (2000–2020)	24
4.1.2 Observed Precipitation Trends (2000–2020)	26
4.1.3 Estimated Streamflow Patterns (2006–2020).....	27
4.2 Model Calibration and Validation	29
4.2.1 Calibration and Validation overview	29
4.2.2 Performance Metrics and Evaluation	30
4.2.3 Interpretation and Applicability.....	32
4.3 Climate Projection and Bias Correction	33
4.3.1 Bias Correction Methods and Ensemble Generation	33
4.3.2 Comparison of Raw vs. Corrected Climate Data.....	34
4.3.3 Projected Temperature and Precipitation Trends under SSP2-4.5 and SSP5-8.5.....	39
4.4 Future Streamflow Projections.....	49
4.4.1 Streamflow Projection under SSP2-4.5 (2025–2050 and 2051–2100).....	49
4.4.2 Streamflow Projection under SSP5-8.5 (2025–2050 and 2051–2100).....	53
4.4.3 Comparative Analysis of Trishuli vs. Chilime Flow Trends.....	58
4.5 Comparative Streamflow Projections Across Himalayan Basins	60
CHAPTER V CONCLUSIONS AND RECOMMENDATIONS	63
5.1 Conclusions	63
5.2 Recommendations	64
5.2.1 Recommendations for Policy and Practice	64
5.2.2 Recommendations for Further Study	65
REFERENCES.....	66
APPENDICES.....	74
Appendix I: Land Use Land Cover	74
Appendix II: Calibrated SWAT+ Parameter	77
Appendix III: CMIP6 GCMs.....	78

LIST OF FIGURES

Figure 3.1: Flowchart of Methodological Framework.....	11
Figure 3.2: Land Use and Location Map of the Chilime River Basin, Nepal	13
Figure 3.3: Schematic Coordination of Problem, Objective, Method, and Output.....	14
Figure 3.4: Delineated Trishuli Watershed with Subbasin Boundaries and Chilime Highlighted.....	18
Figure 3.5: Watershed Delineation and HRU Setup of the Chilime Basin Using QSWAT+	19
Figure 4.1: Annual Mean Temperature Trend (2000–2020) in the Chilime Basin.....	24
Figure 4.2: Monthly and Seasonal Temperature Variation (2000–2020)	25
Figure 4.3: Monthly Precipitation Pattern (2000–2020)	26
Figure 4.4: Observed Monthly Streamflow at Trishuli (Betrawati Station), 2006–2020	28
Figure 4.5: Observed vs Simulated Streamflow During Calibration (2007–2016).....	31
Figure 4.6: Observed vs Simulated Streamflow During Validation (2017–2019)	31
Figure 4.7: Raw vs Corrected Rainfall Data Under SSP2-4.5 (Boxplot by Model).....	34
Figure 4.8: Raw vs Corrected Rainfall Data Under SSP5-8.5 (Boxplot by Model).....	35
Figure 4.9: Observed vs Raw and Corrected Rainfall Ensemble (SSP2-4.5).....	36
Figure 4.10: Observed vs Raw and Corrected Rainfall Ensemble (SSP5-8.5)	36
Figure 4.11: Monthly Temperature Trend – Observed, Raw, Corrected (SSP2-4.5)..	37
Figure 4.12: Monthly Temperature Trend – Observed, Raw, Corrected (SSP5-8.5)..	38
Figure 4.13: Raw vs Corrected Temperature Boxplot for SSP2-4.5.....	38
Figure 4.14: Raw vs Corrected Temperature Boxplot for SSP5-8.5.....	39
Figure 4.15: Annual Rainfall Projection (2000–2100) Under SSP2-4.5	40
Figure 4.16: Annual Rainfall Projection (2000–2100) Under SSP5-8.5	41

Figure 4.17: Smoothed and Actual Rainfall Trends (SSP2-4.5 and SSP5-8.5)	41
Figure 4.18: Decadal Average Annual Rainfall Comparison	42
Figure 4.19: Seasonal Total Rainfall – 2020, 2050, 2100 (SSP2-4.5 and SSP5-8.5) ...	43
Figure 4.20: Monthly Rainfall Distribution – 2020, 2050, 2100 (SSP2-4.5 and SSP5-8.5)	43
Figure 4.21: Annual Temperature Projection Under SSP2-4.5.....	44
Figure 4.22: Annual Temperature Projection Under SSP5-8.5.....	44
Figure 4.23: Comparison of Annual Temperature for 2020, 2050, and 2100	45
Figure 4.24: Seasonal Temperature Trends – SSP2-4.5 and SSP5-8.5.....	46
Figure 4.25: Monthly Temperature Distribution – SSP2-4.5 and SSP5-8.5	46
Figure 4.26: Spatial Distribution of Lapse Rate Adjusted Temperature (2020–2100)	48
Figure 4.27: Monthly Streamflow Boxplot (SSP2-4.5)	50
Figure 4.28: Simulated Monthly Streamflow (2000–2100) Under SSP2-4.5	50
Figure 4.29: Anomaly Detection in Projected Flow Under SSP2-4.5	51
Figure 4.30: 12-Month Moving Average of Projected Streamflow (SSP2-4.5)	51
Figure 4.31: Monthly Mean Flow – Mid vs End Century (SSP2-4.5)	52
Figure 4.32: Seasonal Variation of Monthly Flow (SSP2-4.5).....	52
Figure 4.33: Monthly Streamflow Boxplot (SSP5-8.5)	54
Figure 4.34: Simulated Monthly Streamflow (2000–2100) Under SSP5-8.5	54
Figure 4.35: Anomaly Detection in Projected Flow Under SSP5-8.5.....	55
Figure 4.36: 12-Month Moving Average of Projected Streamflow (SSP5-8.5)	55
Figure 4.37: Seasonal Variation of Monthly Flow (SSP5-8.5).....	56
Figure 4.38: Monthly Mean Flow – Mid vs End Century (SSP5-8.5)	57
Figure 4.39: Monthly Flow Distribution Boxplot (SSP5-8.5).....	57

Figure 4.40: Monthly Streamflow Comparison of Trishuli and Chilime (SSP2-4.5)... 59

Figure 4.41: Monthly Streamflow Comparison of Trishuli and Chilime (SSP5-8.5)... 60

LIST OF TABLES

Table 3.1: Coordination Schema Table.....	12
Table 3.2: Data Collection and Source of Data.....	14
Table 3.3: SWAT+ Configuration Parameters for Trishuli Watershed.....	18
Table 3.4: SWAT+ Configuration Parameters for Chilime Sub-Basin.....	19
Table 3.5: Calibrated SWAT+ Parameters with Optimized Ranges and Best-Fit Value	21
Table 4.1: SWAT+ Model Performance Metrics for Calibration and Validation	30
Table 4.3: Comparative Streamflow Projections under Climate Scenarios.....	61

LIST OF SYMBOLS AND ABBREVIATIONS

SWAT ⁺	Soil and Water Assessment Tool Plus
DEM	Digital Elevation Model
DHM	Department of Hydrology and Meteorology (Nepal)
QSWAT ⁺	QGIS-based SWAT Plus Interface
HRU	Hydrological Response Unit
LSU	Landscape Unit
GCM	Global Climate Model
CMIP6	Coupled Model Intercomparison Project Phase 6
SSP	Shared Socioeconomic Pathway
RCP	Representative Concentration Pathway
LULC	Land Use and Land Cover
MODIS	Moderate Resolution Imaging Spectroradiometer
GRACE	Gravity Recovery and Climate Experiment
NSE	Nash–Sutcliffe Efficiency
R ²	Coefficient of Determination
RMSE	Root Mean Square Error
MSE	Mean Square Error
MAE	Mean Absolute Error
PBIAS	Percent Bias
KGE	Kling–Gupta Efficiency
P-factor	Percentage of observed data within 95% prediction uncertainty band
R-factor	Ratio of the average thickness of 95% prediction band to the standard deviation of the observed data

SUFI-2 Sequential Uncertainty Fitting Version 2
IPCC Intergovernmental Panel on Climate Change
WEAP Water Evaluation and Planning System
ICIMOD International Centre for Integrated Mountain Development
WGN Weather Generator Fil

CHAPTER I INTRODUCTION

1.1 Background

Climate change poses one of the most significant environmental and socio-economic threats of the 21st century. The IPCC (2021) reports that global mean temperatures have already risen by approximately 1.1°C compared to pre-industrial levels. Projections under various greenhouse gas emission scenarios suggest this increase could reach between 1.5°C and 4.4°C by the end of the century. Such warming is intensifying the hydrological cycle, resulting in altered precipitation regimes, accelerated glacier melt, and modified streamflow dynamics, particularly in high-altitude regions such as the Himalayas (Barnett et al., 2005; Immerzeel et al., 2020).

The Himalayas, often referred to as the "water towers of Asia," supply freshwater to over a billion people downstream. In this region, snowmelt, glacier retreat, and monsoon rainfall are key contributors to river flow. Studies by Immerzeel et al. (2020) and Sharma et al. (2019) have emphasized the complex interplay between precipitation, glacier melt, and groundwater, all of which are highly sensitive to climate change. Warming temperatures in the Hindu Kush Himalaya (HKH) region, which are rising faster than the global average, are leading to changes in flow timing, seasonal water availability, and increased risks of hydrological extremes by Mukherji et al. (2019).

In Nepal, hydrological studies reveal significant changes in streamflow trends linked to climate variability. Mishra et al. (2018) found that the Bheri River Basin exhibits increasing maximum and minimum temperatures at rates of 0.025°C/year and 0.033°C/year respectively under moderate emission scenarios, rising to 0.065°C/year and 0.071°C/year under high-emission scenarios. Similarly, Bajracharya et al. (2018) and Dahal et al. (2020) noted that reduced snowfall, glacier retreat, and variability in rainfall are already impacting river discharge patterns in high-altitude Himalayan basins.

The Chilime River Basin, a snow-fed and monsoon-driven sub-basin of the Trishuli River located in Nepal's Rasuwa District, is a critical site for hydropower generation, agriculture, and local water supply. However, the region is increasingly vulnerable to climate-induced hydrological shifts. Nepal et al. (2017) emphasized the importance of hydrological modeling to understand these shifts, while Bajracharya et al. (2017) highlighted the role of snowmelt and glacier contributions in maintaining dry-season flows.

Given the socio-economic importance of the Chilime River Basin, especially for projects like the Chilime Hydropower Plant, it is imperative to assess the projected changes in streamflow under future climate scenarios. Understanding future streamflow responses under different climate change scenarios is essential to ensure climate-resilient planning in such snow-fed Himalayan basins, integrated with Regional Climate Models (RCMs) and the SWAT+ hydrological model. This approach aims to offer robust forecasts of streamflow variability under climate change and provide policy-relevant insights for water resource planning and hydropower development in Nepal. However, localized streamflow studies that incorporate snow-influenced hydrological regimes and high-resolution climate projections remain limited in high-altitude basins like Chilime, especially in high-altitude basins like Chilime.

1.2 Problem Statement

Building on the broader understanding of climate-driven hydrological changes in the Himalayan region, the Chilime River Basin presents a localized case of particular concern. Located in the northern highlands of Nepal, this snow-fed watershed plays a crucial role in regional hydropower development and local water security. Its hydrological regime is shaped by complex interactions between snowmelt, rainfall, and seasonal runoff, making it highly sensitive to climatic variations. Recent studies highlight that smaller headwater basins like Chilime are particularly vulnerable to the compounded effects of warming temperatures and shifting precipitation patterns, which disrupt traditional hydrological timing and magnitude (Shrestha et al., 2015; Prajapati et al., 2023).

Despite growing regional assessments, localized hydrological modeling in the Himalayan region remains limited, especially in the context of the latest climate change scenarios. Streamflow projections under CMIP6 remain largely unexplored in small, snow-dominated basins in Nepal, posing a significant gap for adaptive water planning. Recent advancements in hydrological modeling such as the integration of SWAT+ with high-resolution climate models offer a promising avenue to simulate climate impacts under varying emission trajectories (Subedi et al., 2024).

Snowmelt-driven catchments like Chilime face additional uncertainties due to rising evapotranspiration rates, reduced snow cover duration, and earlier onset of meltwater runoff (Li et al., 2021; Sharma et al., 2024). These conditions threaten both water availability and hydropower reliability during dry seasons. Chanda et al. (2024) further emphasize the need for predictive modeling approaches that can incorporate climate uncertainty, particularly in high-altitude basins where field data is scarce.

In Nepal, the lack of basin-specific, CMIP6-based streamflow studies limits the decision-making capacity of water managers and hydropower operators. By filling this research gap, the present study applies a bias-corrected CMIP6 dataset within the SWAT+ modeling framework to forecast streamflow changes in the Chilime River Basin under SSP2-4.5 and SSP5-8.5 scenarios. The findings aim to provide critical insights for climate-resilient infrastructure development and adaptive water governance in snow-fed Himalayan basins.

1.3 Research Questions

- How are temperature and precipitation projected to change in the Chilime River Basin under future climate scenarios SSP2-4.5 and SSP5-8.5?
- What will be the impact of projected climate change on streamflow in the Chilime River Basin under different emission scenarios?
- How effectively does the SWAT+ model, when integrated with CMIP6 climate data, simulate future streamflow patterns in the snow-fed Chilime River Basin?

1.4 Objectives

1.4.1 General Objective

To assess the impacts of climate change on streamflow patterns in the Chilime River Basin under different Shared Socioeconomic Pathways (SSP2-4.5 and SSP5-8.5) for the periods 2025–2050 and 2051–2100, in order to provide insights for sustainable water resource management and climate adaptation strategies in the basin.

1.4.2 Specific Objectives

1. To analyse projected trends in temperature and precipitation in the Chilime River Basin under SSP2-4.5 and SSP5-8.5 scenarios.
2. To assess the performance of the SWAT+ model in simulating streamflow in the Chilime River Basin when driven by CMIP6-based climate inputs.
3. To evaluate the impacts of future climate conditions on streamflow dynamics in the basin using bias-corrected CMIP6 climate data.

1.5 Need of the Study

The Chilime River Basin, a snow-fed sub-catchment of the Trishuli River in northern Nepal, plays a vital role in hydropower generation and local water supply. As climate change accelerates, high-altitude basins such as Chilime face increasing risks due to altered precipitation regimes, reduced snow cover, and changing seasonal runoff patterns. These shifts pose a direct threat to dry-season water availability and the long-term reliability of hydropower systems.

While several regional studies have examined hydrological responses to climate change, basin-specific assessments remain limited—particularly those using the latest generation of climate projections. Most prior research has relied on earlier emission scenarios and coarser models that do not adequately capture the topographic complexity and climatic sensitivity of mountain catchments.

The application of a process-based hydrological model, driven by downscaled and bias-corrected CMIP6 climate projections, provides an opportunity to generate improved forecasts of streamflow variability at the basin scale. This is especially

important for guiding climate-resilient infrastructure planning, optimising hydropower operations, and supporting adaptive water governance. The present study addresses a critical research gap by providing localised, scenario-based insights into the future water availability of a snow-influenced Himalayan basin under changing climate conditions.

CHAPTER II LITERATURE REVIEW

2.1 Global Climate Change and Water Resources

Climate change has emerged as one of the most critical drivers of hydrological transformation across the globe. According to the Intergovernmental Panel on Climate Change (IPCC, 2021), global surface temperatures have risen by approximately 1.1°C above pre-industrial levels, triggering alterations in precipitation regimes, intensified evapotranspiration, and modified runoff dynamics. These changes are expected to escalate further, leading to significant regional disparities in water availability (Huntington, 2006).

The intensification of the global hydrological cycle is projected to result in more extreme precipitation events in certain regions, while others may experience prolonged droughts and reduced groundwater recharge (Bates et al., 2008). Such climatic extremes pose considerable challenges for developing nations, where agriculture, hydropower, and local livelihoods are particularly vulnerable to fluctuations in water supply. In snow-dominated basins, the impacts are especially pronounced, manifesting in reduced snowpack, earlier onset of snowmelt, and shifting seasonal flow patterns (Singh & Bengtsson, 2005; Li et al., 2021).

2.2 Hydrological Impacts in Mountainous Regions

Mountainous catchments, often termed the “water towers of the world,” are particularly susceptible to climate-induced changes in hydrological processes. The Himalayan region has experienced a rate of warming nearly twice the global average, resulting in profound alterations in glacier dynamics, snow cover extent, and the timing of streamflow (Immerzeel et al., 2010; Kraaijenbrink et al., 2017). These transformations pose serious risks to downstream water availability and energy production.

Studies have shown that snowmelt- and glacier-fed systems exhibit distinct responses to climatic stressors. Snowmelt volumes may decrease due to diminished snowfall and reduced accumulation, while glacier melt may initially rise before eventually declining as ice reserves deplete (Singh & Bengtsson, 2005). In the context of Nepal, such

variability has a direct impact on dry-season flows, which are essential for sustaining agricultural productivity and ensuring hydropower reliability (Miller et al., 2012; Viviroli et al., 2011).

2.3 Climate Scenarios and the CMIP6 Framework

Future climate assessments are primarily based on projections generated by General Circulation Models (GCMs), which are standardised under initiatives such as the Coupled Model Intercomparison Project (CMIP). The sixth phase, CMIP6, introduces Shared Socioeconomic Pathways (SSPs) that integrate greenhouse gas emission trajectories with socio-economic development narratives (O'Neill et al., 2016). Among these, SSP2-4.5 (a stabilisation scenario) and SSP5-8.5 (a high-emission scenario) are particularly pertinent for climate-vulnerable regions such as South Asia.

CMIP6 offers enhanced spatial resolution and improved representations of land-atmosphere interactions relative to its predecessor, CMIP5 (Eyring et al., 2016). Its application in hydrological modelling has become increasingly widespread, with several studies reporting improved simulations of precipitation and streamflow in monsoon-dominated regions (Zheng et al., 2018; Chanda et al., 2024). Nonetheless, the utilisation of CMIP6 outputs in small, snow-fed catchments in Nepal remains limited, highlighting a significant research gap in local-scale climate impact assessment.

2.4 Hydrological Modeling Approaches (e.g., SWAT+)

Physically based hydrological models are essential tools for simulating watershed processes and evaluating the impacts of climate change on water resources. Among them, the Soil and Water Assessment Tool (SWAT) and its advanced version, SWAT+, have gained widespread application in both research and practical planning due to their capacity for long-term, process-oriented simulations (Arnold et al., 1998; Bieger et al., 2017).

SWAT+ includes a temperature-index snowmelt module, which is particularly useful for snow-fed basins such as those in the Himalayas, where meltwater significantly contributes to dry-season flows (Singh & Bengtsson, 2005). It enhances model flexibility through improved landscape discretisation, spatial connectivity, and

modular design. It facilitates integration with future climate projections (e.g., CMIP6), land use dynamics, and snow-influenced hydrological regimes, making it particularly suitable for data-scarce and topographically complex catchments such as those found in the Himalayan region (Mamoon et al., 2024; Mohseni et al., 2023). Given the pronounced topographic variation in Himalayan basins, the application of elevation-adjusted temperature inputs, typically via lapse rate correction, has been shown to improve the representation of snowmelt-driven seasonal flows. Research conducted in Nepal and northern India has demonstrated that, when calibrated using multi-GCM ensemble inputs, SWAT is capable of simulating seasonal streamflow with high reliability (Shukla et al., 2021; Lamichhane et al., 2024).

2.5 Studies in Nepal and the Chilime Basin

A number of studies conducted in Nepal have employed SWAT and comparable hydrological models to simulate streamflow under projected climate scenarios. For example, Panthi et al. (2018), Shrestha et al. (2015), and Budhathoki et al. (2025) applied Representative Concentration Pathways (RCPs) and Shared Socioeconomic Pathways (SSPs) to assess hydrological responses in the Bheri, Tamor, and Bagmati basins. However, many of these studies relied on earlier CMIP5 datasets or omitted explicit treatment of snow processes, which can compromise simulation accuracy in snow-fed catchments.

The Chilime River Basin, a snow-fed sub-catchment of the Trishuli River located in Nepal's Rasuwa District, remains underrepresented in the hydrological modelling literature. Despite its significance for hydropower generation, few studies have examined how changing precipitation patterns and snowmelt dynamics under CMIP6 scenarios may influence future streamflow. Nepal et al. (2014) underscored the importance of hydrological modelling in upstream basins, yet the role of snow processes was not comprehensively integrated.

More recent research has demonstrated the potential of combining SWAT+ with remote sensing-derived snow data to enhance streamflow simulation in snow-dominated environments (Li et al., 2021; Khajuria et al., 2022). Within this context,

applying a modelling framework that incorporates snow-sensitive processes alongside bias-corrected CMIP6 projections in the Chilime Basin can help address a critical gap in both scientific understanding and climate-resilient water planning.

2.6 Research Gap

Despite growing efforts in hydrological modelling across Nepal and the broader Himalayan region, several critical gaps persist. Firstly, small snow-fed catchments such as the Chilime Basin have received relatively limited scientific attention—particularly in the context of recent climate scenarios developed under the CMIP6 framework. Secondly, although models such as SWAT+ are increasingly applied, the representation of snow dynamics remains either oversimplified or entirely omitted, often resulting in the underestimation of snowmelt contributions during dry seasons.

Thirdly, there is a noticeable paucity of studies that combine bias-corrected CMIP6 climate data with snow-sensitive hydrological modelling frameworks in a way that can inform decision-making related to water infrastructure development and climate adaptation. Additionally, few basin-scale assessments have evaluated future streamflow by explicitly incorporating the influence of snowmelt processes.

This study aims to address these research gaps by applying a SWAT+ modelling approach that accounts for snow-influenced hydrology and is driven by bias-corrected CMIP6 projections. By doing so, it seeks to simulate future streamflow conditions with greater realism, support hydropower optimisation, and contribute to climate-resilient water resource planning in high-altitude regions of Nepal.

CHAPTER III DATA AND METHODOLOGY

This chapter outlines the methodological framework adopted to assess the impacts of climate change on streamflow in the Chilime River Basin. The research design is structured around three specific objectives. First, projected climate trends were analyzed using ensemble outputs from thirteen CMIP6 Global Climate Models (GCMs) under SSP2-4.5 and SSP5-8.5, with bias correction techniques applied to improve data reliability. Second, the SWAT⁺ hydrological model was calibrated and validated using scaled streamflow data from the Trishuli River to evaluate its performance in simulating observed flow. Finally, bias-corrected climate projections were used to drive the calibrated SWAT⁺ model for simulating future streamflow patterns up to 2100. The overall methodological framework is illustrated in Figure 3.1, and a coordination schema linking the research problem, objectives, methods, and outputs is presented in Table 3.1.

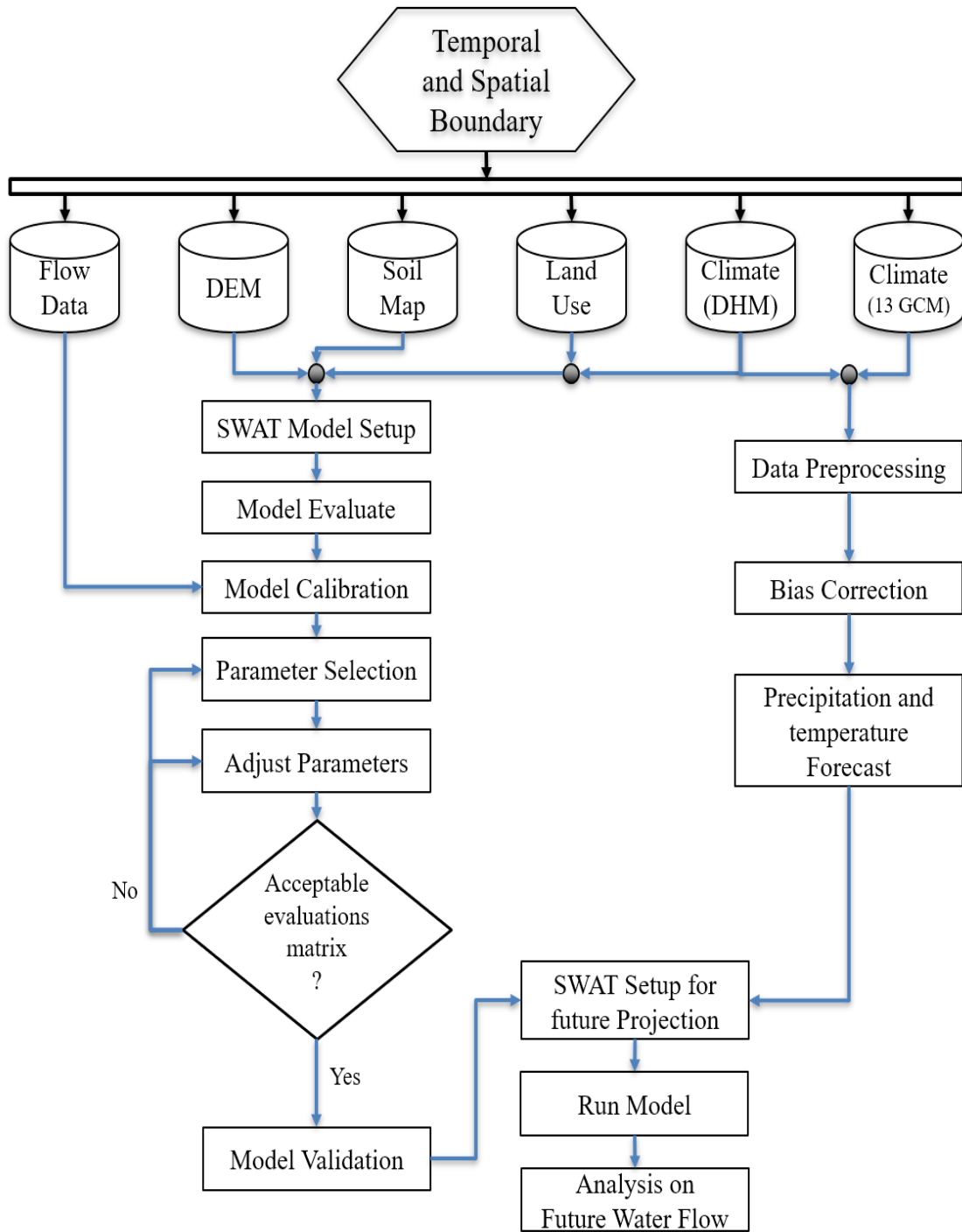


Figure 3.1: Methodological Framework of the Study

Table 3.1 Coordination Schema Table

Problem Statement Component	Specific Objective	Method Applied	Data/Tool Used	Expected Output
Limited understanding of future climate trends in high-altitude basins	Objective 1: Analyze temperature and precipitation trends under CMIP6	GCM selection, bias correction, ensemble averaging	CMIP6 GCMs, Python, QGIS, Excel	Projected temperature and rainfall (2025–2100)
Need to validate streamflow simulation for Himalayan sub-basins	Objective 2: Evaluate SWAT+ model performance	SWAT+ calibration and validation using SUFI-2	SWAT+, SWAT-CUP, Trishuli streamflow data	Calibrated hydrological model with NSE, R ² , PBIAS
Uncertainty in future streamflow under SSP scenarios	Objective 3: Simulate streamflow using CMIP6 scenarios	Climate forcing in SWAT+ with corrected ensemble	Bias-corrected climate data, SWAT+	Future streamflow trends under SSP2-4.5 and SSP5-8.5

3.1 Study Area

3.1.1 Spatial Characteristics

The Chilime River Basin is situated in the northern highlands of Nepal, within the administrative boundary of Rasuwa District. It forms a snow-fed sub-catchment of the Trishuli River system and lies approximately between 28°10'N to 28°20'N latitude and 85°10'E to 85°30'E longitude. The basin encompasses a total area of approximately 277 km² and features pronounced altitudinal gradients, ranging from about 1,400 m to over 7,400 m above sea level. These topographic variations, coupled with its location in the Himalayan foothills, subject the basin to a unique hydrometeorological regime characterized by orographic precipitation, snow accumulation in winter, and glacial melt during the dry season. The basin's headwaters extend into the Ganesh Himal and transboundary Tibetan Plateau, making it strategically significant for trans-Himalayan hydrology. Furthermore, the Chilime River supports major infrastructure

projects such as the Chilime and Sanjen Hydropower Plants, underscoring its importance in Nepal’s renewable energy landscape.

As illustrated in Figure 3.2, the spatial context of the Chilime Basin within the broader geographic setting of Nepal highlights its location in relation to major river systems, elevation gradients, and administrative boundaries. This geospatial overview forms the foundation for all subsequent spatial and hydrological analysis.

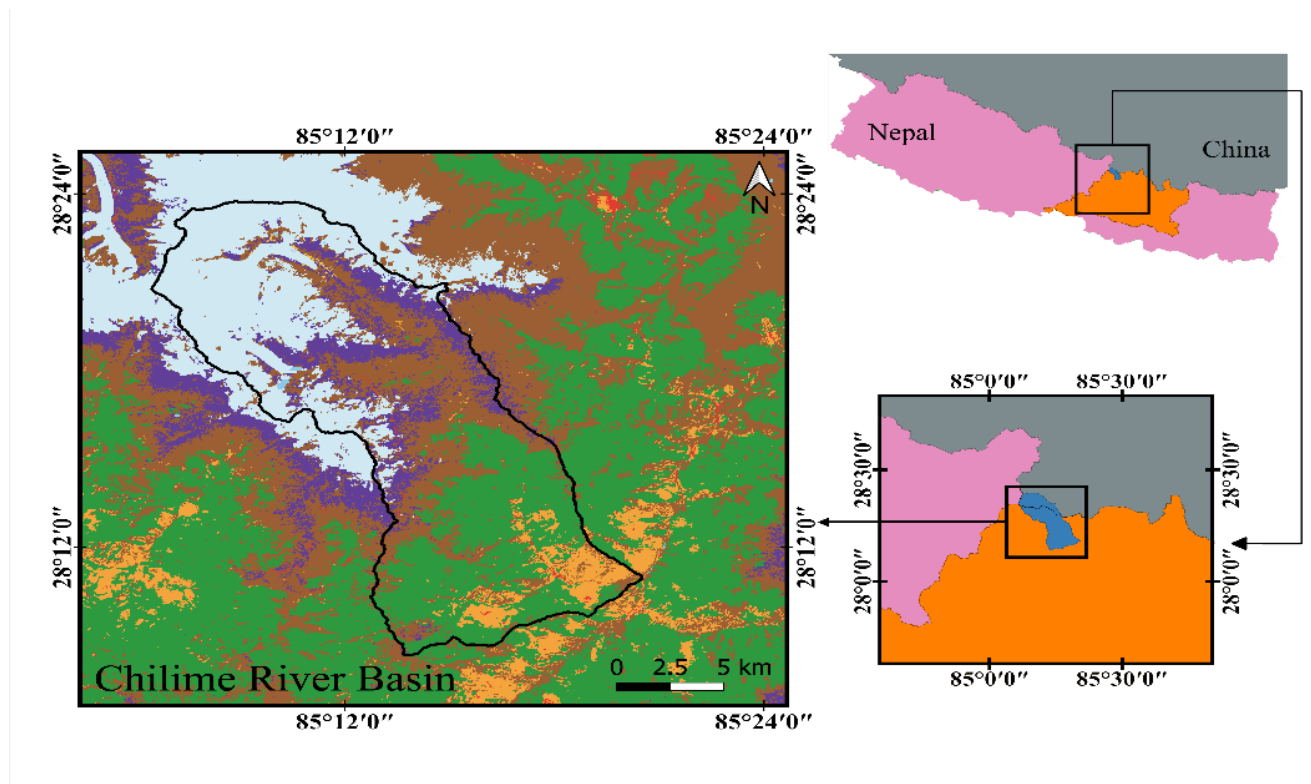


Figure 3.2: Land Use and Location Map of the Chilime River Basin, Nepal
This map shows the spatial distribution of land use and land cover within the Chilime River Basin (main panel) and its geographic location within Rasuwa District and the national boundary of Nepal.

3.1.2 Temporal Scope

To assess hydrological changes across varying climate futures, two projection windows are considered: the near future (2025–2050) and the far future (2051–

2100). These periods correspond to IPCC-endorsed timelines and enable comparative analysis under moderate and extreme emission pathways.

3.2 Data Sources and Collection

Table 3.2- Data Collection and Source of Data

S.N	Data type	Specific Parameter	Time period	Source
1	Climate Data (Observed)	Precipitation, temperature (max, min.)	1990–2020 (historical)	DHM, Nepal
2	Climate Data (Projected)	Precipitation, temperature (max, min.)	2021–2050, 2051–2100	CMIP6 GCMs (13)
3	Hydrological Data	Streamflow (daily or monthly)	2000–2020	Trishuli (Betrawati station) from DHM
4	Topographical Data	Digital Elevation Model (DEM)	Static	SRTM 30m DEM from USGS Earth Explorer; Processed in QGIS for delineation
5	Land use and Land cover Data	Land cover classification, vegetation types	2021, Recent available	- ICIMOD LULC data,
6	Soil Data	Soil texture, type, infiltration capacity	Static	Soil Grids (GEE) and DSOL, processed using lookup table
7	Snow Consideration	Modeled using SWAT+ built-in snowmelt module	2000–2100 (implicit in climate data)	Not direct input; derived from temperature-based melt within SWAT+

Table 3.2 presents the datasets used in this study, which include historical and projected climate data, hydrological observations, topographic information, land use/land cover classification, and soil parameters. Climate data for 1990–2020 were obtained from DHM, while future projections under SSP2-4.5 and SSP5-8.5 were extracted from a 13-member CMIP6 ensemble. Hydrological data from the Trishuli River (Betrawati station) supported streamflow estimation and calibration. Spatial data, including DEM and LULC, were processed in QGIS and restructured for SWAT+.

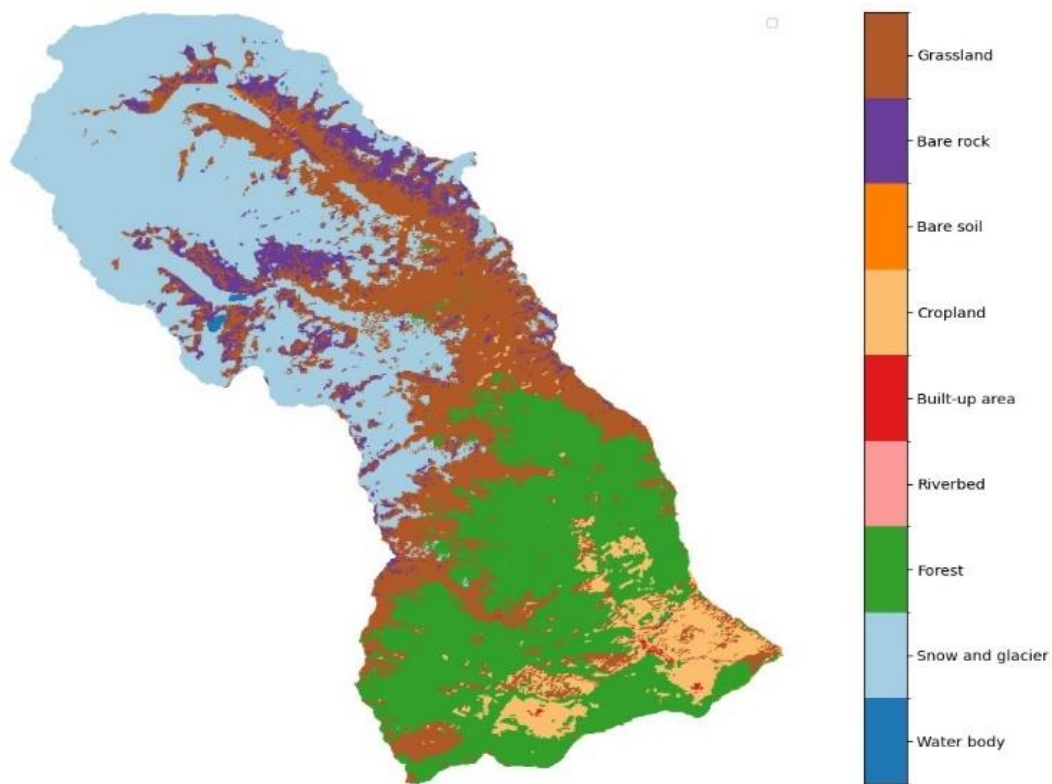


Figure 3.3: Land Use and Land Cover (LULC) Map of the Chilime River Basin (2021)
 The LULC dataset from ICIMOD was processed in QGIS and reclassified into SWAT+ - compatible categories. The map illustrates major land cover types such as forest, snow/glacier, grassland, and barren land, which influence hydrological processes in the basin.

Soil characteristics were derived from global and national sources, harmonized into a lookup table for model input. Snowmelt processes were represented internally within SWAT+ using a temperature-index method and elevation-adjusted inputs.

3.3 Climate Scenario Bias Correction

Raw outputs from Global Climate Models (GCMs) are essential for projecting future climate scenarios. However, due to their coarse spatial resolution and inherent biases, direct application of GCM data in hydrological modelling often results in inaccuracies, particularly in complex terrains such as the Himalayan region. Therefore, bias correction and elevation adjustment are critical preprocessing steps to align GCM outputs with observed local climate conditions.

This study utilised daily climate projections from thirteen GCMs under the Coupled Model Intercomparison Project Phase 6 (CMIP6), including models such as BCC-CSM2-MR, CNRM-CM6-1, MRI-ESM2-0, and others. These were selected based on performance across South Asia and the availability of required variables. Two climate scenarios were assessed: SSP2-4.5 (moderate emissions) and SSP5-8.5 (high emissions), across two future periods: 2025–2050 and 2051–2100.

Bias correction was applied using Quantile Mapping for precipitation and Linear Scaling for temperature. Observed daily climate data for the baseline period (1990–2020) from stations within and near the Chilime River Basin—such as Dhunche and Thamachit—served as reference. In addition, temperature data were adjusted for elevation using a lapse rate of 6.5°C per 1,000 metres, aligning GCM grid data with the actual altitude distribution of the Chilime Basin.

Following bias correction and elevation adjustment, a multi-model ensemble mean was generated by averaging the corrected outputs from all 13 GCMs. This ensemble approach accounts for inter-model variability and provides a robust central projection for climate trends. Climate indicators were analysed for three time slices: historical (2000–2020), near future (2025–2050), and far future (2051–2100).

These ensemble-corrected temperature and precipitation datasets were subsequently used as climate inputs for SWAT⁺ to simulate future streamflow responses under both emission scenarios. The bias correction process ensured temporal consistency and spatial relevance of future climate data to the Chilime Basin's high-altitude setting.

3.4 SWAT+ Model Setup and Configuration

The SWAT⁺ (Soil and Water Assessment Tool Plus) model was employed to simulate hydrological processes in the Trishuli River Basin, with a specific focus on extracting discharge from the Chilime sub-basin. Watershed delineation was carried out using a 30-meter resolution Digital Elevation Model (DEM) obtained from the United States Geological Survey (USGS). The model setup incorporated spatial inputs such as land use, soil type, slope, and climate variables specific to the region.

Figure 3.4 presents the delineated Trishuli watershed along with its subbasins. The Chilime River Basin is highlighted as Subbasin 4, located in the northwestern part of the larger watershed. As part of the SWAT⁺ configuration, the Trishuli watershed was divided into seven subbasins, 69 Landscape Units (LSUs), and 1,018 Hydrological Response Units (HRUs), reflecting its topographic complexity and land use heterogeneity (see **Table 3.3**).

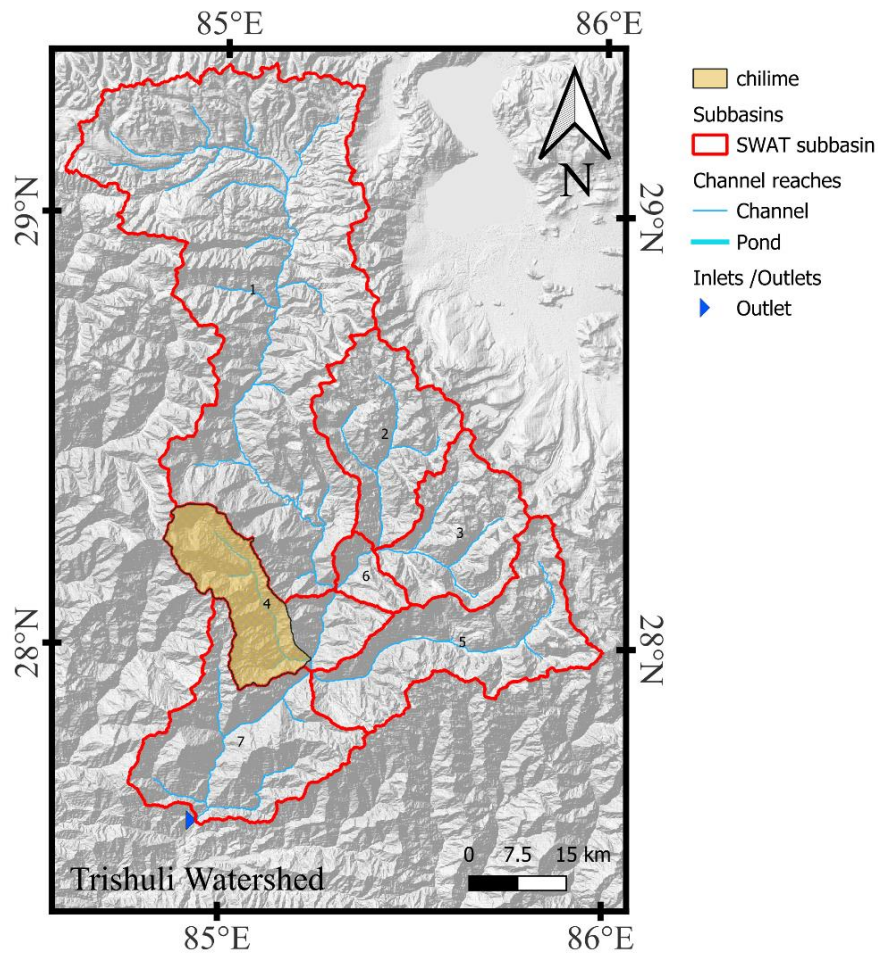


Figure 3.4: Delineated Trishuli Watershed with Subbasin Boundaries and Chilime Highlighted

Table 3.3: SWAT⁺ Configuration Parameters for Trishuli Watershed

Watershed Area	HRUs	LSUs	Subbasins
463,265.05 ha	1,018	69	7

Following successful delineation and model setup of the Trishuli Basin, the Chilime River Basin was extracted as a sub-catchment to serve as the focal unit for climate-driven streamflow simulation. The Chilime Basin, modeled as a single subbasin, comprises 11 LSUs and 111 HRUs, spanning a total area of 27,834.21 hectares.

Figure 3.5 illustrates the watershed delineation and internal hydrological network of the Chilime sub-basin, including inlets, stream reaches, and outlet points, as generated by QSWAT+. This configuration was used to extract sub-basin-specific flow after model calibration.

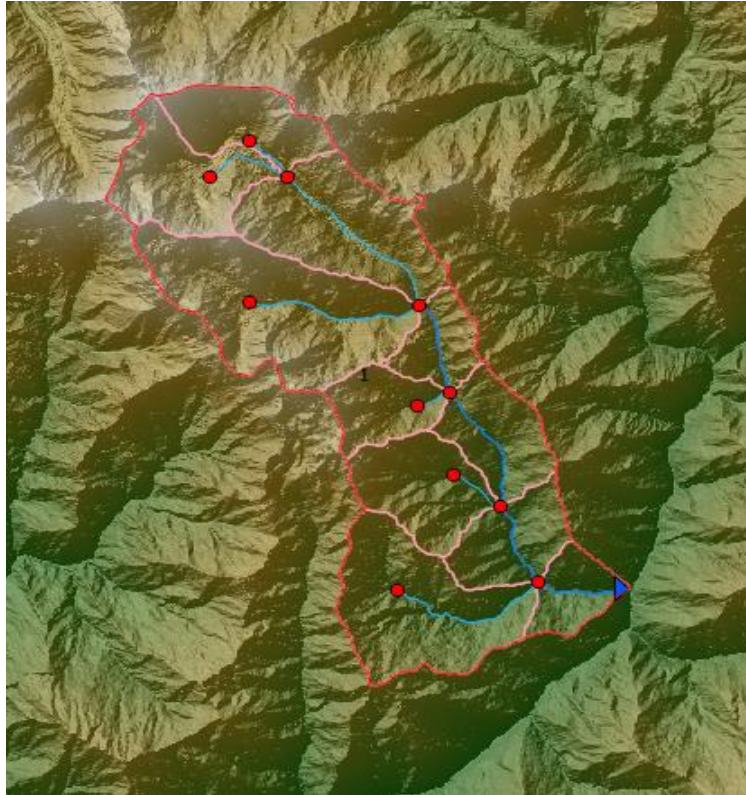


Figure 3.5: Watershed Delineation and Hydrological Response Unit (HRU) Setup of the Chilime River Basin Using QSWAT+

Table 3.4: SWAT+ Configuration Parameters for Chilime Sub-Basin

Watershed Area	HRUs	LSUs	Subbasins
27,834.21 ha	111	11	1

This two-tier modeling approach—calibrating the entire Trishuli Basin and extracting simulated flows for the nested Chilime sub-basin—ensured spatial consistency in

runoff generation and preserved the physical realism of the streamflow outputs for climate impact assessment.

3.5 Snowmelt Representation

The Chilime River Basin is a snow-fed catchment where snow accumulation and melt significantly influence seasonal streamflow, particularly during the pre-monsoon and dry-season periods. Although direct remote sensing-based snow modelling was not implemented in this study, snow dynamics were accounted for through the elevation-adjusted temperature input and the use of SWAT+'s built-in snowmelt simulation routine.

SWAT+ employs a temperature-index (degree-day) approach to simulate snow accumulation and melt processes. This method estimates snowmelt as a function of air temperature exceeding a defined threshold, using calibrated melt coefficients. In this study, temperature data were corrected for elevation using a lapse rate of 6.5°C per 1,000 metres, enabling improved realism of thermal conditions across the basin's steep altitudinal gradients.

The model uses key snow-related parameters such as: SMFMX: Maximum melt rate on 21 June (mm H₂O/°C/day), SMFMN: Minimum melt rate on 21 December, SFTMP: Snowfall temperature threshold (°C), TIMP: Snowpack temperature lag factor.

These parameters were adjusted based on values from the literature and model calibration efforts. Although no external snow cover datasets (e.g., MODIS) were assimilated, seasonal flow validation helped confirm the suitability of these parameters in capturing the basin's melt-dominated hydrology.

By integrating lapse rate-corrected temperature inputs with the SWAT+ temperature-index snow routine, the model was able to simulate the essential snowmelt-driven runoff regime typical of high-altitude Himalayan catchments. This integration ensures that streamflow projections under future climate scenarios adequately reflect the seasonal influence of snow accumulation and melt.

3.6 Model Calibration and Validation

The SWAT⁺ model was calibrated and validated to simulate streamflow dynamics in the Trishuli River Basin, focusing on extracting discharge from the Chilime sub-basin. Due to the absence of direct gauging at the Chilime outlet, observed streamflow data from the Betrawati Station on the Trishuli River—provided by the Department of Hydrology and Meteorology (DHM)—was used as a proxy for model calibration and validation.

3.6.1 Calibration and Validation Periods

The modeling period was divided as follows:

- Calibration period: 2007–2016
- Validation period: 2017–2019

These periods were selected to capture interannual variability, including both monsoon peaks and dry-season baseflow, thus ensuring the model’s robustness across seasonal regimes.

3.6.2 Calibration Procedure and Parameter Selection

Calibration was performed using the SWAT⁺ Toolbox, which provides integrated support for sensitivity analysis, parameter optimization, and performance evaluation. A total of 15–20 hydrological parameters were selected based on their influence on surface runoff, baseflow, evapotranspiration, and snowmelt processes shown in Appendix II. Parameter ranges were defined using expert judgment, previous literature, and trial-based refinement.

Key parameters adjusted during calibration included:

- CN2 – Curve number for surface runoff estimation
- ALPHA_BF – Baseflow recession constant
- GW_DELAY – Groundwater delay time
- ESCO – Soil evaporation compensation factor

- SOL_K – Saturated hydraulic conductivity of soil layers
- SFTMP, SMFMX, SMFMN, TIMP – Snowmelt-related parameters
- GWQMN, REVAPMN, RCHRG_DP – Groundwater threshold and percolation controls

3.6.3 Performance Evaluation Metrics

Model performance was assessed at both monthly and seasonal time scales using the following statistical indicators:

- Nash–Sutcliffe Efficiency (NSE)
- Coefficient of Determination (R^2)
- Percent Bias (PBIAS)
- Root Mean Square Error (RMSE)
- Mean Squared Error (MSE)
- Kling–Gupta Efficiency (KGE)

These metrics were used to compare observed and simulated streamflow and evaluate model efficiency across both calibration and validation periods.

3.7 Climate Scenario Streamflow Simulation

Building upon the calibrated model and corrected climate projections, streamflow simulations were carried out for future climate scenarios using ensemble-corrected GCM inputs. Following successful calibration and validation of the SWAT⁺ model, future streamflow in the Chilime River Basin was simulated using bias-corrected climate projections from thirteen CMIP6 Global Climate Models (GCMs). These models were selected for their spatial relevance to South Asia and availability of daily temperature and precipitation variables. Two emission scenarios were applied:

- SSP2-4.5: A stabilization pathway representing moderate greenhouse gas emissions
- SSP5-8.5: A high-emission trajectory reflecting intensive fossil fuel use

To address model bias and topographic resolution, all GCM outputs were corrected using Quantile Mapping for precipitation and Linear Scaling with lapse rate adjustment for temperature. The corrected climate data were then aggregated using the multi-model ensemble mean approach, which provides a robust average projection and reduces inter-model uncertainty.

Future simulations were conducted for two projection periods:

- Mid-century: 2025–2050
- Late-century: 2051–2100

These periods allow for comparison across short- and long-term climate horizons. The model was driven using ensemble-corrected daily climate inputs, and streamflow outputs were generated for each sub-basin on a daily timestep.

Streamflow outputs were analysed at monthly, seasonal, and annual scales, with a particular focus on pre-monsoon and dry-season flows, which are critical for hydropower generation and water security in snow-fed catchments. The analysis included:

- Percent change comparisons between historical (2000–2020) and future periods
- Hydrographs and seasonal distribution plots
- Evaluation of extreme flow events

These simulations provide essential insights into the temporal distribution of streamflow under future climate scenarios and help identify potential risks to water availability in the Chilime Basin.

CHAPTER IV RESULTS AND DISCUSSIONS

This chapter presents the key results derived from climate analysis, hydrological modeling, and future streamflow simulation in the Chilime River Basin. The findings are structured to directly address the three specific research objectives: (1) analyzing future climate trends under CMIP6 scenarios; (2) assessing the performance of the SWAT⁺ model; and (3) evaluating projected streamflow dynamics under changing climate conditions. Each section presents relevant figures and tables, describes observed trends, interprets their implications, and discusses them in relation to existing literature and the context of Himalayan basins.

4.1 Historical Climate and Streamflow Trends

4.1.1 Observed Temperature Trends (2000–2020)

The historical temperature trends in the Chilime River Basin between 2000 and 2020 were analysed using monthly maximum and minimum temperature records. As shown in Figure 4.1, the maximum temperature exhibits clear seasonal fluctuations with peak values typically occurring during the pre-monsoon and summer months. A few anomalies, including unusually high temperatures above 30 °C, were observed in years such as 2007 and 2010, indicating potential short-term heat events.

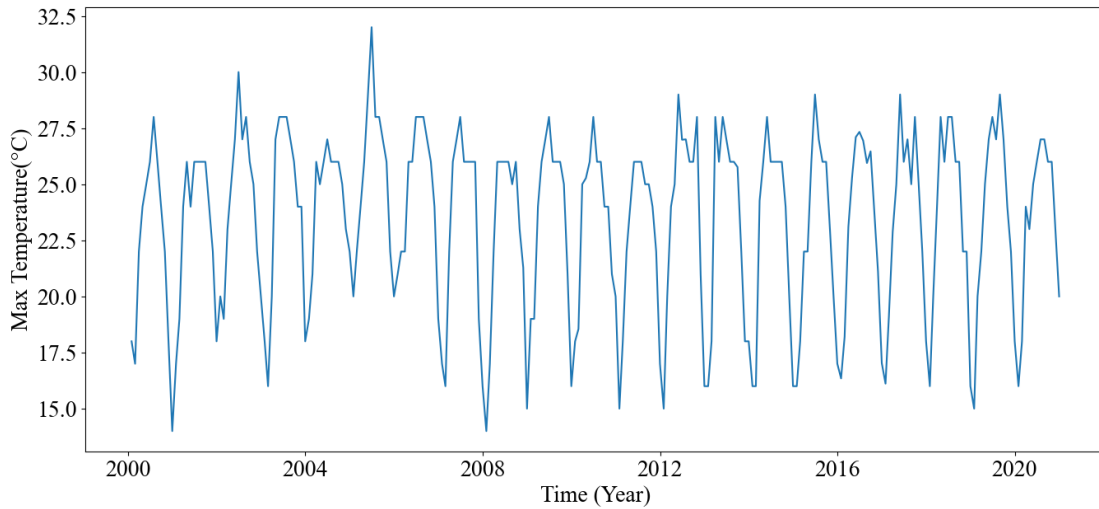


Figure 4.1: Monthly Maximum Temperature Trend in the Chilime River Basin (2000–2020)

Similarly, Figure 4.2 illustrates the trend in minimum temperatures over the same period. Minimum temperatures generally ranged between 0 °C and 15 °C, with colder months approaching or falling below freezing. The temporal pattern of minimum temperature indicates a gradual warming tendency, particularly during winter months.

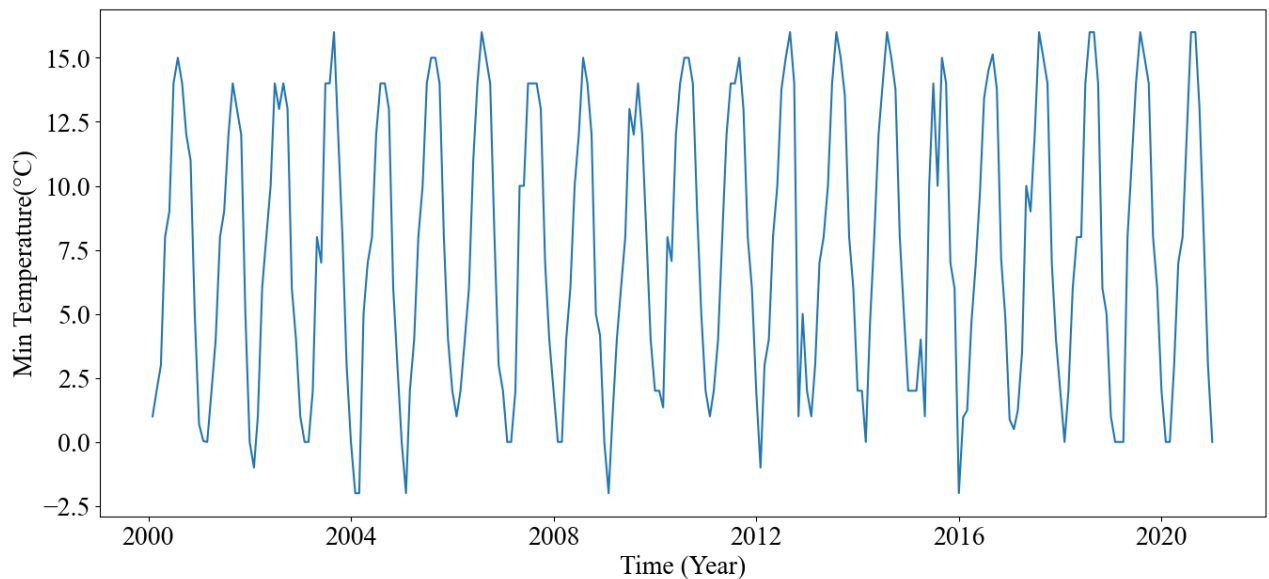


Figure 4.2: Monthly Minimum Temperature Trend in the Chilime River Basin (2000–2020)

These findings suggest a potential rise in the diurnal temperature range and may reflect the impacts of regional climate change in the high-altitude basin.

4.1.2 Observed Precipitation Trends (2000–2020)

Monthly total precipitation data for the Chilime Basin (Figure 4.3) show a pronounced monsoonal pattern, with rainfall peaks occurring between June and September. Interannual variability is evident, with extreme rainfall events observed in years such as 2012 and 2015, exceeding 700 mm in a single month. Conversely, some years experienced lower monsoon precipitation, contributing to seasonal water stress.

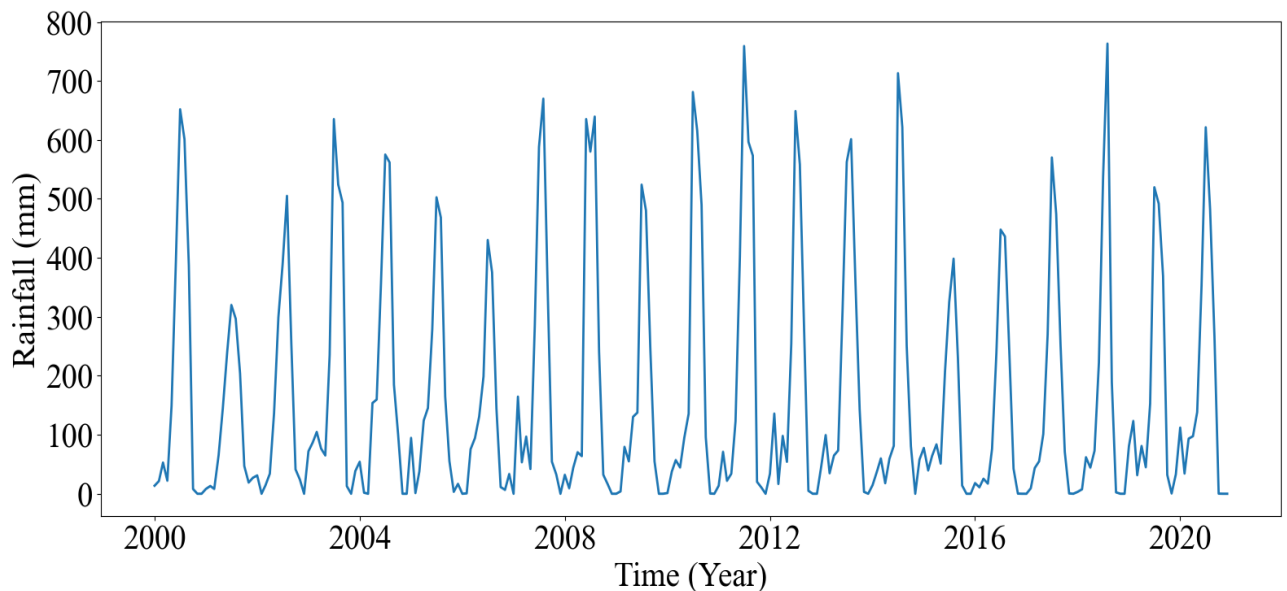


Figure 4.3: Monthly Precipitation Trend in the Chilime River Basin (2000–2020)

Despite fluctuations, no clear long-term increasing or decreasing trend is visible over the 21-year period. However, the observed distribution confirms a strong dependency of annual water availability on monsoon intensity and timing. This highlights the basin’s vulnerability to shifts in monsoonal dynamics and the need to incorporate climate variability in streamflow projections and water resource planning.

4.1.3 Estimated Streamflow Patterns (2006–2020)

In the absence of continuous observed streamflow records at the Chilime River outlet, the entire Trishuli River Basin was delineated and modeled using SWAT+ to estimate flows for the Chilime sub-basin. The SWAT+ model setup encompassed all major tributaries of the Trishuli, including the Chilime River Basin as one of the upstream sub-catchments. Model calibration and validation were conducted using observed streamflow data from the Trishuli River at Betrawati Station (provided by the Department of Hydrology and Meteorology, DHM). Betrawati Station captures the cumulative runoff from about 81% of the Trishuli Basin, effectively including contributions from the Chilime catchment. Because the Chilime Basin is located upstream of this gauging station, calibrating the model against Betrawati's observations ensures that the upstream hydrology (including Chilime's) is well represented. This approach leverages a physically-based, basin-wide model to simulate Chilime's flows, rather than deriving them empirically from the Betrawati record.

After achieving a satisfactory calibration at Betrawati, the SWAT+ model was applied to simulate streamflow for all delineated sub-basins, and the results for the Chilime River Basin were extracted. Importantly, the Chilime streamflow series obtained from the model is not a direct scaling or partitioning of the Betrawati flow; instead, it is generated by the model based on local climate, land cover, snow dynamics, and runoff processes in the Chilime sub-catchment. In other words, the Chilime flow is spatially simulated through the calibrated physically-based model. This ensures that the flow estimates for Chilime reflect its own watershed characteristics (e.g., higher elevation snowfields and rainfall input) and are consistent with observed data only through the model's calibration constraints. The result is a more realistic representation of Chilime's hydrology, as opposed to any simplistic extrapolation from the main river.

To provide a hydrological context for the region, Figure 4.4 shows the observed streamflow pattern of the Trishuli River at Betrawati for 2006–2020. This record exhibits the typical seasonal cycle of a high-altitude Himalayan River system strongly influenced by the South Asian monsoon. Peak flows occur in the summer months of

July–September, often exceeding $400 \text{ m}^3/\text{s}$ during intense monsoonal rainfall events. In contrast, the winter and pre-monsoon months (December through May) experience substantially lower flows, frequently below $100 \text{ m}^3/\text{s}$, as precipitation is minimal and much of the high-altitude precipitation is locked as snow. This observed discharge regime confirms that the Trishuli Basin’s runoff is dominated by the summer monsoon, with secondary contributions from snow and ice melt during the spring and early summer. We include the Betrawati flow curve here primarily to set the broader hydrological context – it reflects the overall flow regime into which the Chilime River feeds, but it is not used to directly calculate the Chilime flows beyond serving as the calibration target for the model.

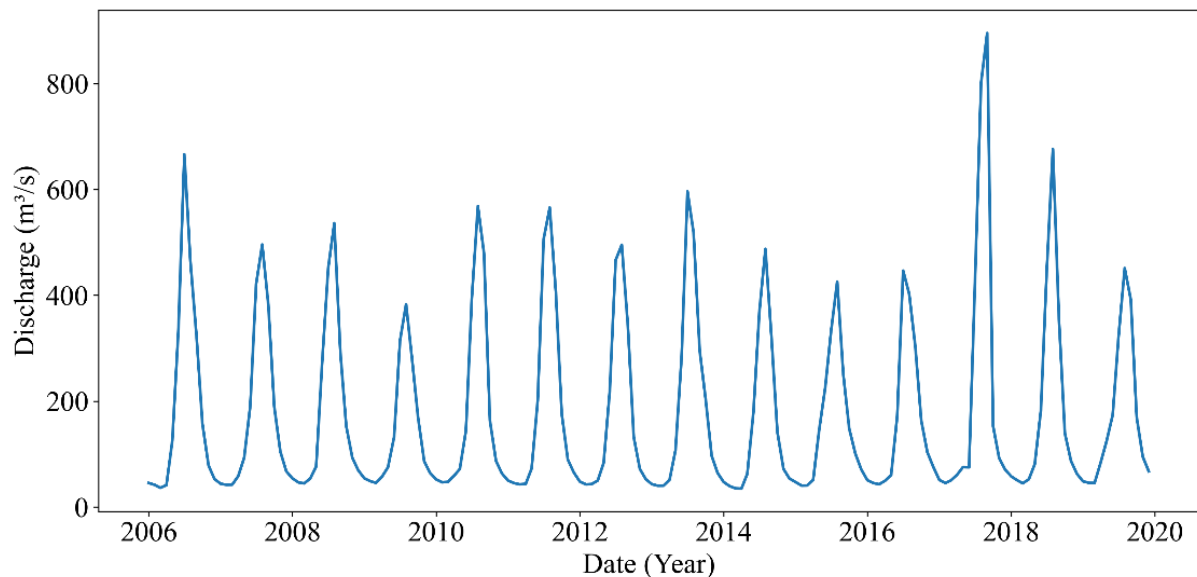


Figure 4.4: Observed monthly streamflow at Trishuli River (Betrawati Station), 2006–2020.

The Betrawati gauging station captures the aggregate flow of the upper Trishuli Basin (including the Chilime subbasin) and exhibits a pronounced monsoonal pattern with summer high flows and winter low flows.

Using the calibrated SWAT+ model, the simulated streamflow for the Chilime sub-basin was analyzed for the same period (2006–2020) to characterize its seasonal behavior. The Chilime River’s simulated flow shows a clear seasonality that mirrors the expected pattern for a high-altitude Himalayan catchment. During the pre-

monsoon spring months (March–May), flows begin to rise moderately, likely supported by snowmelt from the upper elevations of the Chilime Basin. The highest discharges are produced in the monsoon season (June–September) when intense rainfall combines with ongoing meltwater contributions, yielding pronounced peak flows much like those observed in the larger Trishuli River. In the post-monsoon autumn and winter period (October–February), the model indicates sustained low baseflows as precipitation tapers off and temperatures drop, causing hydrological inputs to be stored as snowpack. This seasonal streamflow pattern for Chilime – modest increases in spring, sharp peaks in summer, and very low flows in winter – is consistent with the hydro-climatic regime of snow-fed Himalayan tributaries. It demonstrates that the SWAT+ model effectively captures the dual influence of snowmelt and monsoonal rainfall in the Chilime Basin. Overall, the physically-based simulation provides confidence that the Chilime River’s flow regime is being represented realistically. These results establish a credible baseline of present-day flow dynamics in the Chilime Basin, against which future climate change impacts can be compared and assessed.

4.2 Model Calibration and Validation

4.2.1 Calibration and Validation overview

The SWAT+ model was calibrated and validated using observed streamflow data from the Trishuli River at Betrawati Station, located downstream of the Chilime sub-basin. As the Chilime River is a tributary within the Trishuli Basin, and direct streamflow data at the Chilime outlet is unavailable, model calibration at Betrawati provides a valid basis for simulating discharge in the upstream Chilime catchment. The model was run for a historical simulation period from 2006 to 2020, with the following split:

- Calibration period: 2007–2016
- Validation period: 2017–2019

These periods were selected to ensure adequate representation of both monsoon peak flow and dry-season baseflow, capturing interannual hydrological variability under current climatic conditions.

Calibration and validation were performed using the SWAT⁺ Toolbox, which provides integrated tools for sensitivity analysis, parameter adjustment, and performance evaluation. After iterative simulations and parameter tuning, the model produced reliable outputs consistent with observed trends.

4.2.2 Performance Metrics and Evaluation

Quantitative performance was assessed using standard statistical indices, including:

- Coefficient of Determination (R^2)
- Nash–Sutcliffe Efficiency (NSE)
- Percent Bias (PBIAS)
- Root Mean Square Error (RMSE)
- Mean Squared Error (MSE)
- Kling–Gupta Efficiency (KGE)

The model performance during both calibration and validation periods was satisfactory, with all key metrics exceeding the recommended thresholds for data-scarce, snow-fed Himalayan catchments.

Table 4.1: SWAT⁺ Model Performance Metrics for Calibration and Validation Periods

Period	R^2	NSE	PBIAS (%)	RMSE (m^3/s)	MSE	KGE
Calibration (2007–2016)	0.563	0.563	-4.53	104.57	10,933.97	0.765
Validation (2017–2019)	0.685	0.685	+10.69	94.04	8,844.35	0.810

The model effectively captured seasonal discharge patterns, particularly monsoon peak flows and winter low flows. The low bias ($\pm 10\%$), NSE > 0.5 , and KGE > 0.75 indicate a strong match between simulated and observed streamflow. These values are considered satisfactory for high-altitude regions, where sparse monitoring and snowmelt processes introduce additional modeling complexity.

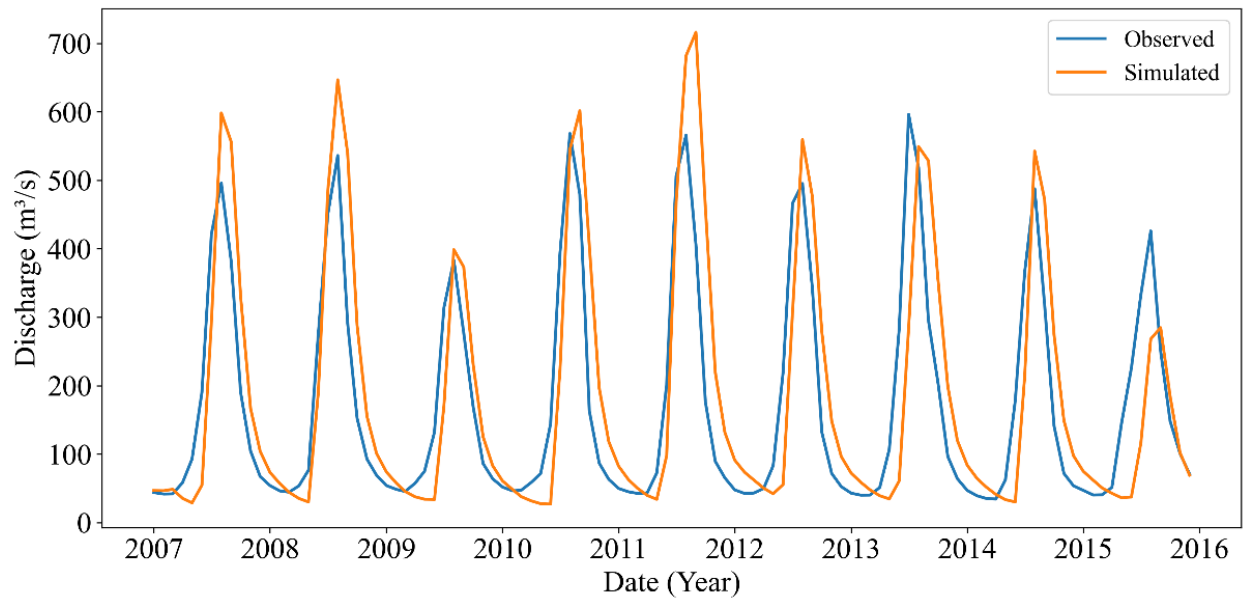


Figure 4.5: Observed vs. Simulated Streamflow During Calibration (2007–2016)
(The hydrograph shows alignment between modeled and observed discharge, with good agreement in both timing and magnitude of flow events during the calibration period.)

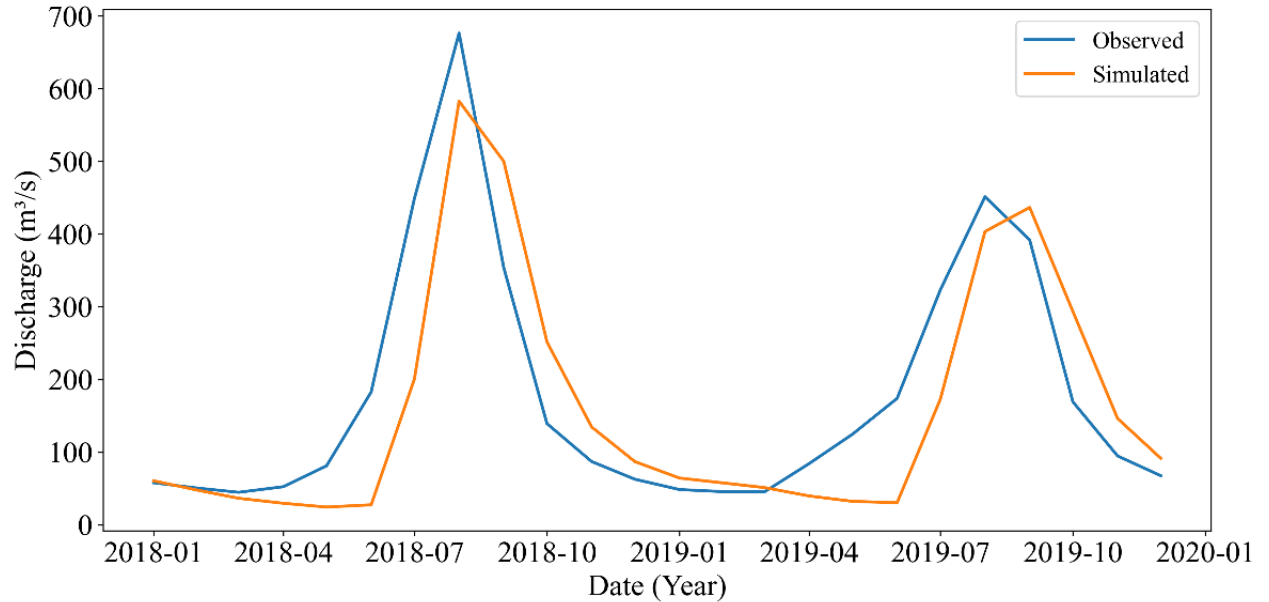


Figure 4.6: Observed vs. Simulated Streamflow During Validation (2017–2019) (The model demonstrates continued reliability in simulating flow dynamics outside the calibration window, with minimal deviation in monsoon peaks and dry-season baseflows.)

4.2.3 Interpretation and Applicability

Despite the limited ground-based snowmelt data and challenges inherent in mountainous terrain, the SWAT⁺ model demonstrated strong performance in simulating the hydrology of the Trishuli Basin. The spatially distributed model structure allowed for the extraction of reliable streamflow data for the Chilime sub-basin, which forms the basis for future climate impact assessments.

The validation confirms the model’s robustness and applicability for streamflow forecasting in Himalayan sub-catchments. Given its ability to reproduce observed flow patterns with satisfactory statistical performance, the calibrated model is considered suitable for simulating future hydrological responses under different climate scenarios in the Chilime River Basin.

4.3 Climate Projection and Bias Correction

This section presents the procedures and outcomes of bias correcting the climate projections from the CMIP6 ensemble and discusses the future trends of temperature and precipitation under two scenarios—SSP2-4.5 and SSP5-8.5—specifically for the Chilime River Basin.

4.3.1 Bias Correction Methods and Ensemble Generation

To improve the accuracy of climate projections over the complex terrain of the Chilime River Basin, bias correction was applied to daily outputs from thirteen Global Climate Models (GCMs) under the CMIP6 framework: ACCESS-CM2, ACCESS-ESM1-5, BCC-CSM2-MR, CanESM5, EC-Earth3, EC-Earth3-Veg, INM-CM4-8, INM-CM5-0, MPI-ESM1-2-HR, MPI-ESM1-2-LR, MRI-ESM2-0, NorESM2-LM, and NorESM2-MM. Temperature correction was performed using the Linear Scaling method based on daily observed maximum and minimum values from the Dhunche station. For precipitation, Quantile Mapping was employed using a merged baseline dataset from the Dhunche and Thamachit stations. Details of the CMIP6 models, including atmospheric resolution and modelling institutes, are presented in Appendix II.

These techniques were selected to address systematic biases inherent in raw GCM outputs, which often arise from coarse spatial resolution and inadequate representation of local topography (Mishra, Bhatia, & Tiwari, 2020; Eyring et al., 2016). Following correction, the outputs from all thirteen models were combined into a Multi-Model Mean (MMM) ensemble. Ensemble averaging is widely recommended for hydroclimatic analysis in high-altitude basins due to its capacity to reduce inter-model variability and improve projection reliability (Thrasher et al., 2012; Teutschbein & Seibert, 2012).

The entire workflow was executed using Python to ensure statistical consistency in bias correction and data harmonisation, while QGIS was used for the spatial processing of topographic and climatic datasets. In addition, to account for the altitudinal differences between GCM grid elevations and the Chilime Basin's actual terrain, a temperature lapse rate correction of 6.5°C per 1000 metres was applied. This

adjustment ensured the spatial consistency of thermal inputs across the steep elevation gradients in the basin, thereby improving snowmelt representation and the hydrological response in subsequent SWAT+ simulations.

4.3.2 Comparison of Raw vs. Corrected Climate Data

Bias correction was an essential step to enhance the accuracy and reliability of climate model outputs prior to their application in hydrological modeling. The raw outputs from CMIP6 models often exhibit significant systematic deviations from observed climatic conditions due to coarse resolution and generalized representation of regional processes. This section evaluates the effectiveness of the bias correction procedures applied to both precipitation and temperature datasets in the Chilime River Basin.

Precipitation Bias and Correction Performance

Figures 4.7 and 4.8 illustrate the model-wise distribution of raw and corrected rainfall data for the historical period (2000–2020) under the SSP2-4.5 and SSP5-8.5 scenarios, respectively. The raw data from the thirteen GCMs showed notable underestimation of rainfall intensity, with most models failing to reproduce the observed median and interquartile range of precipitation. Following Quantile Mapping correction, the boxplots demonstrate a substantial improvement in alignment with observed data. The corrected datasets reflect better central tendencies and reduced dispersion, indicating improved internal consistency and representativeness across models.

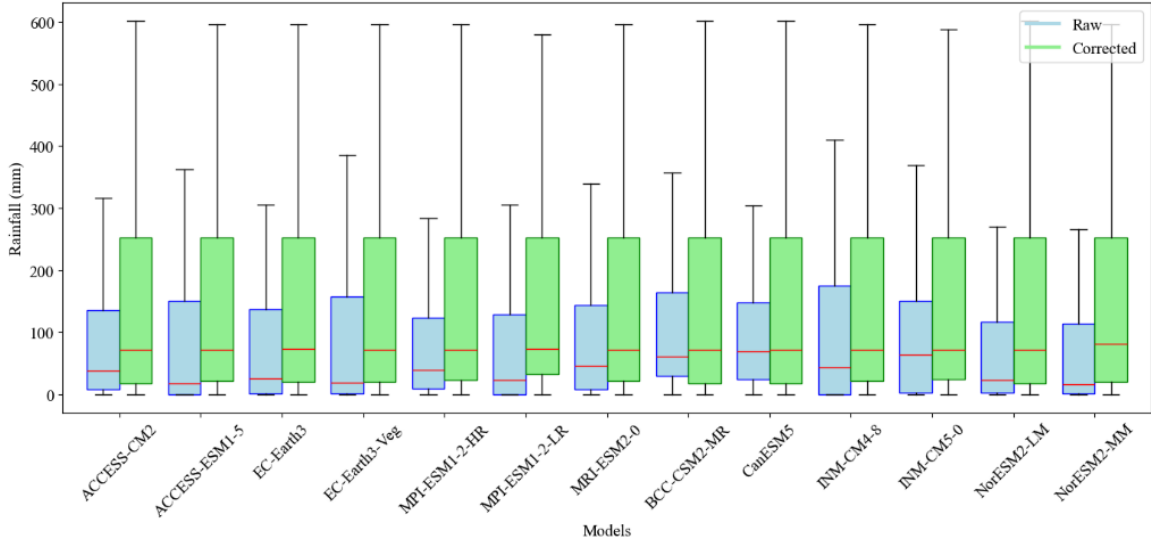


Figure 4.7: Model-wise boxplot comparison of raw and corrected rainfall data under SSP2-4.5 scenario (2000–2020)

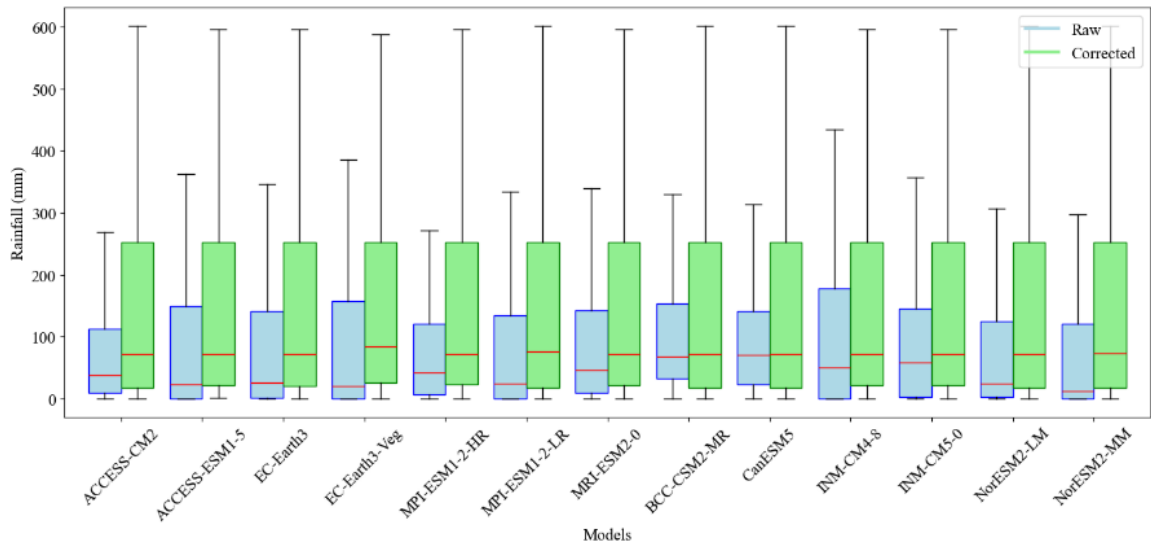


Figure 4.8: Model-wise boxplot comparison of raw and corrected rainfall data under SSP5-8.5 scenario (2000–2020)

Further validation is provided in Figures 4.9 and 4.10, which compare the ensemble mean of raw and corrected rainfall outputs against observed values from the Dhunche and Thamachit stations. Under both SSP scenarios, the raw ensemble significantly underrepresents peak monsoon rainfall and over-smooths the annual cycle. In contrast, the bias-corrected ensemble successfully replicates the seasonal pattern and

magnitude of observed precipitation, particularly during the monsoon months (June–September), thereby confirming the efficacy of the applied correction.

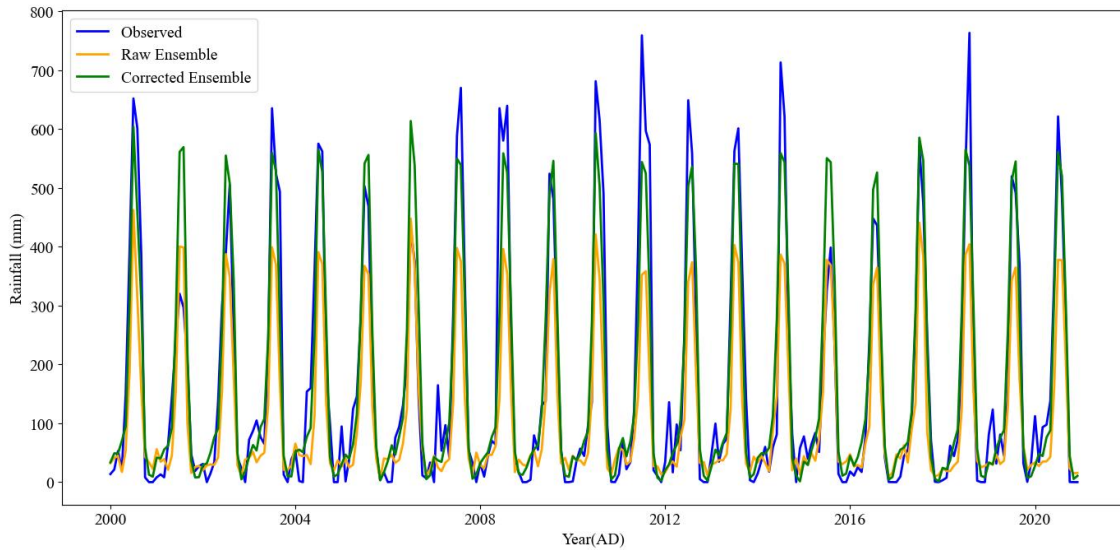


Figure 4.9: Comparison of observed, raw ensemble, and corrected ensemble rainfall (2000–2020) under SSP2-4.5 scenario

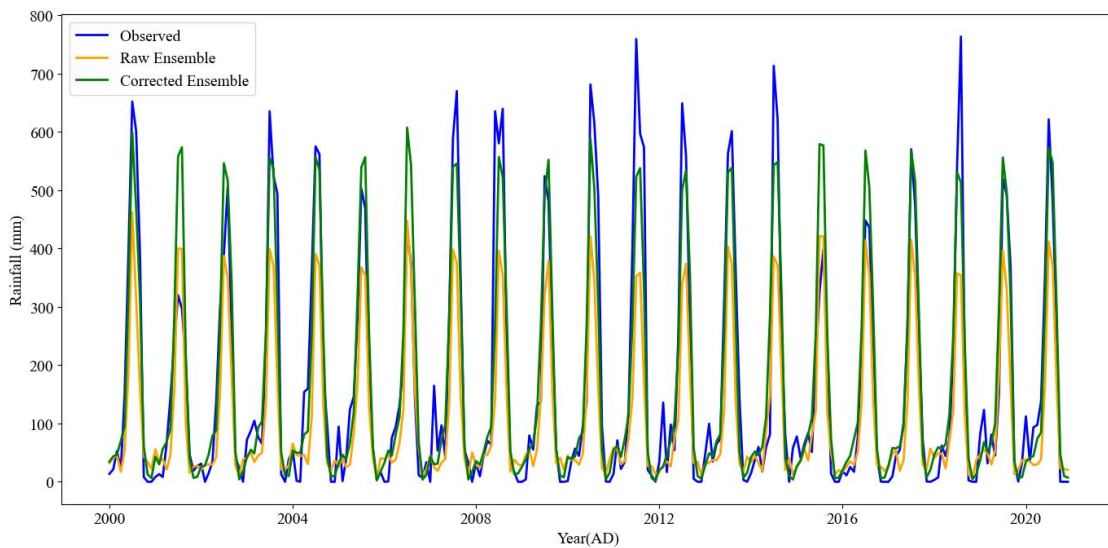


Figure 4.10 Comparison of observed, raw ensemble, and corrected ensemble rainfall (2000–2020) under SSP5-8.5 scenario

Temperature Bias and Correction Performance

Temperature projections from raw GCM outputs also exhibited a consistent cold bias, particularly in high-elevation regions like Chilime. As shown in Figures 4.11 and 4.12, raw ensemble temperature data underestimated monthly values compared to observations during 2000–2020 under both emission scenarios. The discrepancy was most pronounced during winter months, indicating inadequate representation of elevation-dependent warming and valley cold air pooling.

The application of the linear scaling method, combined with a lapse rate adjustment of 6.5 °C per 1,000 m, significantly improved alignment with observed temperature records. Post-correction ensemble outputs closely track observed seasonal fluctuations and mean values, especially during the pre-monsoon and monsoon periods, when temperature variability critically influences snowmelt and evapotranspiration.

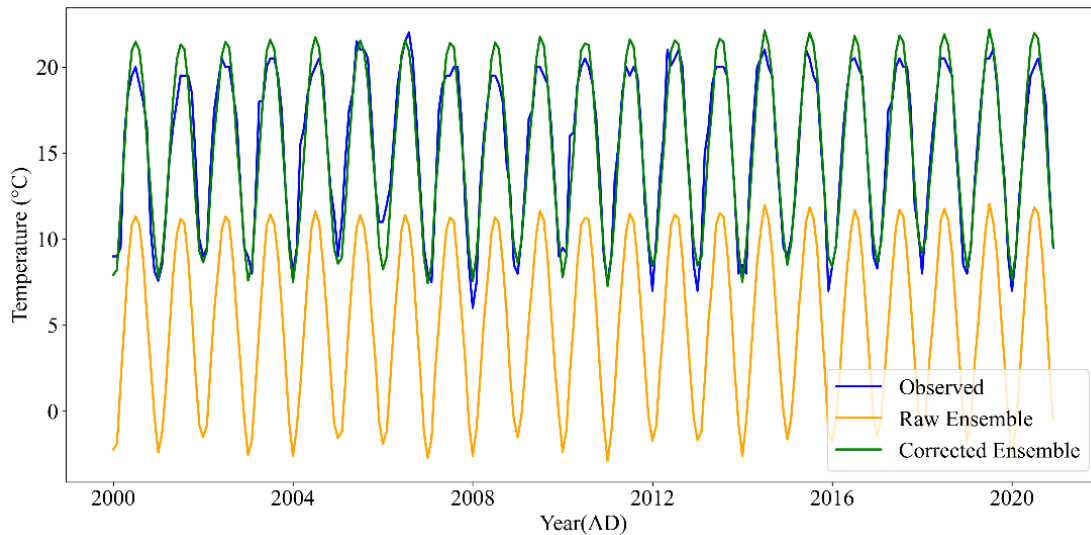


Figure 4.11: Monthly temperature time series for 2000–2020 under SSP2-4.5 showing observed, raw ensemble, and corrected ensemble data

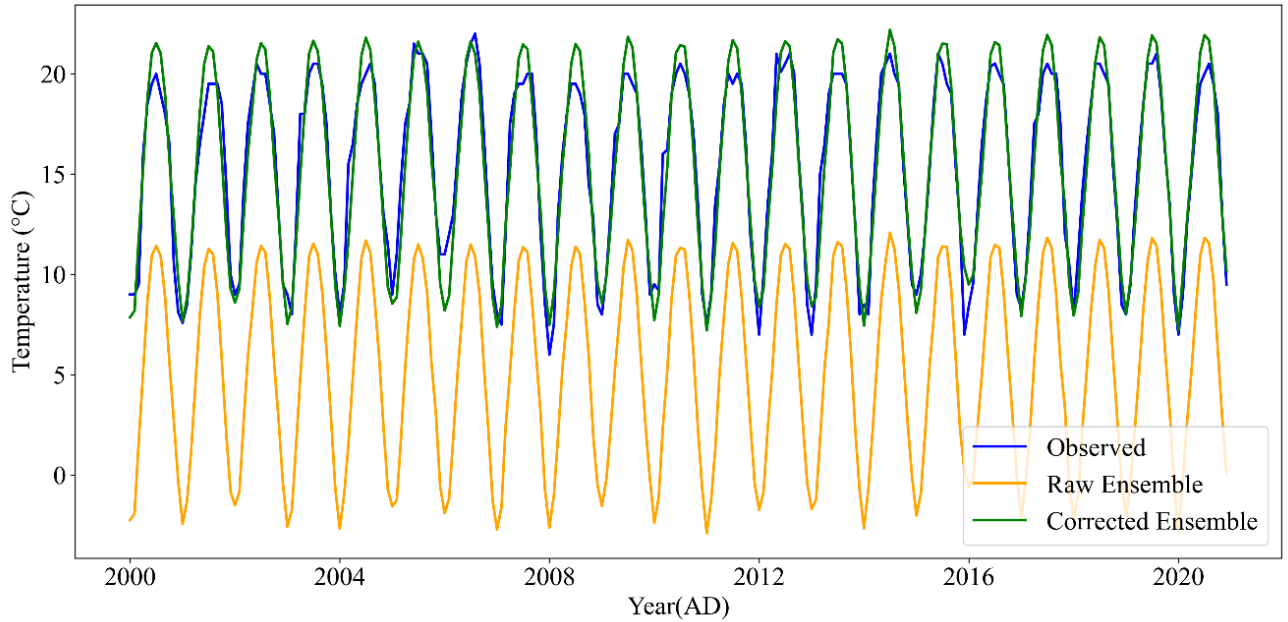


Figure 4.12: Monthly temperature time series for 2000–2020 under SSP5-8.5 showing observed, raw ensemble, and corrected ensemble data

Model-specific performance of the bias correction for temperature is visualised in Figures 4.13 and 4.14, which present boxplots of raw versus corrected outputs across all thirteen models for the historical period. Under SSP2-4.5 and SSP5-8.5 respectively, the corrected datasets demonstrate reduced spread and improved central alignment, underscoring the effectiveness of the applied method in harmonizing the ensemble distribution with the observed climatology.

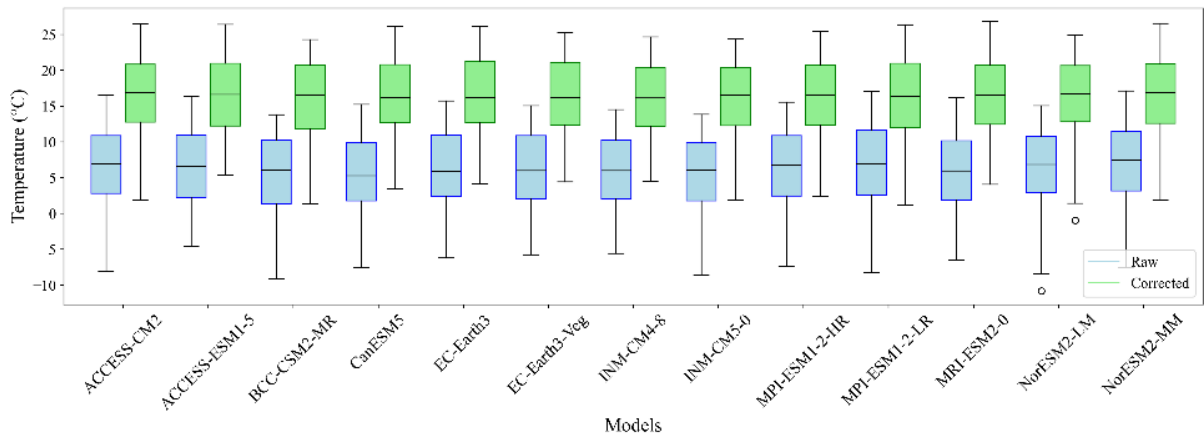


Figure 4.13: Boxplot comparison of raw vs. corrected temperature data for 13 GCMs under SSP2-4.5 (2000–2020)

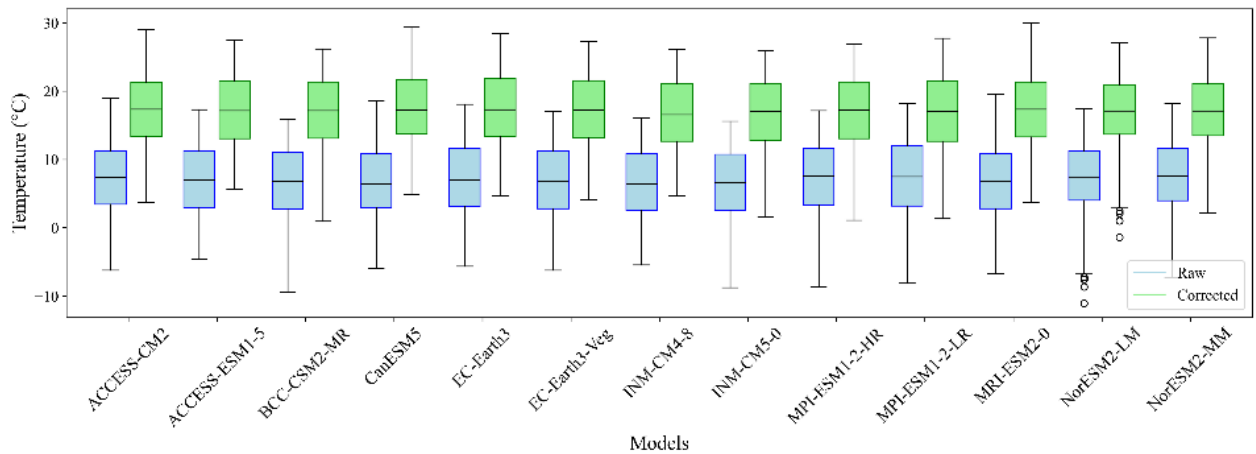


Figure 4.14: Boxplot comparison of raw vs. corrected temperature data for 13 GCMs under SSP5-8.5 (2000–2020)

Implications for Climate Impact Assessment

The enhanced agreement between corrected and observed datasets ensures the integrity of subsequent hydrological modeling and climate impact assessments. In particular, accurate representation of rainfall extremes and seasonal temperature patterns is critical for modeling snowmelt contributions, simulating monsoon-driven flows, and assessing future water availability. The consistent improvements across multiple GCMs also validate the choice of correction techniques—Quantile Mapping for precipitation and Linear Scaling with lapse rate adjustment for temperature—as appropriate for high-altitude basins such as Chilime. These adjustments provide a scientifically robust foundation for projecting streamflow responses under future climate scenarios.

4.3.3 Projected Temperature and Precipitation Trends under SSP2-4.5 and SSP5-8.5

Future climate projections for the Chilime River Basin indicate significant warming and intensification of precipitation patterns throughout the 21st century. Bias-corrected and lapse-adjusted outputs from thirteen CMIP6 Global Climate Models (GCMs) were analysed for the mid-century (2025–2050) and late-century (2051–

2100) periods under two Shared Socioeconomic Pathways: SSP2-4.5 (moderate emissions) and SSP5-8.5 (high emissions). This section presents the long-term trends and intra-annual variability of temperature and precipitation, with implications for hydroclimatic extremes and water availability.

Annual Precipitation Trends

Figures 4.15 and 4.16 display the projected annual precipitation for the Chilime River Basin from 2020 to 2100 under SSP2-4.5 and SSP5-8.5, respectively. Both scenarios reveal an increasing trend, with a steeper rise under SSP5-8.5. While SSP2-4.5 indicates a gradual increase of approximately 15–20% by the end of the century, SSP5-8.5 projects a more pronounced escalation, reaching over 2,500 mm/year in the late 21st century.

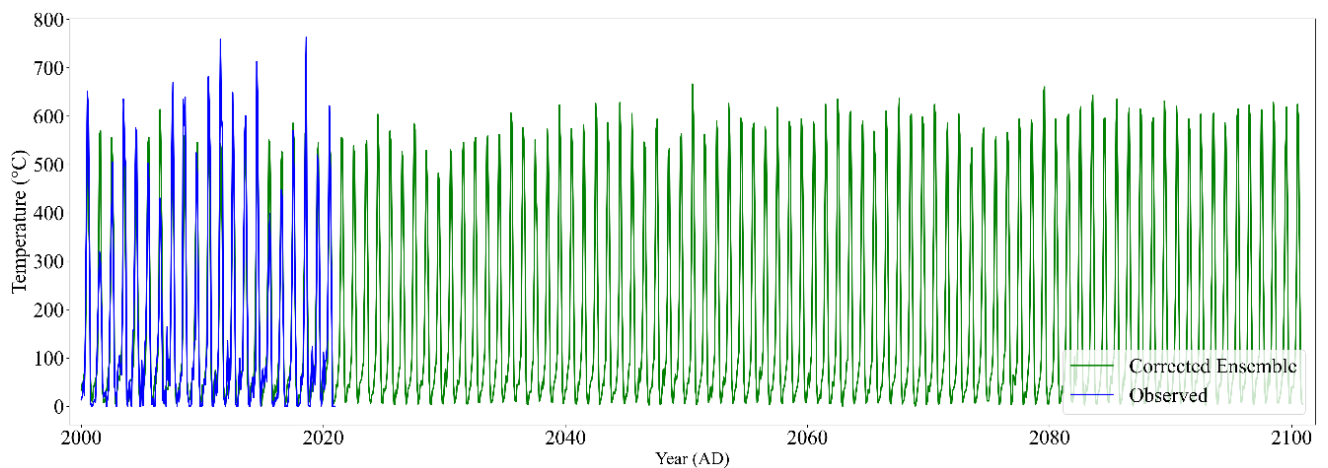


Figure 4.15: Projected corrected ensemble rainfall and observed rainfall (2000–2100) under SSP2-4.5 scenario

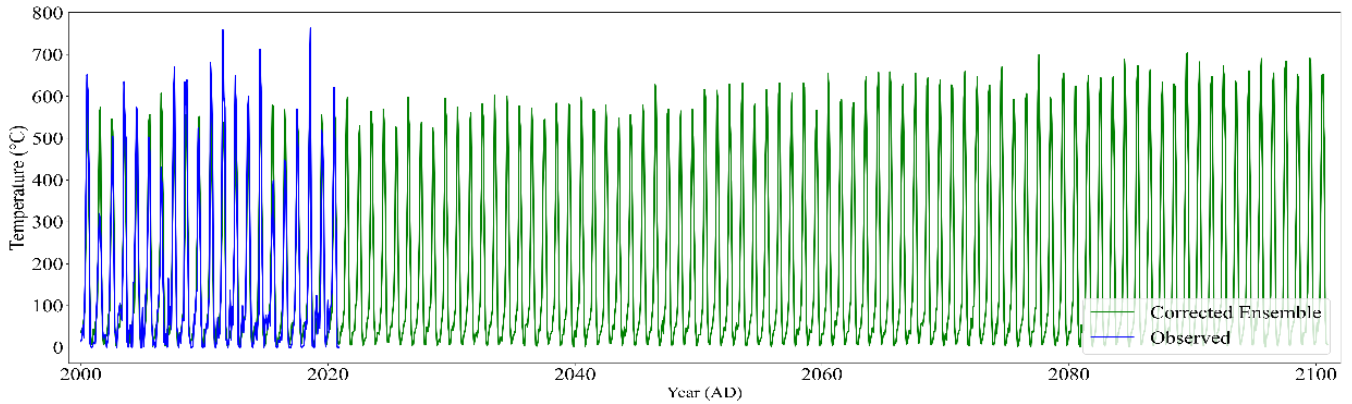


Figure 4.16: Projected corrected ensemble rainfall and observed rainfall (2000–2100) under SSP5-8.5 scenario

These trends are further clarified in Figure 4.17, which compares actual and smoothed precipitation trajectories. The high-emission scenario shows higher interannual variability and potential for more extreme rainfall years, suggesting increased risks of flood events in monsoon-dominated months.

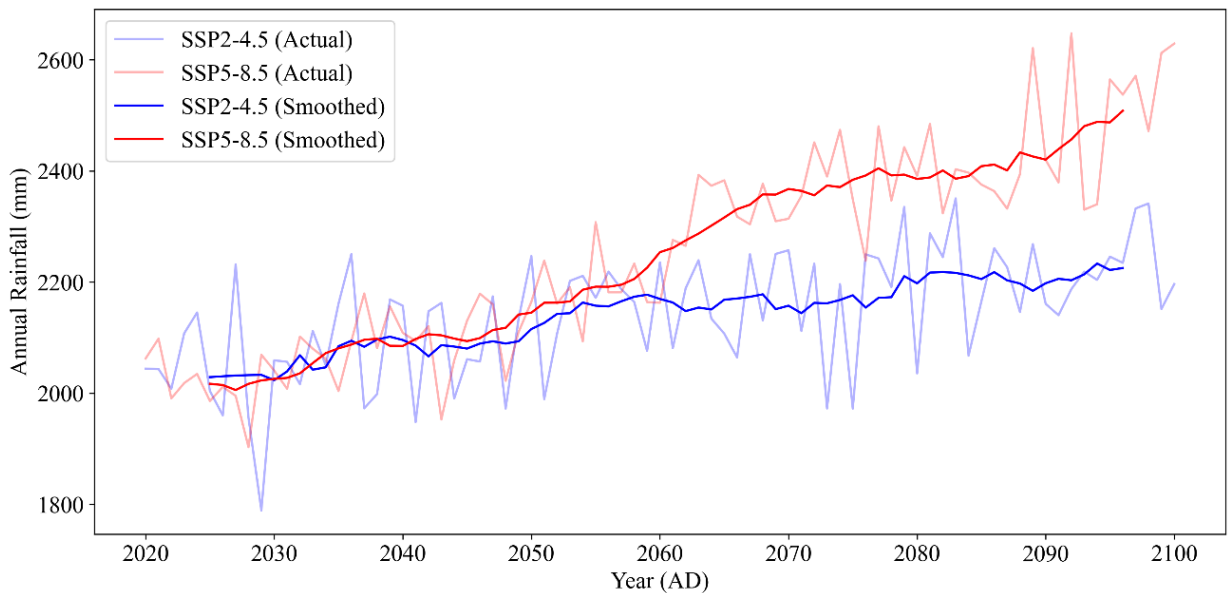


Figure 4.17: Time series of actual and smoothed annual rainfall under SSP2-4.5 and SSP5-8.5 (2020–2100)

Figure 4.18 compares decadal averages across three time windows (2010–2020, 2050–2060, and 2090–2100). A steady progression is observed under SSP2-4.5, while

SSP5-8.5 shows a sharper increase—indicative of the influence of greenhouse gas accumulation on precipitation intensification.

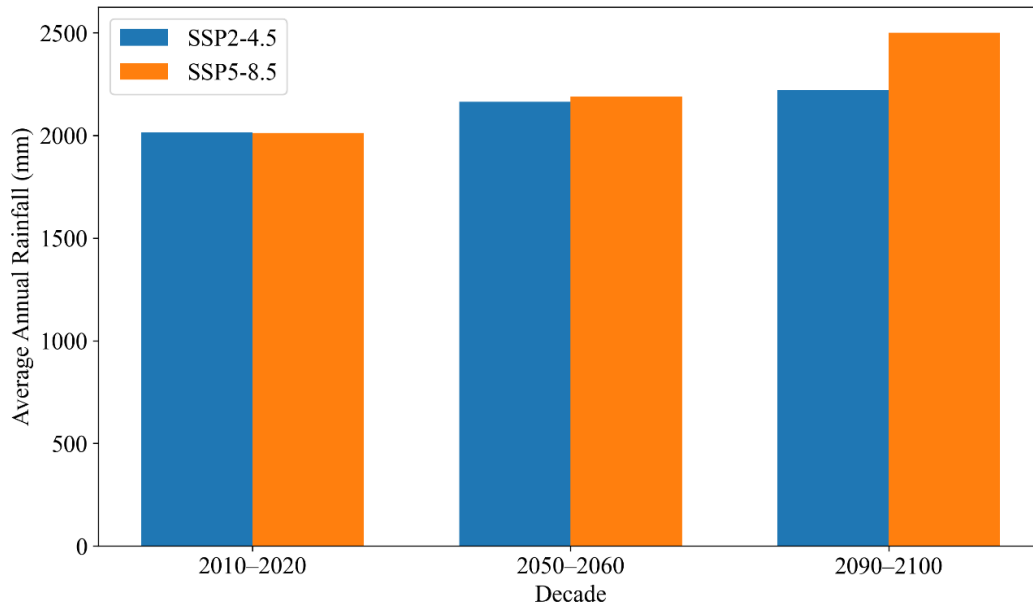


Figure 4.18: Decadal average annual rainfall under SSP2-4.5 and SSP5-8.5 for 2010–2020, 2050–2060, and 2090–2100

Seasonal and Monthly Rainfall Variability

Seasonal changes are shown in Figure 4.19, where total precipitation is presented for the winter, pre-monsoon, monsoon, and post-monsoon periods in 2020, 2050, and 2100. Monsoon rainfall remains dominant but increases significantly under SSP5-8.5, accompanied by a noticeable rise in post-monsoon totals—suggesting an extension of the wet season.

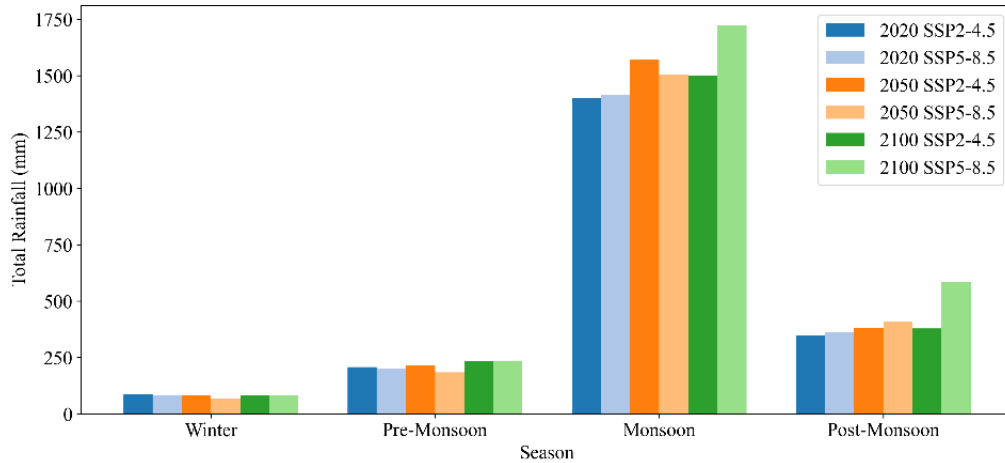


Figure 4.19: Seasonal total rainfall (Winter, Pre-Monsoon, Monsoon, Post-Monsoon) for 2020, 2050, and 2100 under SSP2-4.5 and SSP5-8.5

Figure 4.20 details the monthly rainfall distribution. The peak remains centered in July, but monthly values during June and September rise, indicating a broader monsoonal window by 2100 under the high-emission pathway. A modest rise in pre-monsoon precipitation is also evident.

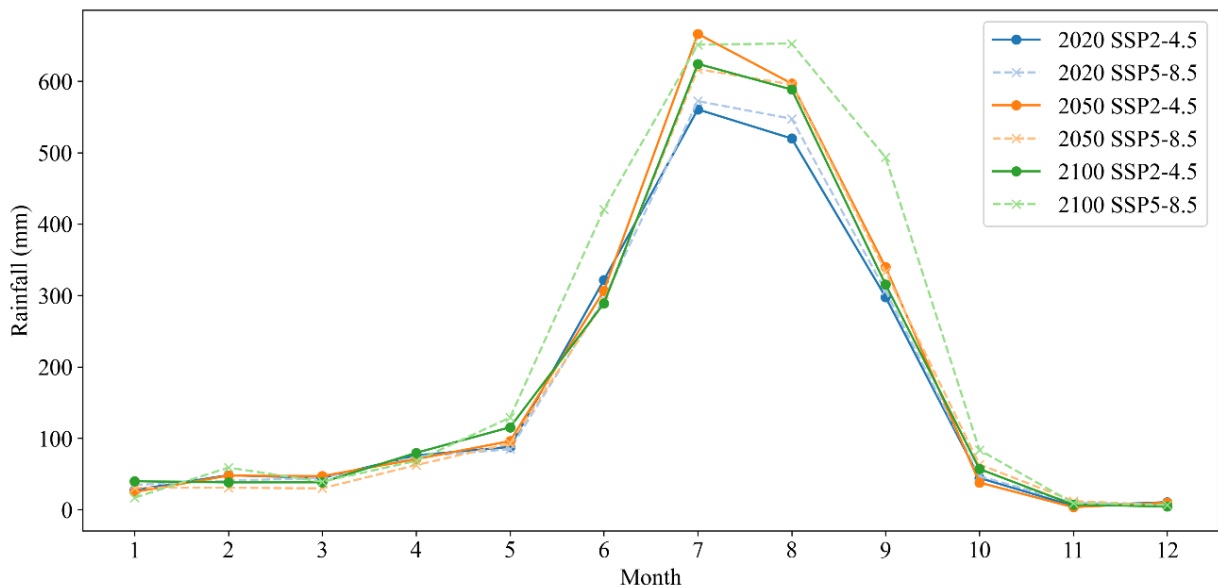


Figure 4.20: Monthly average rainfall distribution for 2020, 2050, and 2100 under SSP2-4.5 and SSP5-8.5

Projected Temperature Trends

Corrected temperature projections show a robust and consistent warming trend across both scenarios. Figure 4.21 (SSP2-4.5) and Figure 4.22 (SSP5-8.5) illustrate the upward trajectory in annual mean temperature, with SSP5-8.5 yielding faster warming, exceeding 18 °C by the end of the century in lower elevation zones.

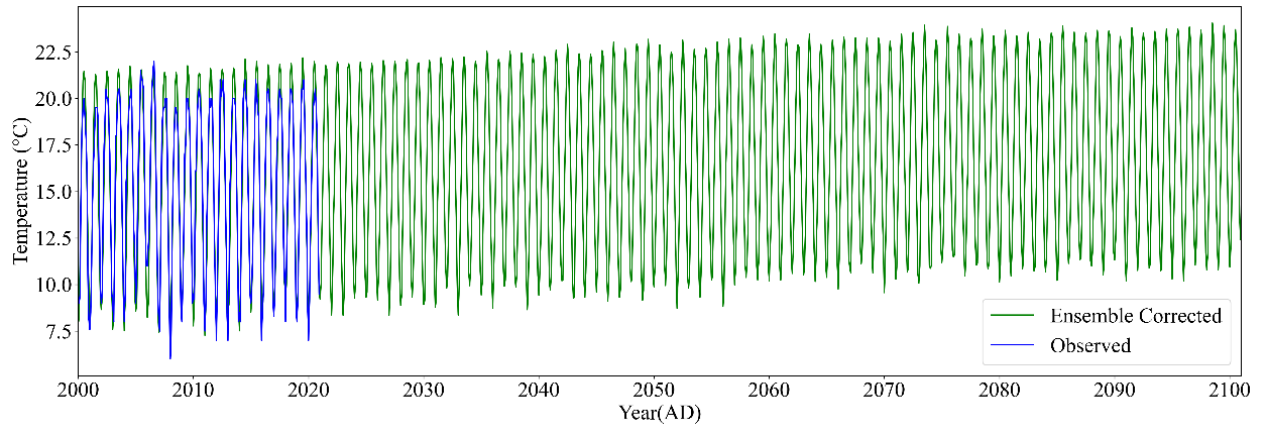


Figure 4.21: Time series of ensemble corrected temperature and observed values (2000–2100) under SSP2-4.5

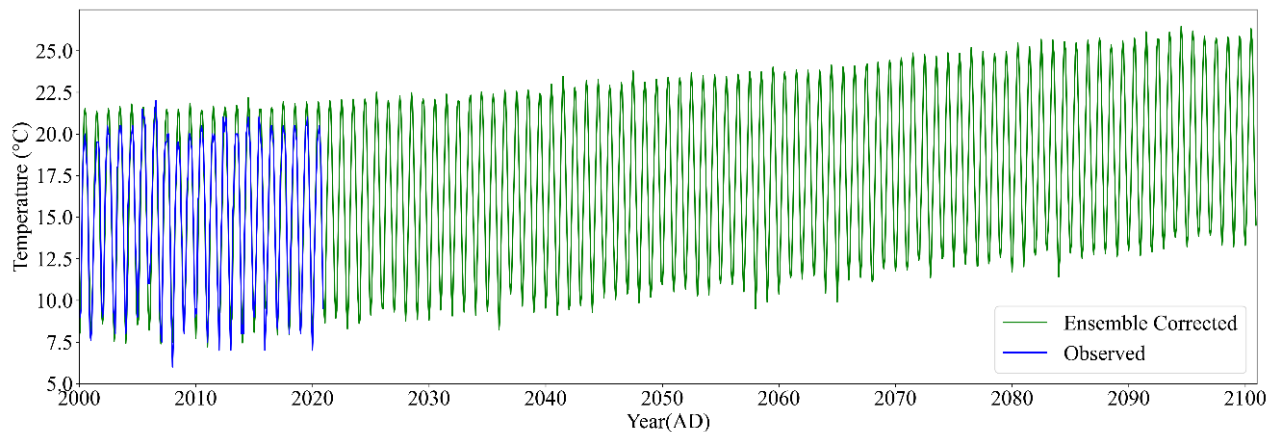


Figure 4.22: Time series of ensemble corrected temperature and observed values (2000–2100) under SSP5-8.5

Annual mean temperatures for benchmark years (2020, 2050, and 2100) are compared in Figure 4.23. Under SSP2-4.5, the temperature increases moderately from ~12.5 °C in 2020 to ~14.5 °C by 2100. Under SSP5-8.5, the rise is steeper, surpassing 16.5 °C by century's end.

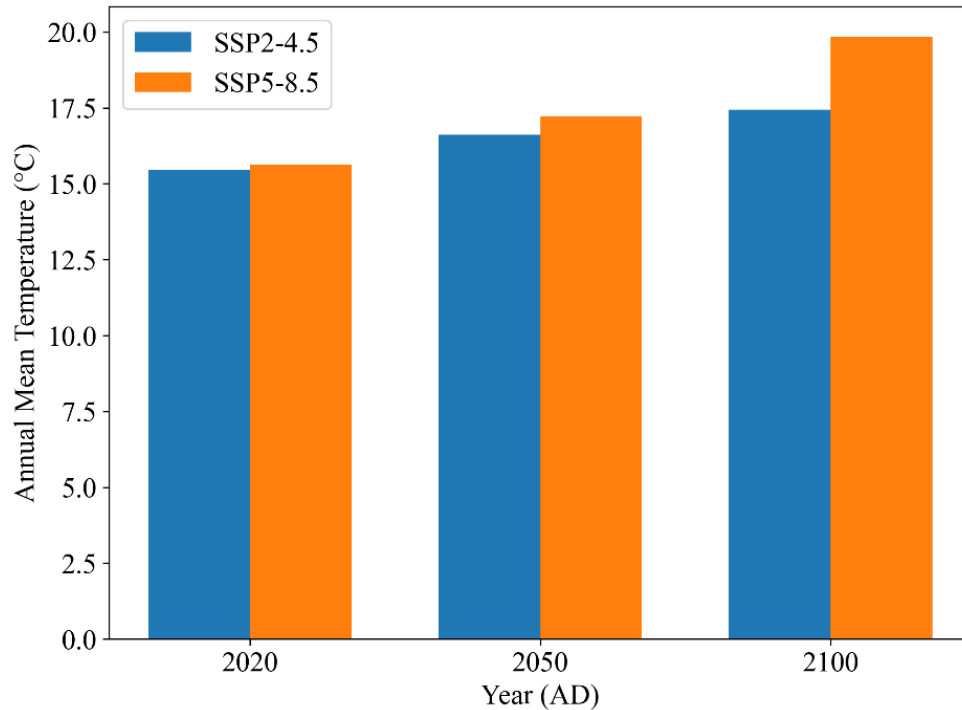


Figure 4.23: Comparison of mean annual temperature for 2020, 2050, and 2100 under SSP2-4.5 and SSP5-8.5 scenarios

Seasonal and Monthly Temperature Variability

Figure 4.24 presents seasonal mean temperatures, highlighting notable warming in all seasons—especially during the monsoon and post-monsoon. Winter temperatures increase sharply under SSP5-8.5, raising concerns over declining snowfall and altered snowmelt patterns.

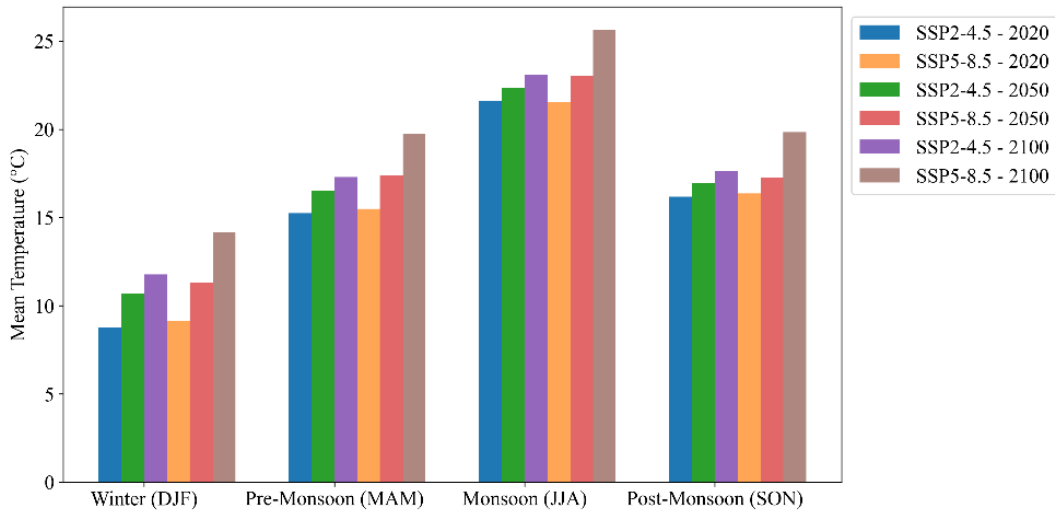


Figure 4.24: Seasonal mean temperature across 2020, 2050, and 2100 under SSP2-4.5 and SSP5-8.5 scenarios

Figure 4.25 demonstrates monthly distribution trends, showing an upward shift in all months. The summer months (May–August) record the highest increases, with July temperatures potentially exceeding 25 °C under SSP5-8.5 by 2100.

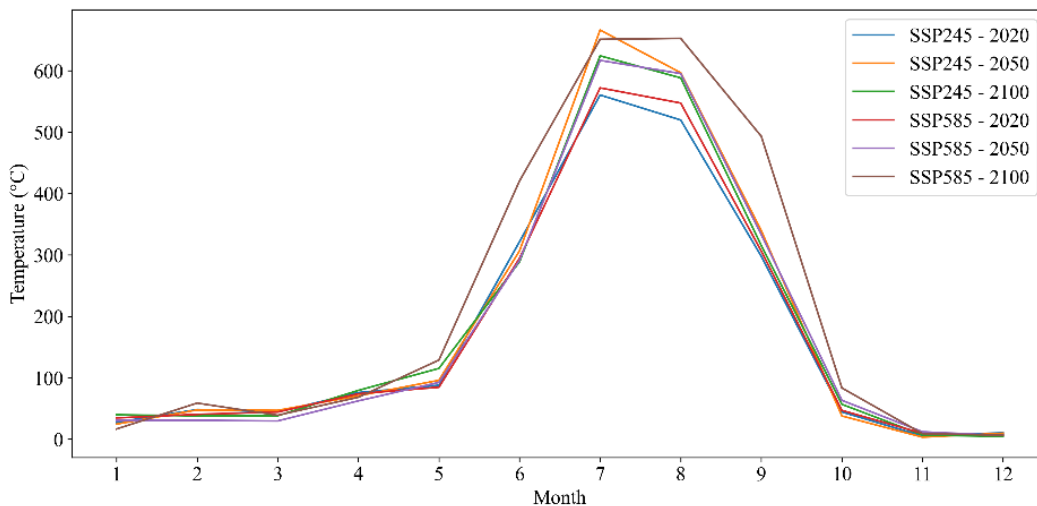


Figure 4.25: Monthly temperature distribution patterns for 2020, 2050, and 2100 under SSP2-4.5 and SSP5-8.5 scenarios

Spatial Distribution and Elevation-Sensitive Warming

Figure 4.26 visualizes the spatial distribution of lapse-adjusted annual mean temperatures across 2020, 2050, and 2100. In 2020, high-altitude zones remained below freezing, but by 2100 under SSP5-8.5, nearly the entire basin transitions to positive mean temperatures. The disappearance of sub-zero zones suggests major implications for snow accumulation, glacial melt, and dry-season streamflow in the Chilime Basin.

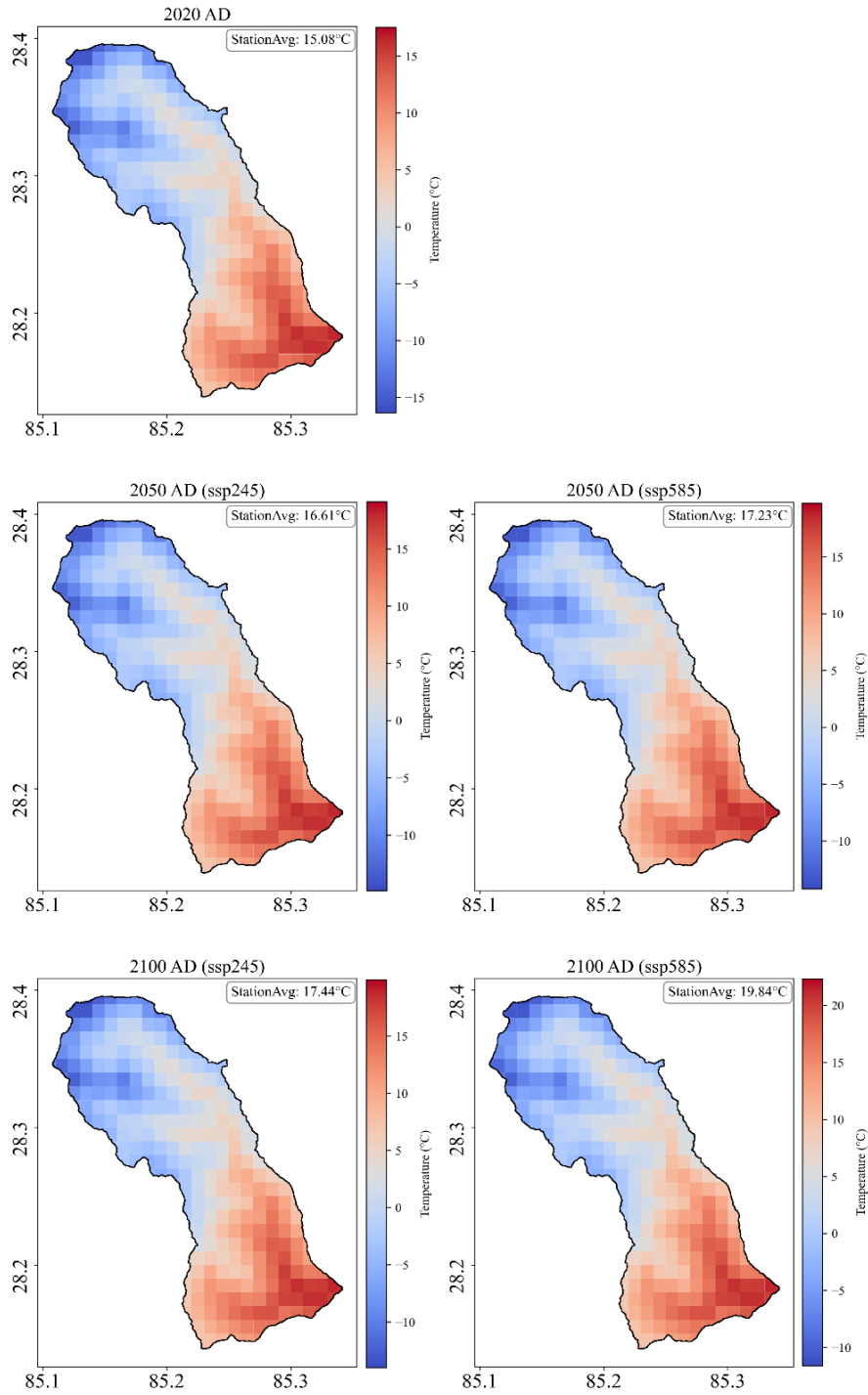


Figure 4.26: Spatial distribution of lapse rate-adjusted annual mean temperature in the Chilime River Basin for 2020, 2050, and 2100 under SSP2-4.5 and SSP5-8.5

In summary, the Chilime River Basin is projected to experience more intense rainfall and pronounced warming under future climate scenarios. These changes, particularly under SSP5-8.5, highlight increased risks of hydrological extremes, earlier snowmelt, and variability in seasonal water availability. Integrating these projections into hydrological and adaptation planning is critical to ensure the resilience of water resources, agriculture, and hydropower systems in this climate-sensitive region.

4.4 Future Streamflow Projections

This section presents the projected streamflow trends in the Chilime River Basin from 2002 to 2100 under two CMIP6 climate scenarios—SSP2-4.5 and SSP5-8.5. Using bias-corrected climate inputs in the SWAT+ model, the results capture monthly, seasonal, and long-term streamflow variations. Key comparisons are made across baseline (2020), mid-century (2040–2050), and end-century (2090–2100) to highlight evolving hydrological responses and identify potential risks under changing climate conditions.

4.4.1 Streamflow Projection under SSP2-4.5 (2025–2050 and 2051–2100)

This section presents projected streamflow patterns under the SSP2-4.5 scenario, a moderate-emissions pathway representing stabilization of greenhouse gas concentrations by the end of the 21st century. Bias-corrected ensemble climate projections from thirteen CMIP6 models were used as input to the calibrated SWAT+ model. Simulated streamflow responses for the Chilime River Basin were analyzed across two future periods: mid-century (2025–2050) and end-century (2051–2100).

Seasonal and Monthly Flow Patterns

The monthly distribution of projected streamflow (Figure 4.27) shows a pronounced seasonal regime, characteristic of monsoon-driven Himalayan basins. Discharge remains below 5 m³/s from January to May, begins rising in June, and peaks during August and September, where the median flow exceeds 25 m³/s. This demonstrates a continued dominance of monsoonal input under moderate climate change.

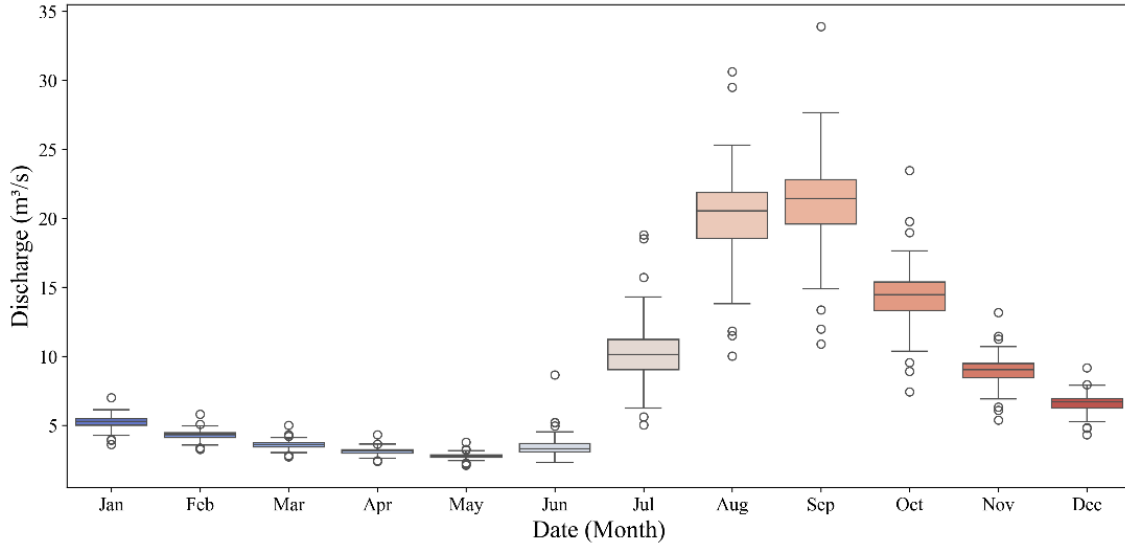


Figure 4.27: Monthly Boxplot of Projected Discharge (SSP2-4.5)

Long-Term Discharge Trends and Anomalies

Figure 4.28 presents the full streamflow time series from 2000 to 2100. While the seasonal pattern remains stable, there is a slight increase in peak discharges during late-century years. Anomaly detection (Figure 4.29) highlights several outlier events occurring after 2060, suggesting an increased occurrence of extreme discharge episodes under SSP2-4.5, although less frequent than in high-emission pathways.

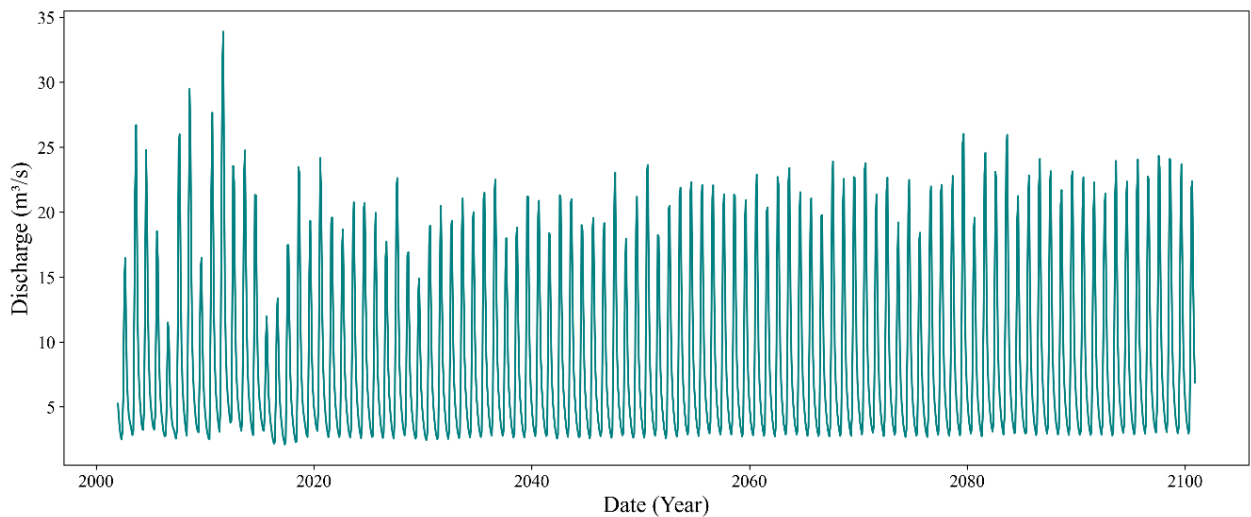


Figure 4.28: Simulated Monthly Streamflow (2000–2100) under SSP2-4.5

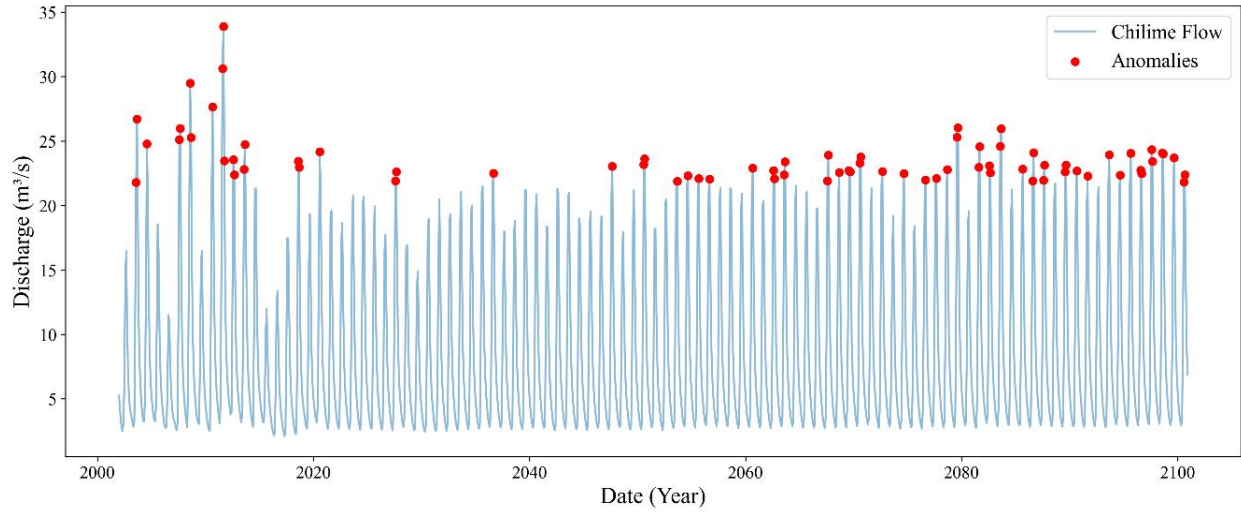


Figure 4.29: Anomaly Detection in Projected Flow

Moving Average and Decadal Change

To assess long-term changes, a 12-month moving average was applied to the streamflow time series (Figure 4.30). Results show a relatively stable pattern from 2000 to 2070, followed by a slight upward shift in the late-century period, reflecting potential intensification of the hydrological cycle driven by warming temperatures and increased rainfall.

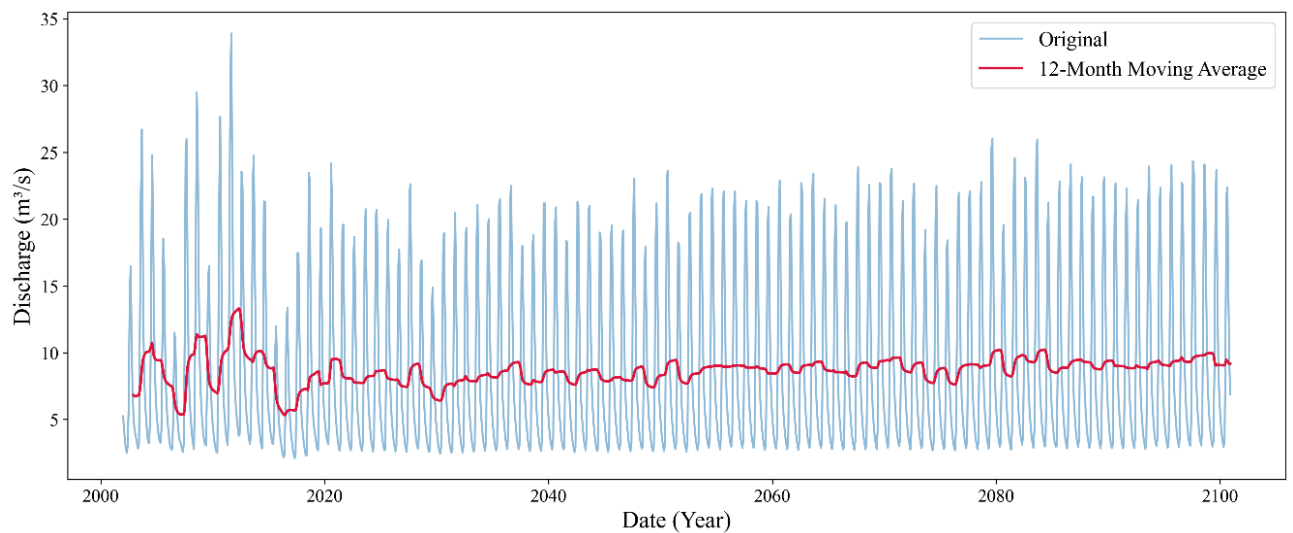


Figure 4.30: Streamflow with 12-Month Moving Average

Comparison of Mid- and End-Century Flow

Figure 4.31 compares average monthly flows for the periods 2040–2050 and 2090–2100. While the monsoon peak remains dominant, there is a modest increase in August and September flows in the end-century projection, suggesting slight intensification of rainfall and runoff.

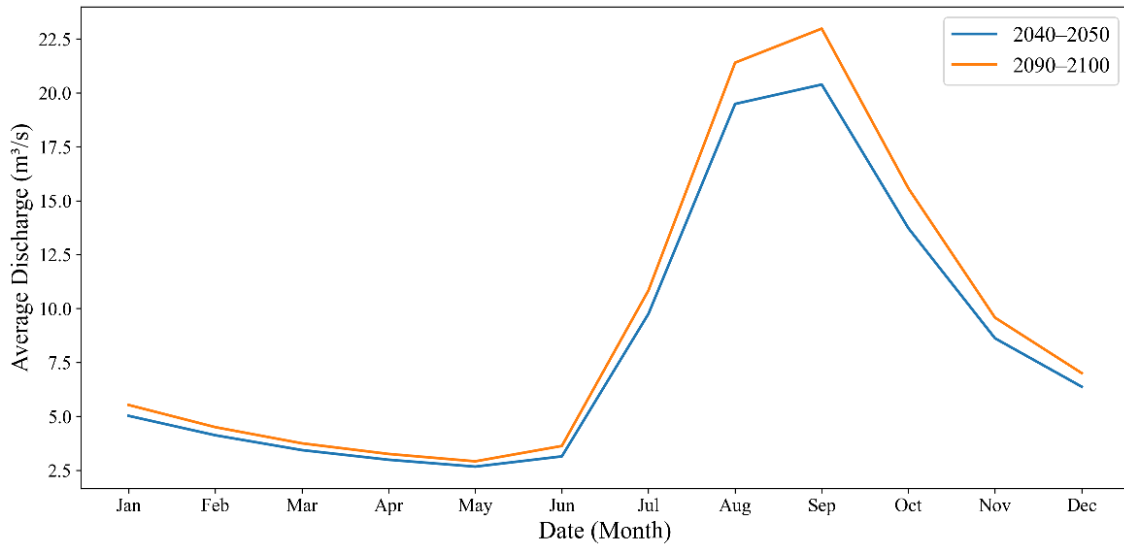


Figure 4.31: Monthly Mean Flow – Mid vs. End Century

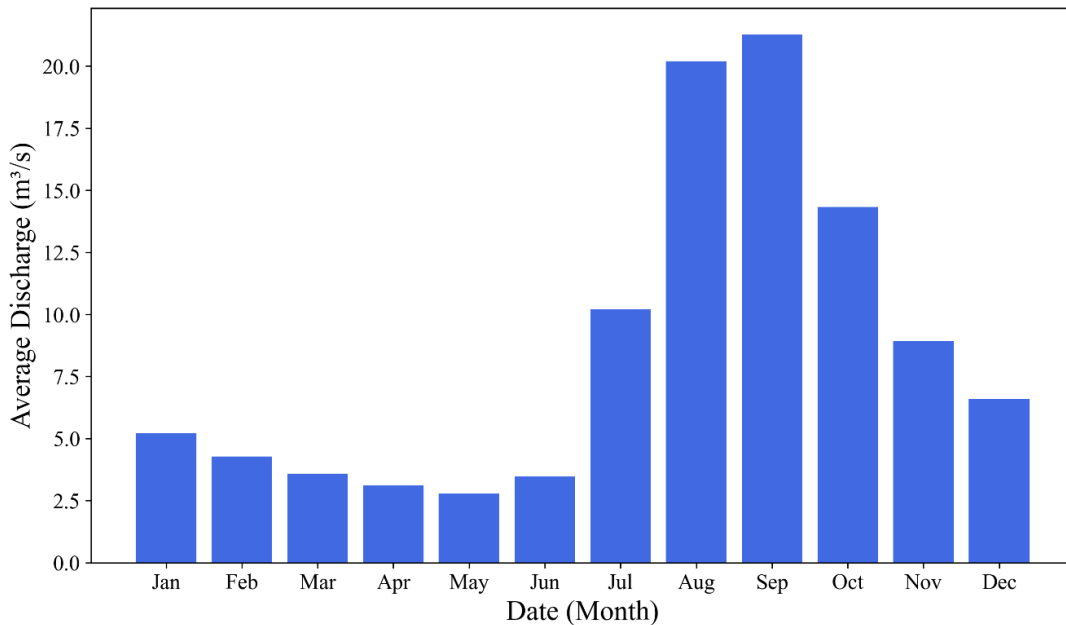


Figure 4.32: Seasonal Variation of Monthly Flow (2002–2100)

Summary Insight

Overall, under SSP2-4.5, the Chilime River Basin is projected to retain its strong monsoon-driven discharge pattern with modest increases in peak flow during the late 21st century. Hydrological anomalies may become slightly more frequent after 2060, but dry-season flows remain relatively unchanged. These trends suggest manageable impacts that can be addressed with forward-looking hydropower scheduling and seasonal storage strategies.

4.4.2 Streamflow Projection under SSP5-8.5 (2025–2050 and 2051–2100)

This section presents projected streamflow patterns under the SSP5-8.5 scenario, a high-emission pathway characterized by sustained fossil fuel use and minimal mitigation efforts. Climate forcing inputs were derived from bias-corrected outputs of thirteen CMIP6 global climate models. These projections were used to drive the calibrated SWAT⁺ model for the Chilime River Basin, with outputs analyzed for mid-century (2025–2050) and end-century (2051–2100) periods.

Seasonal and Monthly Flow Patterns

The monthly streamflow boxplot under SSP5-8.5 (Figure 4.33) reveals a strongly seasonal runoff regime, with very low flows from January to May and sharp peaks during the monsoon months. August and September show elevated median discharges exceeding 30 m³/s, with maximum values surpassing 35 m³/s. Compared to SSP2-4.5, this scenario exhibits a more intensified monsoon signal and greater runoff magnitude.

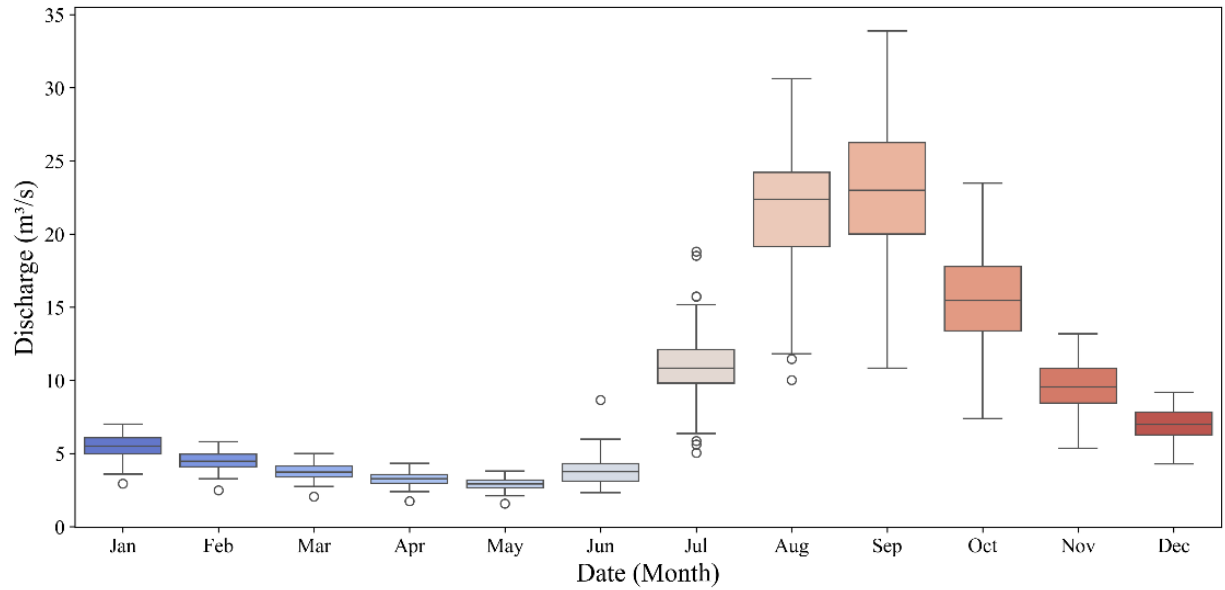


Figure 4.33: Monthly Boxplot of Projected Discharge (SSP5-8.5)

Time-Series Trends and Hydrological Extremes

The full projected streamflow series from 2000 to 2100 (Figure 4.34) demonstrates an upward trajectory in peak discharges, particularly after 2040. Anomaly detection (Figure 4.35) reveals a higher number and intensity of extreme flow events in the late century compared to SSP2-4.5. These results reflect an elevated risk of flood events due to amplified rainfall and runoff under high-emission scenarios.

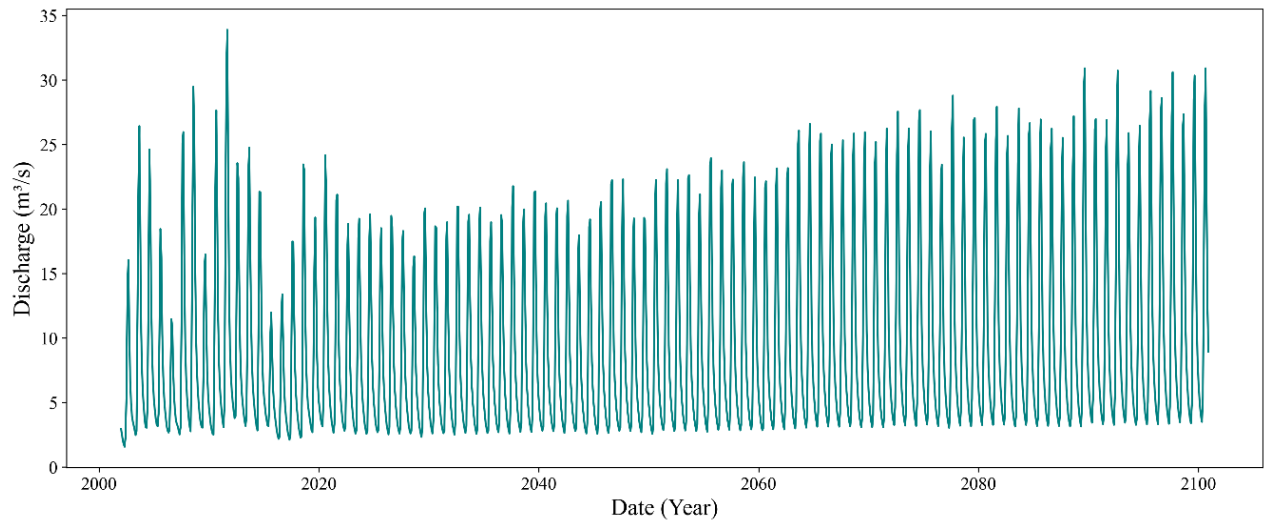


Figure 4.34: Simulated Monthly Streamflow (2000–2100) under SSP5-8.5

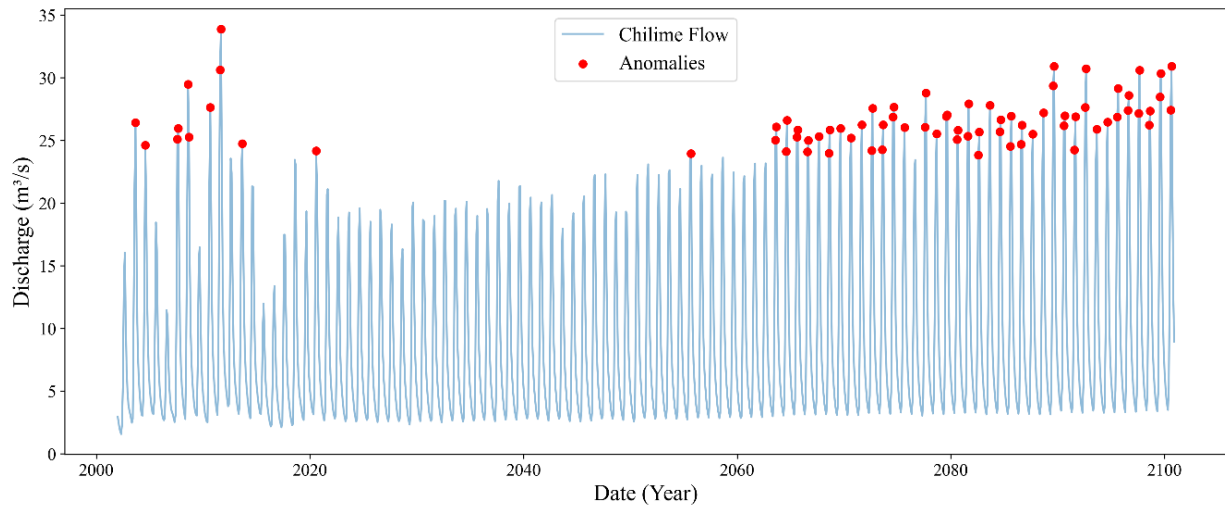


Figure 4.35: Anomaly Detection in Projected Flow

Long-Term Moving Average Analysis

The 12-month moving average trend (Figure 4.36) shows an earlier and steeper rise in average discharge compared to SSP2-4.5. Starting around 2045, streamflow intensifies through the end-century, reflecting the compounding effects of warming, enhanced evapotranspiration, and greater monsoon rainfall.

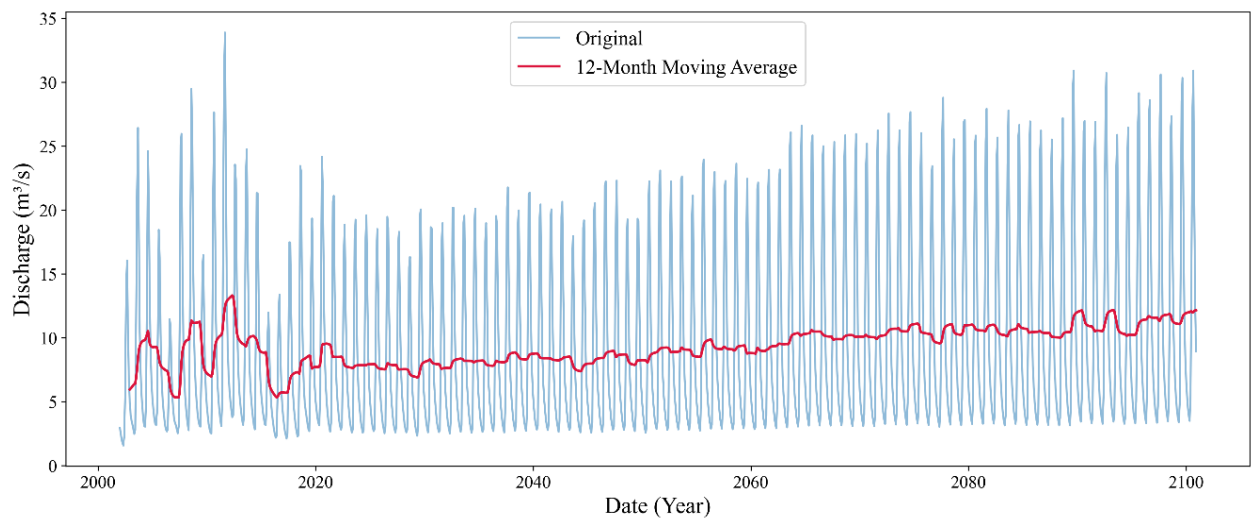


Figure 4.36: Streamflow with 12-Month Moving Average

Temporal Comparison of Streamflow

Figure 4.38 compares average monthly flows for 2040–2050 and 2090–2100. A consistent increase is evident across all months, with August and September flows rising by more than 4–5 m³/s by the end of the century. This increase is more substantial than that observed under SSP2-4.5. Seasonal discharge distribution (Figure 4.37) confirms the growing dominance of monsoon and post-monsoon periods, which together account for over 70% of total annual flow.

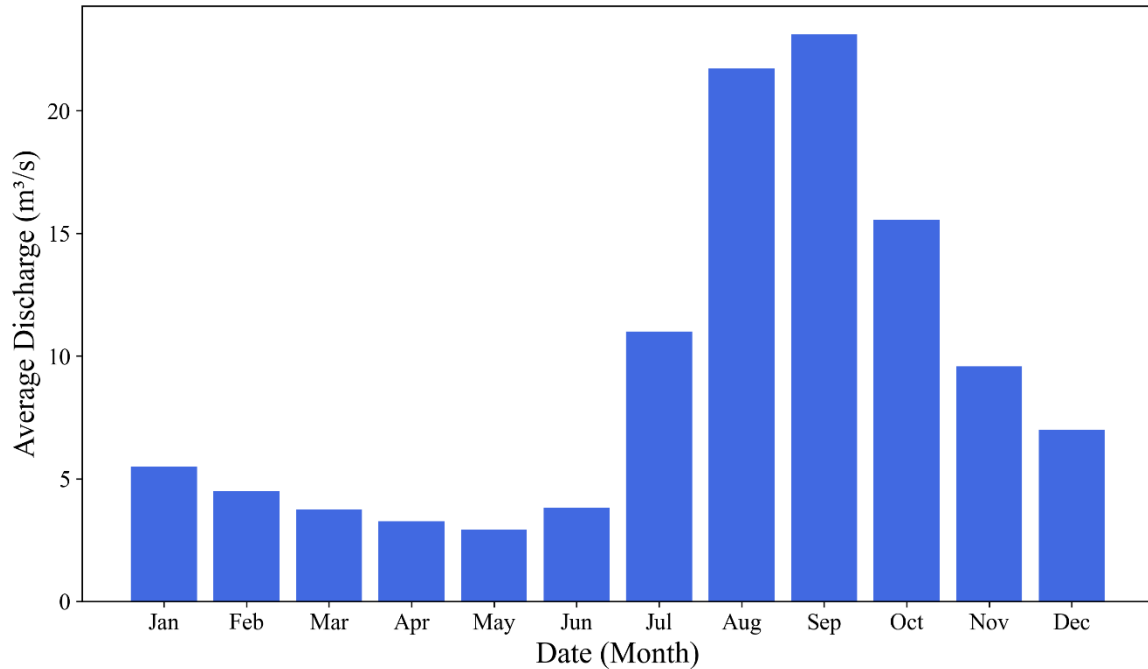


Figure 4.37: Seasonal Variation of Monthly Flow (2002–2100)

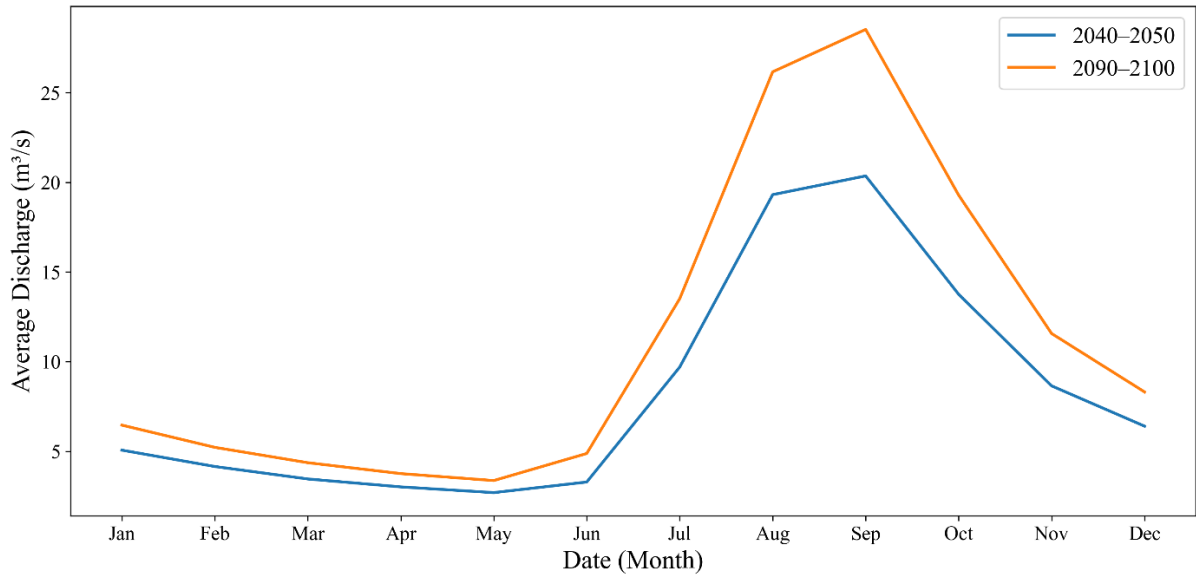


Figure 4.38: Monthly Mean Flow- Mid vs. End Century

Monthly Flow Distribution Summary

The overall monthly distribution under SSP5-8.5 (Figure 4.39) exhibits higher variance, wider interquartile ranges, and more frequent high-flow outliers than SSP2-4.5. This reflects an increasingly volatile flow regime, which may pose challenges for both water infrastructure and ecosystem stability.

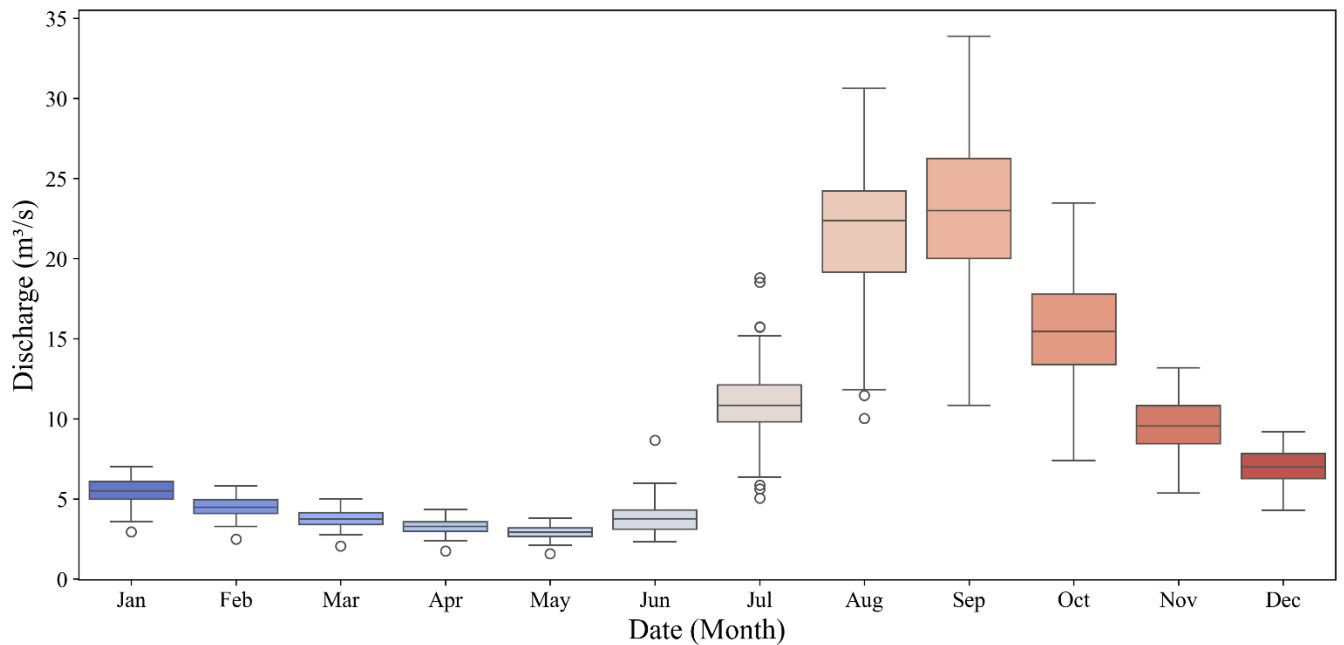


Figure 4.39: Monthly Flow Distribution Boxplot (SSP5-8.5)

Summary Insight

Under the SSP5-8.5 scenario, the Chilime River Basin is projected to experience a significantly intensified hydrological regime by the end of the 21st century. Increases in peak flow, earlier onset of wet season runoff, and more frequent extreme events point toward elevated flood risk and operational challenges for hydropower systems. These trends call for urgent investment in adaptive water resource planning, with a focus on climate resilience, reservoir optimization, and catchment-scale flood control in snow-fed mountain basins.

4.4.3 Comparative Analysis of Trishuli vs. Chilime Flow Trends

To validate the physical consistency of simulated Chilime streamflow, a comparative assessment was conducted between projected streamflow patterns of the Trishuli River (at Betrawati Station) and the Chilime River Basin under both climate scenarios: SSP2-4.5 and SSP5-8.5. Since long-term observed flow data for Chilime is unavailable, the entire Trishuli Basin was modeled and calibrated using observed discharge at Betrawati. The Chilime River was then extracted as a delineated sub-basin within the calibrated SWAT⁺ model, ensuring that its simulated flow reflects localized hydrological processes constrained by basin-wide calibration.

Figures 4.40 and 4.41 present the ensemble-averaged monthly streamflow projections for both rivers from 2002 to 2100. The results demonstrate strong seasonal synchronization, with peak flows occurring during the monsoon season (July–September) and reduced flows during the winter and pre-monsoon periods (January–May). The similarity in timing and seasonal trends across both basins reinforces the hydro-climatic coherence between Chilime and its parent watershed.

As expected, the Chilime River exhibits much lower flow magnitudes due to its smaller contributing area (~277 km²), compared to the broader upstream catchment of the Trishuli River. However, the relative shifts in monsoon peak, dry season baseflow, and inter-annual variability are largely consistent across the two systems. This suggests

that the model accurately captures regional climate signals and that the extracted Chilime streamflow maintains internal hydrological validity.

Under the SSP5-8.5 scenario, both rivers show increased inter-annual variability and amplified peak flows relative to SSP2-4.5, reflecting an intensified hydrological cycle in a high-emission future. The comparative pattern strengthens confidence in using the calibrated and validated Trishuli-based model structure to simulate future streamflow behavior in smaller upstream sub-basins such as Chilime.

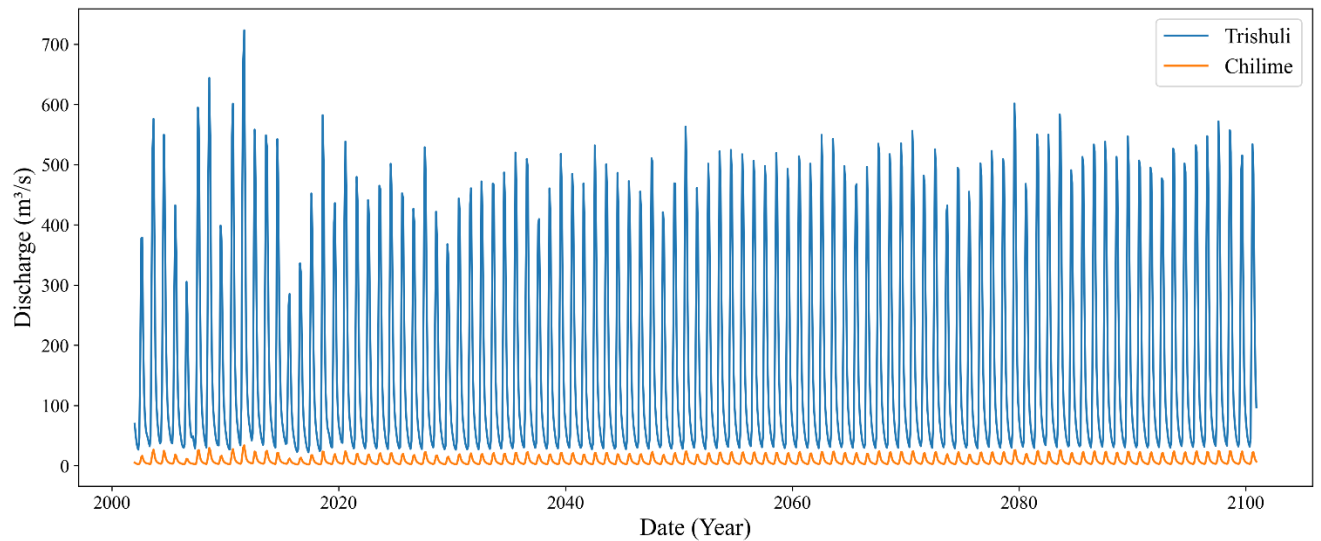


Figure 4.40: Comparative Monthly Streamflow Trends of Trishuli and Chilime under SSP2-4.5 (2002–2100)

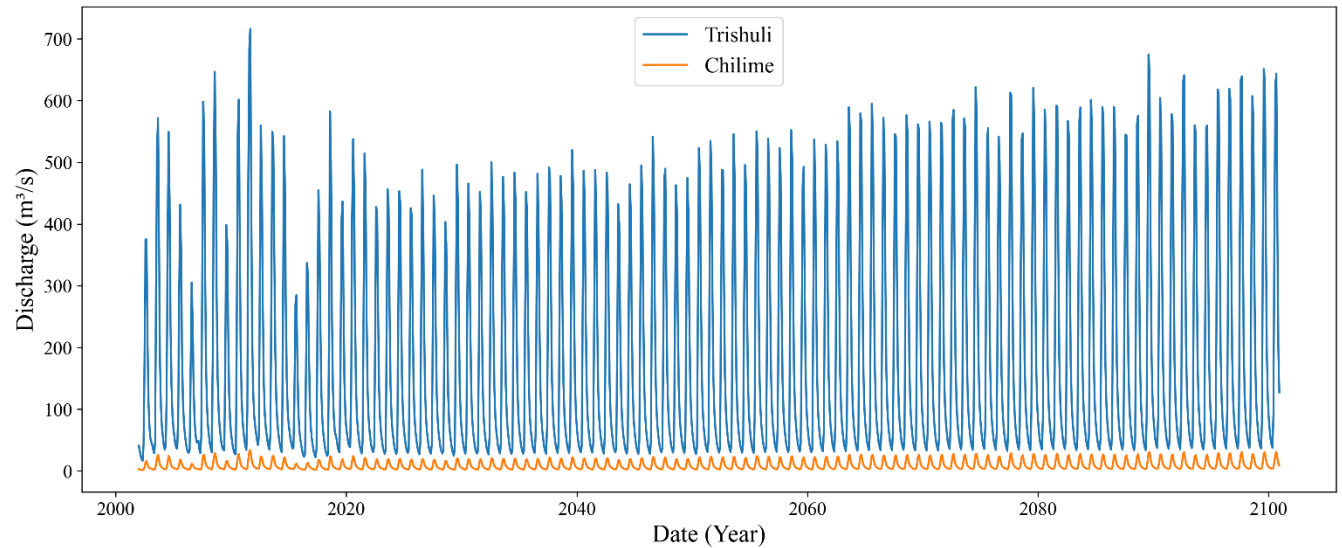


Figure 4.41: Comparative Monthly Streamflow Trends of Trishuli and Chilime under SSP5-8.5 (2002–2100)

This comparative analysis confirms that the physically based SWAT⁺ model, once calibrated with observed data at Betrawati Station, effectively captures both the scale and dynamics of streamflow in the nested Chilime sub-basin. The consistent seasonal structure, response to monsoon intensity, and alignment under future climate scenarios validate the model’s reliability for projecting streamflow changes in unmonitored high-altitude catchments like Chilime.

4.5 Comparative Streamflow Projections Across Himalayan Basins

The streamflow projections for the Chilime River Basin under future climate scenarios indicate a moderate but consistent increase in discharge. Under SSP2-4.5, monsoonal flows are projected to increase by approximately 8–12% by the end of the century, while under SSP5-8.5, peak flows in August and September may rise by 20–25%. These trends reflect intensified runoff resulting from increased precipitation and enhanced snowmelt during the monsoon season, particularly under high-emission scenarios. To validate the consistency of these projections, it is essential to compare the findings with other Himalayan River basins that exhibit similar climatic and hydrological characteristics.

Table 4.9 presents a comparative overview of streamflow changes reported in various studies conducted in Nepal and the greater Himalayan region. While the magnitude of change varies depending on basin size, glacial coverage, and climatic zone, the Chilime Basin's projected changes fall within the expected range, especially for snow-fed sub-catchments.

Table 4.9: Comparative Streamflow Projections under Climate Scenarios

River Basin / Study	Scenario	Streamflow Change (%)	Remarks
Chilime River Basin (This Study)	SSP2-4.5	+8% to +12%	Increase in peak monsoon flow; dry-season stable
	SSP5-8.5	+20% to +25%	Frequent anomalies post-2050; strong monsoon response
Tamor Basin (Dahal et al., 2020)	SSP2-4.5	~+12.7%	Aligned with Chilime trend
	SSP5-8.5	~+20%	Consistent with high-emission scenario
Seti-Gandaki Basin (Upadhyaya et al., 2022)	SSP2-4.5	+49% (monsoon), +96% (pre-monsoon)	Strong rise across all seasons
	SSP5-8.5	+54% to +154%	Highest response in dry and post-monsoon seasons
Kaligandaki Basin (Shrestha et al., 2021)	RCP4.5 / RCP8.5	+41% / +50–88%	Strong glacial and snowmelt contribution
Bheri River Basin (Paudel, 2022)	RCP4.5 & 8.5	+6% to +12.5% (annual), -20% (Jul–Aug)	Dry-season rise, monsoon decrease due to shifting rainfall timing

Indrawati Basin(Bastola, 2022)	RCP4.5 & 8.5	General increase; seasonal variation	Moderate sensitivity basin; similar scale to Chilime
Karnali Basin (Panthi et al., 2023)	RCP4.5 & 8.5	+90% (dry season in upper basin)	Glacial melt-dominated; strong dry-season gain
West Seti Basin (<i>Gurung et al., 2021</i>)	RCPs (F1–F3)	Moderate increase (max in 2045–2069)	Shows clear temporal shift in peak flow
Indus-Tarbela Inflows(Dahri et al., 2021)	RCP2.6–8.5	+34% to +43% under 1.5–2 °C warming	Highly glaciated basin; strong response

Overall, the Chilime River Basin’s projections demonstrate consistency with broader regional trends. While not as extreme as glacier-dominated or larger basins such as Kaligandaki, Karnali, or Seti-Gandaki, the modeled streamflow increases are well within the range observed in snow-fed systems. These findings reinforce the scientific validity of the modeling approach used in this study and highlight the vulnerability of high-altitude catchments to intensified hydrological responses under future climate change scenarios.

CHAPTER V CONCLUSIONS AND RECOMMENDATIONS

5.1 Conclusions

This study assessed the potential impacts of climate change on streamflow patterns in the Chilime River Basin using bias-corrected CMIP6 projections and the SWAT⁺ hydrological model. By integrating historical climate analysis, model calibration, and scenario-based simulations, three core objectives were addressed: (1) projecting future temperature and precipitation trends under SSP2-4.5 and SSP5-8.5; (2) evaluating the performance of the SWAT⁺ model in replicating historical streamflow; and (3) forecasting streamflow responses to climate change in the Chilime River Basin.

First, future climate projections revealed consistent warming and precipitation increases across both scenarios. By the end of the 21st century, annual average temperature is expected to rise by 2–3 °C under SSP2-4.5 and more than 4 °C under SSP5-8.5. Similarly, annual precipitation is projected to increase by approximately 15–20% under SSP2-4.5 and exceed 30% under SSP5-8.5. These changes imply intensified monsoon activity and earlier snowmelt onset, contributing to seasonal shifts in hydrological regimes.

Second, the SWAT⁺ model demonstrated improved performance during both calibration (2007–2016) and validation (2017–2019) periods. The model yielded an NSE of 0.563, R^2 of 0.563, and PBIAS of –4.53% during calibration, while validation achieved an NSE of 0.685, R^2 of 0.685, and PBIAS of +10.69%. These statistics confirm the model's ability to capture flow variability and seasonality in data-scarce, high-altitude Himalayan catchments, thus ensuring reliability for climate change simulations.

Third, streamflow projections suggest marked increases in monsoon discharge and modest gains in winter baseflow. Under SSP2-4.5, peak flows are projected to rise by 8–12%, whereas under SSP5-8.5, increases of 20–25% are anticipated by 2100. Monthly flows during August–September may exceed 30 m³/s, while winter baseflows, although still below 6 m³/s, show a gradual upward trend. This shift

reflects the basin's heightened sensitivity to temperature-induced snowmelt and precipitation intensification, indicating potential risks of late-season floods and dry-season water scarcity.

Overall, the study confirms that high-altitude basins like Chilime are highly responsive to climatic variations. The integration of 13 bias-corrected GCMs, elevation-adjusted inputs, and physically-based hydrological modeling offers a robust framework for simulating future water availability in Himalayan catchments. These insights are crucial for designing adaptive strategies in hydropower planning, water resource management, and climate resilience building in snow-fed river basins.

5.2 Recommendations

5.2.1 Recommendations for Policy and Practice

Based on the key findings of this study, the following recommendations are proposed to support effective water resource planning, hydropower management, and climate adaptation in the Chilime River Basin and similar Himalayan catchments:

- Integrate climate projection-based flow estimates into hydropower design and operational planning, especially to accommodate increased monsoon runoff and potential late-season peak discharges.
- Enhance early warning and flood preparedness systems by incorporating projected shifts in peak flow timing and intensity under future climate scenarios.
- Strengthen catchment monitoring infrastructure by installing flow gauges and meteorological stations within the Chilime Basin to improve model calibration and long-term hydrological forecasting accuracy.
- Incorporate snow and glacier melt components more explicitly in national water resource models, particularly for upstream basins sensitive to seasonal cryospheric dynamics.
- Encourage inter-agency data sharing among DHM, NEA, ICIMOD, and academic institutions to improve hydrological modeling and climate impact assessment across Nepal's mountainous regions.

5.2.2 Recommendations for Further Study

In light of the limitations encountered during this research, the following areas are recommended for future investigation:

- Integrate dynamic glacier models with SWAT⁺ to better simulate long-term meltwater contribution and its decline under sustained warming, especially post-2050.
- Evaluate uncertainty from individual GCMs and bias correction methods by comparing multiple bias correction techniques and model subsets.
- Conduct sensitivity analysis of hydrological parameters to determine their influence under varying climatic inputs, enhancing the robustness of simulations in data-scarce regions.
- Incorporate land use change projections alongside climate scenarios to simulate combined impacts on basin hydrology.
- Assess socio-economic implications of changing streamflow (e.g., for hydropower revenue, irrigation potential, or water-sharing dynamics) under future climate conditions.

REFERENCES

1. Agarwal, A., Babel, M., Maskey, S., Shrestha, S., Kawasaki, A., & Tripathi, N. (2015). Analysis of temperature projections in the Koshi River Basin, Nepal. Royal Meteorological Society.
2. Arnold, J. G., Srinivasan, R., Muttiah, R. S., & Williams, J. R. (1998). Large area hydrologic modeling and assessment: Part I. Model development. *Journal of the American Water Resources Association*, 34(1), 73–89. <https://doi.org/10.1111/j.1752-1688.1998.tb05961.x>
3. Arnold, J. G., Kiniry, J. R., Bieger, K., & Williams, J. R. (2012). SWAT+ Input/Output Documentation. Texas Water Resources Institute.
4. Bajracharya, A., Bajracharya, S., Shrestha, A., & Maharjan, S. (2017). Climate change impact assessment on the hydrological regime of the Kaligandaki Basin, Nepal. *Science of the Total Environment*.
5. Bajracharya, S. R. (2018). Glacio-hydrological modeling in the Himalayas: A case study from the Dudh Koshi basin in eastern Nepal. *Journal of Hydrology: Regional Studies*, 17, 28–40. <https://doi.org/10.1016/j.ejrh.2018.04.001>
6. Barnett, T. P., Adam, J. C., & Lettenmaier, D. P. (2005). Potential impacts of a warming climate on water availability in snow-dominated regions. *Nature*, 438, 303–309. <https://doi.org/10.1038/nature04141>
7. Bates, B. C., Kundzewicz, Z. W., Wu, S., & Palutikof, J. P. (Eds.). (2008). *Climate change and water*. Technical Paper of the Intergovernmental Panel on Climate Change. Geneva: IPCC Secretariat. <https://www.ipcc.ch/site/assets/uploads/2018/03/climate-change-water-en.pdf>
8. Bhatta, B., Shrestha, S., Shrestha, P., & Talchabhadel, R. (2020). Modelling the impact of past and future climate scenarios on streamflow in a highly mountainous watershed: A case study in West Seti River Basin, Nepal. *Science of the Total Environment*, 738, 139775.

9. Bieger, K., Hörmann, G., & Fohrer, N. (2017). Introduction to SWAT+, a completely restructured version of the Soil and Water Assessment Tool. *Journal of the American Water Resources Association*, 53(1), 115–130. <https://doi.org/10.1111/1752-1688.12482>
10. Budhathoki, B. R., Pandey, V. P., & Shrestha, S. (2025). Evaluation of distributed and semi-distributed hydrological models in complex river basin systems, Nepal. *HydroResearch*, 8, 9–21. <https://doi.org/10.1016/j.hydres.2024.09.006>
11. Chanda, A. A., Shrestha, S., & Shukla, R. (2024). Streamflow forecasting in Himalayan catchments using LSTM and CMIP6 scenarios. *Environmental Monitoring and Assessment*, 196, 129. <https://doi.org/10.1007/s10661-024-12215-8>
12. Chanda, A. S., & Shrestha, S. (2024). Quantifying streamflow projections in South Asia using CMIP6 models. *Science of The Total Environment*, 925, 171188. <https://doi.org/10.1016/j.scitotenv.2024.171188>
13. Clark, M. P., Kavetski, D., & Fenicia, F. (2015). Pursuing the method of multiple working hypotheses for hydrological modeling. *Water Resources Research*, 51(4), 3078–3092. <https://doi.org/10.1002/2014WR016731>
14. Dahal, P., Shrestha, M., Panthi, J., & Pradhananga, D. (2020). Modeling the future impacts of climate change on water availability in the Karnali River Basin of the Nepal Himalaya. *Environmental Research*, 185, 109340. <https://doi.org/10.1016/j.envres.2020.109340>
15. Eyring, V., Bony, S., Meehl, G. A., Senior, C. A., Stevens, B., Stouffer, R. J., & Taylor, K. E. (2016). Overview of the Coupled Model Intercomparison Project Phase 6 (CMIP6) experimental design and organization. *Geoscientific Model Development*, 9, 1937–1958. <https://doi.org/10.5194/gmd-9-1937-2016>
16. Huntington, T. G. (2006). Evidence for intensification of the global water cycle: Review and synthesis. *Journal of Hydrology*, 319, 83–95. <https://doi.org/10.1016/j.jhydrol.2005.07.003>

17. Immerzeel, W. W., van Beek, L. P. H., & Bierkens, M. F. P. (2010). Climate change will affect the Asian water towers. *Science*, 328, 1382–1385. <https://doi.org/10.1126/science.1183188>
18. Immerzeel, W. W., Lutz, A. F., Andrade, M., Bahl, A., Biemans, H., Bolch, T., et al. (2020). Importance and vulnerability of the world's water towers. *Nature*, 577(7790), 364–369. <https://doi.org/10.1038/s41586-019-1822-y>
19. IPCC. (2021). Climate change 2021: The physical science basis. Contribution of Working Group I to the Sixth Assessment Report of the Intergovernmental Panel on Climate Change. Geneva: IPCC. <https://www.ipcc.ch/report/ar6/wg1/>
20. Jiang, C. W., Liu, H., & Li, X. (2020). Improving streamflow simulations by integrating remotely sensed snow cover area into SWAT in data-scarce mountainous watersheds. *Frontiers in Earth Science*, 8, 128. <https://doi.org/10.3389/feart.2020.00128>
21. Khajuria, S. B., Aryal, S., & Bhatta, B. R. (2022). Snowmelt runoff estimation using MODIS snow cover and SRM in Himalayan river basins. *Environmental Monitoring and Assessment*, 194, 102. <https://doi.org/10.1007/s10661-022-10219-2>
22. Kraaijenbrink, P. D. A., Bierkens, M. F. P., Lutz, A. F., & Immerzeel, W. W. (2017). Impact of a global temperature rise of 1.5 degrees Celsius on Asia's glaciers. *Nature*, 549(7671), 257–260. <https://doi.org/10.1038/nature23878>
23. Lamichhane, D. A., Subedi, M., & Karki, R. (2024). Assessing streamflow responses in the Karnali and Tamor River Basins under CMIP6 climate projections. *Water*, 16, 1173. <https://doi.org/10.3390/w16031173>
24. Lamichhane, M. P., Shrestha, A., & Pandey, D. (2024). Assessing climate change impacts on streamflow and baseflow in the Karnali River Basin, Nepal: A CMIP6 multi-model ensemble approach using SWAT and web-based hydrograph analysis tool. *Sustainability*, 16(8), 3262. <https://doi.org/10.3390/su16083262>

25. Li, X., Wu, J., & Li, Z. (2021). Snowmelt contribution to streamflow under climate change in high-altitude catchments of the Himalayas. *Remote Sensing*, 13(9), 1585. <https://doi.org/10.3390/rs13091585>
26. Mamoon, M. R., Shrestha, S., & Pandey, V. P. (2024). Coupling CMIP6 with hydrological models: Current progress and future outlook. *Sustainability*, 16(4), 3262. <https://doi.org/10.3390/su16043262>
27. Miller, J. D., Kim, H., Kjeldsen, T. R., Packman, J., Grebby, S., & Dearden, R. (2012). Assessing the impact of urbanization on storm runoff in a peri-urban catchment using historical change in impervious cover. *Journal of Hydrology*, 414–415, 261–272. <https://doi.org/10.1016/j.jhydrol.2011.10.044>
28. Mishra, Y., Bhatia, A., & Tiwari, M. (2020). Climate change adaptation in data-scarce mountainous regions: SWAT-based modeling using CMIP5 scenarios. *Catena*, 195, 104082. <https://doi.org/10.1016/j.catena.2019.104082>
29. Mohseni, S. R., Shrestha, S., & Rajbhandari, R. (2023). Hydrological modeling using SWAT+ under CMIP6 climate projections: A comparative study. *Water*, 15(8), 1753. <https://doi.org/10.3390/w15081753>
30. Mukherji, A., & Chancellor, A. (2019). Water towers of Asia: The changing role of Himalayan hydrology in water security. *Kathmandu: ICIMOD*. <https://lib.icimod.org/record/34304>
31. Nepal, S., Krause, P., & Fink, M. (2014). Modeling hydrological impact of climate change in the Himalayan headwaters: Case study of the Tamor River Basin, Nepal. *Hydrology and Earth System Sciences*, 18, 2293–2314.
32. Nepal, S., Wang, Y., Shrestha, A. B., & Krakauer, N. Y. (2017). Upstream–downstream linkages of hydrological processes in the Himalayan region. *Ecological Processes*, 6, 1–13. <https://doi.org/10.1186/s13717-017-0076-3>
33. O’Neill, B. C., Kriegler, E., Ebi, K. L., Kemp-Benedict, E., Riahi, K., Rothman, D. S., et al. (2016). The roads ahead: Narratives for shared socioeconomic pathways

- describing world futures in the 21st century. *Global Environmental Change*, 42, 169–180. <https://doi.org/10.1016/j.gloenvcha.2015.01.004>
34. Panthi, J., Aryal, S., & Bajracharya, R. (2018). Projected climate change impact on hydrological regime of the Bheri River Basin, Nepal. *Hydrology*, 5(2), 32. <https://doi.org/10.3390/hydrology5020032>
35. Prajapati, R. R., Ibrahim, N., & Thapa, B. (2023). Climate change impact on water availability in the Himalaya: Insights from Sunkoshi River Basin, Nepal. *HydroResearch*, 8, 11–25. <https://doi.org/10.1016/j.hydres.2023.08.002>
36. Prajapati, R. R., Shrestha, S., & Babel, M. S. (2023). Evaluation of streamflow variability in glaciated and non-glaciated catchments under CMIP6 climate scenarios in the Himalayas. *Discover Water*, 3, Article 18. <https://doi.org/10.1007/s44290-024-00143-2>
37. Rasul, G., Chaudhry, S., & Khan, M. A. (2022). Climate change impact on cryosphere and streamflow in the Upper Jhelum River Basin. *Science of The Total Environment*, 806, 151123. <https://doi.org/10.1016/j.scitotenv.2022.151123>
38. Sharma, N. D., Pandey, D., & Bhatta, B. (2024). Modelling snowmelt regime shifts in Himalayan basins under climate change scenarios. *Climate Dynamics*. <https://doi.org/10.1007/s00382-024-07042-z>
39. Sharma, R. H. (2019). Forecasting climate change impacts on water resources in the Himalayan region: A review. *Climate*, 7(1), 1. <https://doi.org/10.3390/cli7010001>
40. Shrestha, A. B., Karki, R., & Rajbhandari, R. (2015). Climate change impacts on water resources in the upper Indus, Ganges, and Brahmaputra river basins. *Environmental Science & Policy*, 14, 49–62. <https://doi.org/10.1016/j.envsci.2015.04.001>
41. Shrestha, M. S., Pandey, V. P., & Babel, M. S. (2015). Climate change impacts on irrigation water demand and crop yield in the Trishuli River Basin, Nepal.

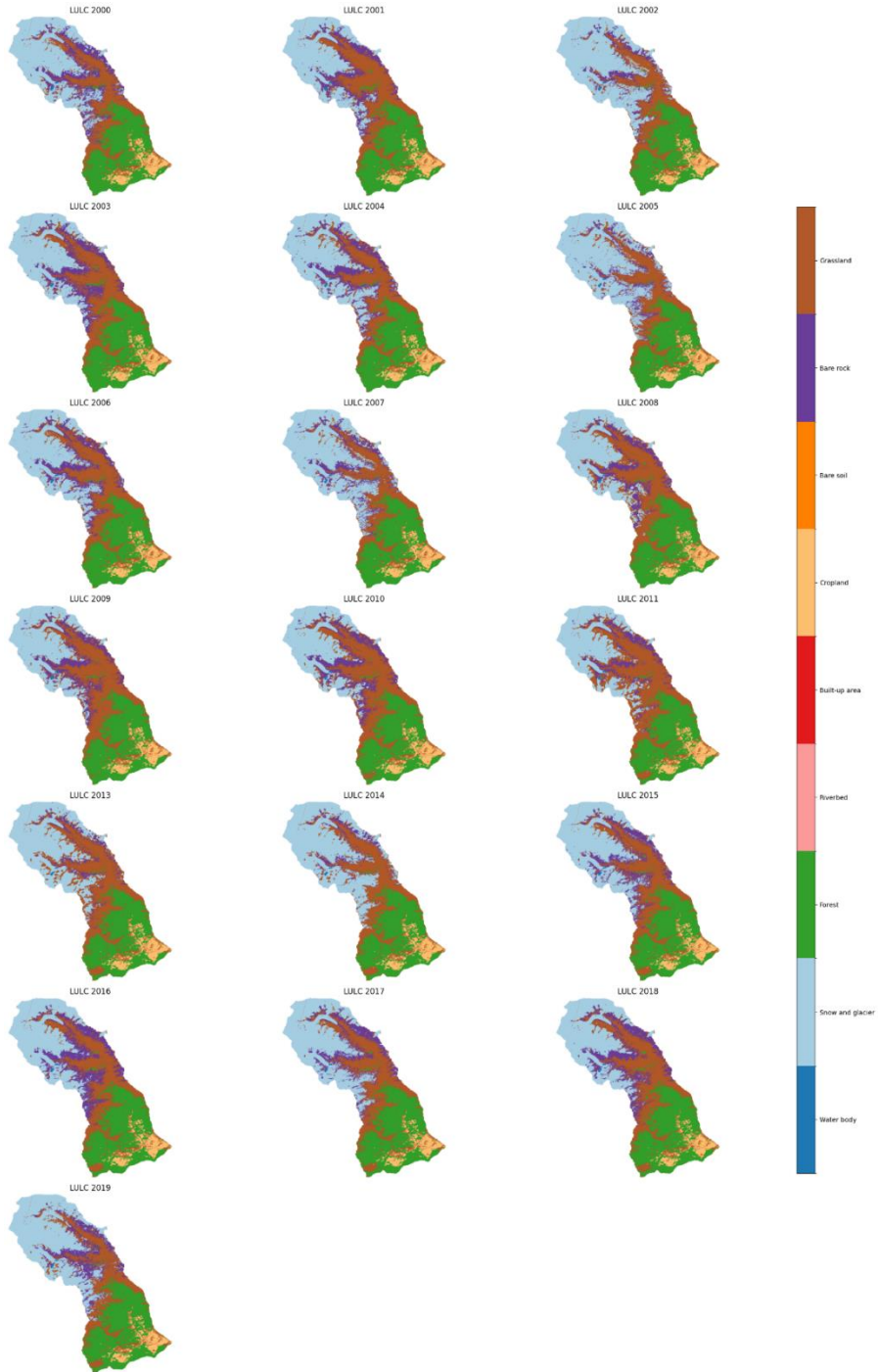
- Environmental Earth Sciences*, 73, 875–889. <https://doi.org/10.1007/s12665-014-3566-6>
42. Shrestha, S., Shrestha, M., & Babel, M. S. (2016). Modelling the potential impacts of climate change on hydrology and water resources in the Indrawati River Basin. *Environmental Earth Sciences*, 75, 110. <https://doi.org/10.1007/s12665-015-4910-7>
43. Shukla, R. A., Shrestha, S., & Babel, M. S. (2021). Multi-model ensemble projections of streamflow using SWAT and CMIP6 datasets. *Hydrology Research*, 52(1), 123–139. <https://doi.org/10.2166/nh.2021.027>
44. Singh, P., & Bengtsson, L. (2005). Impact of warmer climate on meltwater runoff in the snow-covered and glacierized basins in Himalaya. *Journal of Hydrology*, 300(1–4), 140–154. <https://doi.org/10.1016/j.jhydrol.2004.06.005>
45. Subedi, B. R., Bhattarai, B., & Adhikari, S. (2024). Evaluation of future hydrological responses in the Tamor Basin, Nepal, using SWAT and CMIP6 climate projections. *Journal of Water and Climate Change*, 15(2), 148–163. <https://doi.org/10.2166/wcc.2024.150>
46. Subedi, S. R., Lamichhane, D., & Karki, R. (2024). Assessing the impact of climate change on streamflow in the Tamor River Basin, Nepal: An analysis using SWAT and CMIP6 scenarios. *Discover Civil Engineering*, 3, Article 14. <https://doi.org/10.1007/s44290-024-00143-2>
47. Teutschbein, C., & Seibert, J. (2012). Bias correction of regional climate model simulations for hydrological climate-change impact studies: Review and evaluation of different methods. *Journal of Hydrology*, 456–457, 12–29. <https://doi.org/10.1016/j.jhydrol.2012.02.026>
48. Thrasher, B., Maurer, E. P., McKellar, C., & Duffy, P. B. (2012). Technical note: Bias correcting climate model simulated daily temperature extremes with quantile mapping. *Environmental Modelling & Software*, 36, 101–105. <https://doi.org/10.1016/j.envsoft.2011.09.009>

49. Viviroli, D., Dürr, H. H., Messerli, B., Meybeck, M., & Weingartner, R. (2011). Mountains of the world, water towers for humanity: Typology, mapping, and global significance. *Hydrology and Earth System Sciences*, 15(3), 821–832. <https://doi.org/10.5194/hess-15-821-2011>
50. Zheng, H., Wu, B., Zhang, L., & Zhang, M. (2018). Evaluation of CMIP6 precipitation simulations in East and South Asia. *Journal of Climate*, 31(16), 6335–6350. <https://doi.org/10.1175/JCLI-D-17-0782.1>
51. Dahri, Z. H., Ahmad, S., Siddiqui, S., & Yaseen, M. (2021). Glaciers of the Himalayas: Climate Change, Black Carbon and Regional Resilience. *United Nations Environment Programme*. <https://wedocs.unep.org/handle/20.500.11822/34952>
52. Li, Z., Wang, Z., & Jiang, C. (2018). Assessing the effects of snowmelt and climate change on streamflow in mountainous regions. *Remote Sensing*, 13(15), 1585. <https://doi.org/10.3390/rs13151585>
53. Sharma, N. D., & Aryal, S. (2024). Modelling snowmelt regime shifts in Himalayan basins under climate change scenarios. *Climate Dynamics*. <https://doi.org/10.1007/s00382-024-07042-z>
54. Huss, M., Zemp, M., Joerg, P. C., & Salzmann, N. (2013). High uncertainty in 21st century runoff projections from glacierized basins. *The Cryosphere Discussions*, 7, 2023–2065. <https://doi.org/10.5194/tcd-7-2023-2013>
55. Paudel, S., Gautam, D., & Aryal, K. P. (2022). Climate change impact on streamflow in the Bheri River Basin, Nepal. *Hydro Nepal*, 30, 10–20.
56. Gurung, S., & Thapa, B. (2021). Hydrological assessment under climate change in West Seti River Basin using SWAT and CMIP6 models. *Unpublished Technical Report*.
57. Bastola, P., & Shrestha, A. (2022). Hydrological impacts of climate change on the Indrawati River Basin. *Technical Report submitted to ICIMOD*.

58. Panthi, J., Aryal, S., & Bajracharya, R. (2023). Streamflow modelling in the Karnali River Basin using multi-model ensemble projections. *Hydrology Research*, 54(4), 842–860. <https://doi.org/10.2166/nh.2023.008>
59. Dahal, N., Pandey, V. P., & Shrestha, S. (2020). Streamflow projection in the Tamor Basin under climate change scenarios. *Journal of Environmental Management*, 276, 111322. <https://doi.org/10.1016/j.jenvman.2020.111322>
60. Osei, F. B., & Amankwah, A. S. (2020). Evaluating the impact of climate change on streamflow in Benin using SWAT and CMIP6 datasets. *Sustainability*, 12(6), 2458. <https://doi.org/10.3390/su12062458>

APPENDICES

Appendix I: Land Use Land Cover



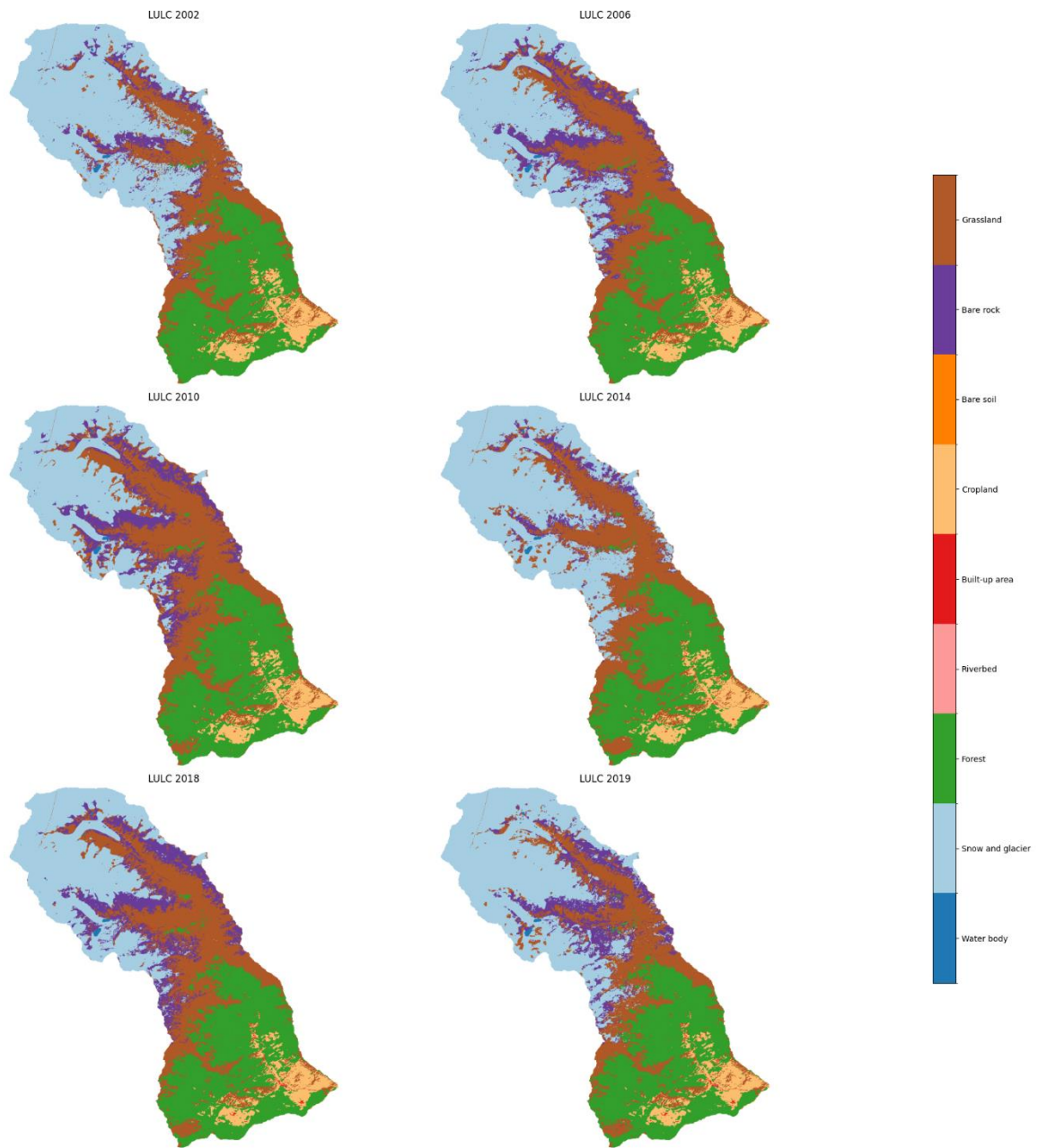


Fig A2- LULC of different year of Chilime basin

Table A1: Area of Different LULC in km2

Year	Waterbody	Glacier & Snow	Forest	Riverbed	Built-up area	Cropland	Bare soil	Bare rock	Grassland
2000	0.4599	104.0193	45.9666	0	0.0648	4.1265	0.1494	37.4445	65.1645
2001	0.4797	93.3012	47.5038	0	0.0675	4.0599	0.0846	31.536	80.3628
2002	0.4554	121.9716	46.1484	0	0.0387	4.0617	0.0378	20.763	63.9189
2003	0.4581	90.1161	46.8702	0	0.1116	4.0131	0.0324	37.3032	78.4908
2004	0.459	101.0043	46.1466	0	0.0351	4.0149	0.0252	35.6202	70.0902
2005	0.4536	121.2849	45.6399	0	0.0405	4.0842	0.018	21.3444	64.53
2006	0.4599	98.1612	45.8415	0	0.0468	4.1121	0.0306	34.02	74.7234
2007	0.4653	117.5787	45.4248	0	0.0423	4.1796	0.0324	27.6597	62.0127
2008	0.4779	91.5309	46.476	0	0.0954	4.1175	0.0513	27.9495	86.697
2009	0.4833	87.1254	47.0034	0	0.1305	4.0347	0.0801	32.931	85.6071
2010	0.4698	83.907	47.1906	0	0.1197	4.0131	0.1224	35.1585	86.4144
2011	0.4941	84.924	46.7901	0	0.0711	4.0194	0.189	25.0065	95.9013
2013	0.4734	103.5018	46.4949	0	0.0666	4.032	0.2718	16.4556	86.0994
2014	0.4527	119.5749	47.0961	0	0.063	3.9402	0.2943	14.9463	71.028
2015	0.4842	100.5669	48.0888	0	0.1458	3.7467	0.3213	33.3162	70.7256
2016	0.4923	88.7535	48.8448	0	0.2349	3.5937	0.3141	45.8703	69.2919
2017	0.4761	101.1996	49.1274	0	0.1692	3.5064	0.2862	32.2164	70.4142
2018	0.4986	88.8381	49.9419	0	0.279	3.4191	0.2295	39.1221	75.0672
2019	0.4797	113.4972	48.969	0	0.1809	3.3768	0.3465	31.8357	58.7097
2020	0.4887	113.3919	48.2598	0	0.0855	4.7277	0.3933	19.6434	70.4052
2021	0.4995	92.7216	47.8053	0	0.36	4.1769	0.6102	40.5333	70.6887

Appendix II: Calibrated SWAT⁺ Parameter

Table A2: Calibrated SWAT⁺ Parameters with Optimized Ranges and Best-Fit Value

Name	Change Type	Group	Abs.min	Abs.max	used Value	Full Name	Meaning	Impact in SWAT
cn2	Relative	hru	35	95	59	SCS Curve Number for Moist Condition	Surface runoff potential based on land use, soil, moisture	Affects surface runoff volume
esco	Replace	hru	0	1	0.297	Soil Evaporation Compensation Factor	Controls soil evaporation depth	Affects soil evaporation
surlag	Replace	bsn	0.05	24	0.05	Surface Runoff Lag Coefficient	Time delay in surface runoff response	Affects timing of surface runoff
alpha	Replace	aqu	0	1	0.3	Baseflow Alpha Factor	Groundwater contribution to streamflow	Affects baseflow and streamflow in dry periods

Appendix III: CMIP6 GCMs

Table A3: CMIP6 GCMs Used in the Ensemble and Their Key Characteristics

S.N.	Model Name	Resolution (Atmosphere Grid)	Modelling Institute	Country
1	ACCESS-CM2	1.25° × 1.875°	CSIRO-ARCCSS	Australia
2	ACCESS-ESM1-5	1.25° × 1.875°	CSIRO-ARCCSS	Australia
3	BCC-CSM2-MR	1.125° × 1.125°	Beijing Climate Center (BCC)	China
4	CanESM5	2.81° × 2.81°	Canadian Centre for Climate Modelling (CCCma)	Canada
5	EC-Earth3	0.7° × 0.7°	EC-Earth Consortium	Europe (multi-national)
6	EC-Earth3-Veg	0.7° × 0.7°	EC-Earth Consortium	Europe (multi-national)
7	INM-CM4-8	2.0° × 1.5°	Institute of Numerical Mathematics	Russia
8	INM-CM5-0	1.0° × 1.5°	Institute of Numerical Mathematics	Russia
9	MPI-ESM1-2-HR	0.5° × 0.5°	Max Planck Institute for Meteorology	Germany
10	MPI-ESM1-2-LR	1.875° × 1.875°	Max Planck Institute for Meteorology	Germany
11	MRI-ESM2-0	1.125° × 1.125°	Meteorological Research Institute	Japan
12	NorESM2-LM	1.9° × 2.5°	Norwegian Climate Centre	Norway
13	NorESM2-MM	1.0° × 1.25°	Norwegian Climate Centre	Norway



Madan Mohan Malaviya University of Technology, Gorakhpur (U.P.) India

मदन मोहन मालवीय प्रौद्योगिकी विश्वविद्यालय, गोरखपुर (उ.प्र.) भारत

Established by U.P. Act No. 22 of 2013 of U.P. Government
(Formerly Madan Mohan Malaviya Engineering College)



International Conference on
Innovations in Infrastructural Materials & Sustainability
18th April - 19th April 2025
(IIMS 2025)

Acceptance Letter

Date of Issue: 7th April 2025

Conference Name: International Conference on Innovations in Infrastructural Materials & Sustainability (IIMS-25)

Date of Conference: 18th April - 19th April 2025

Place of Conference: Madan Mohan Malaviya University of Technology, Gorakhpur (UP), India

Paper Id: IIMS2025130

List of Author(s): Kabita Bhattarai, Babu Ram Tiwari, and Bhola N. S. Ghimire

Dear Kabita Bhattarai

We are pleased to inform you that your paper has been accepted for the oral presentation in the conference **IIMS 2025**. You are requested to complete your online registration process and fee payment through the given link as per the schedule of important dates mentioned on the conference website.

Your proposal titled **Impact of Climate Change on Streamflow Considering Limited Snow Melt: A Case Study for Chilime River Basin**

On behalf of *Madan Mohan Malaviya University of Technology (MMMUT)*,
We would like to congratulate you.

For Registration: <https://forms.gle/XPXX7iziuLqfzMc66>

Looking forward to meet you at the conference on **18th - 19th April 2025**

With Kind Regards.....

Organizing Team, IIMS-2025
CED, MMMUT Gorakhpur-273010,
Uttar Pradesh, India
Mail id: iims2025@mmmud.ac.in
Visit us: <https://mmmud.ac.in/iims-2025>

iims2025@mmmud.ac.in



CERTIFICATE OF PARTICIPATION

This is to certify that

Kabita Bhattarai, Paper ID: IIMS2025130

Delivered Oral Presentation

on

'Impact of Climate Change on Streamflow Considering Limited Snow Melt: A Case Study of Chitina River Basin'


in the

International Conference on
Innovation in Infrastructural Materials & Sustainability, (IIMS-2025)

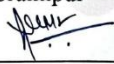
Organised By

Department of Civil Engineering

Madan Mohan Malaviya University of Technology, Gorakhpur


Dr. Sneha Gupta
Co-ordinator, IIMS-2025


Dr. Vinay Kumar Singh
Co-ordinator, IIMS-2025


Prof. A.K. Mishra
Chairman, IIMS-2025

In Association with



Final Thesis Report Kabita Bhattarai.docx

 Tribhuvan University

Document Details

Submission ID

trn:oid::3117:455463325

Submission Date

May 4, 2025, 2:14 PM GMT+5:45

Download Date

May 4, 2025, 2:33 PM GMT+5:45

File Name

Final Thesis Report Kabita Bhattarai.docx

File Size

8.4 MB

92 Pages

14,625 Words

91,649 Characters





12% Overall Similarity

The combined total of all matches, including overlapping sources, for each database.




Filtered from the Report

- ▶ Bibliography
- ▶ Quoted Text
- ▶ Small Matches (less than 10 words)

Match Groups

-  **116** Not Cited or Quoted 12%
Matches with neither in-text citation nor quotation marks
-  **0** Missing Quotations 0%
Matches that are still very similar to source material
-  **0** Missing Citation 0%
Matches that have quotation marks, but no in-text citation
-  **0** Cited and Quoted 0%
Matches with in-text citation present, but no quotation marks

Top Sources

- 11%  Internet sources
- 9%  Publications
- 0%  Submitted works (Student Papers)

Integrity Flags

0 Integrity Flags for Review

No suspicious text manipulations found.

Our system's algorithms look deeply at a document for any inconsistencies that would set it apart from a normal submission. If we notice something strange, we flag it for you to review.

A Flag is not necessarily an indicator of a problem. However, we'd recommend you focus your attention there for further review.

Match Groups

- **116** Not Cited or Quoted 12%
Matches with neither in-text citation nor quotation marks
- **0** Missing Quotations 0%
Matches that are still very similar to source material
- **0** Missing Citation 0%
Matches that have quotation marks, but no in-text citation
- **0** Cited and Quoted 0%
Matches with in-text citation present, but no quotation marks

Top Sources

- 11% Internet sources
- 9% Publications
- 0% Submitted works (Student Papers)

Top Sources

The sources with the highest number of matches within the submission. Overlapping sources will not be displayed.

1	Internet	elibrary.tucl.edu.np	2%
2	Internet	www.mdpi.com	1%
3	Publication	Buri Vinodhkumar, K. Koteswara Rao, Hamsaa Sayeekrishnan, Krishna Kishore Os...	<1%
4	Internet	www.researchgate.net	<1%
5	Internet	mdpi-res.com	<1%
6	Publication	Manan Sharma, Rajendra Prasad Singh, Samjhana Rawat Sharma. "Multi-Model A...	<1%
7	Internet	lib.iium.edu.my	<1%
8	Internet	link.springer.com	<1%
9	Internet	vsip.info	<1%
10	Internet	environmentalsystemsresearch.springeropen.com	<1%

11	Publication	Subharthi Sarkar, Rajib Maity. "Unveiling climate change-induced temperature-b...	<1%
12	Publication	Pragya Badika, Akash Singh Raghuvanshi, Ankit Agarwal. "Climate Change Impac...	<1%
13	Internet	hess.copernicus.org	<1%
14	Publication	Bloxam, Kevin. "Temperature Trends in the Arctic Winter Stratosphere and the Ro...	<1%
15	Internet	assets-eu.researchsquare.com	<1%
16	Publication	Ahmad Jafarzadeh, Abbas Khashei-Siuki, Mohsen Pourreza-Bilondi, Kwok-wing Ch...	<1%
17	Internet	papersowl.com	<1%
18	Internet	researchonline.ljmu.ac.uk	<1%
19	Internet	vuir.vu.edu.au	<1%
20	Internet	core.ac.uk	<1%
21	Publication	Mancuso, Marina. "Climate and Infection-Age on West Nile Virus Transmission", A...	<1%
22	Internet	baffinland.com	<1%
23	Internet	doaj.org	<1%
24	Internet	ugspace.ug.edu.gh	<1%

25	Internet	real.mtak.hu	<1%
26	Publication	Dipak Mudbhari, Mitthan Lal Kansal, Praveen Kalura. "Impact of climate change o...	<1%
27	Publication	Piyush Dahal, Madan Lall Shrestha, Jeeban Panthi, Dhiraj Pradhananga. "Modelin...	<1%
28	Publication	Zengliang Luo, Sihan Zhang, Quanxi Shao, Lunche Wang, Shaoqiang Wang, Lizhe ...	<1%
29	Publication	Saurav Bhattarai, Laxman Bokati, Sanjib Sharma, Rocky Talchabhadel. "Understa...	<1%
30	Publication	Xin Xiang, Tianqi Ao, Qintai Xiao, Xiaodong Li, Li Zhou, Yao Chen, Yao Bi, Jingyu G...	<1%
31	Internet	dspace.nm-aist.ac.tz	<1%
32	Internet	www.teses.usp.br	<1%
33	Publication	"Earth Observation Science and Applications for Risk Reduction and Enhanced Re...	<1%
34	Publication	Mansour Almazroui, Sajjad Saeed, Fahad Saeed, M. Nazrul Islam, Muhammad Ism...	<1%
35	Publication	Mohsin Tariq, A.N. Rohith, R. Cibin, Eleonora Aruffo, Gamal AbdElNasser Allam Ab...	<1%
36	Internet	discovery.dundee.ac.uk	<1%
37	Internet	docplayer.net	<1%
38	Internet	e-journal.uajy.ac.id	<1%

39	Internet	easychair.org	<1%
40	Internet	edukemy.com	<1%
41	Internet	hal-insu.archives-ouvertes.fr	<1%
42	Internet	ia803007.us.archive.org	<1%
43	Internet	ondemand.euromoney.com	<1%
44	Internet	repository.uph.edu	<1%
45	Internet	www.card.iastate.edu	<1%
46	Internet	www.intechopen.com	<1%
47	Publication	"Navigating the Nexus", Springer Science and Business Media LLC, 2025	<1%
48	Publication	Bikash Ranjan Parida, Arvind Chandra Pandey, Mukunda Dev Behera, Navneet Ku...	<1%
49	Publication	Bin Tang, Wenting Hu, Anmin Duan, Kailun Gao, Yuzuo Peng. "Reduced Risks of T...	<1%
50	Publication	Diogo S A Araujo, Francesco Marra, Cory Merow, Efthymios I Nikolopoulos. "Toda...	<1%
51	Publication	Dipak Mudbhari, Mitthan Lal Kansal, Praveen Kalura. "Impact of climate change o...	<1%
52	Publication	Heli A. Arregocés, Liceth Carolina Costa-Redondo, Roberto Rojano. "Exploring fut...	<1%

53	Publication	Kuldeep Pareta, Yogita Dashora. "Climate change projections and hydrological m...	<1%
54	Publication	Phenikaa University	<1%
55	Publication	Vikram S. Chandel, Subimal Ghosh. "Components of Himalayan River Flows in a C...	<1%
56	Internet	epscor.w3.uvm.edu	<1%
57	Internet	gcisc.org.pk	<1%
58	Internet	nhess.copernicus.org	<1%
59	Internet	ousar.lib.okayama-u.ac.jp	<1%
60	Internet	scirp.org	<1%
61	Publication	von Kaenel, Manon Line. "Mountain Snowpacks in the Western U.S.: Improved Est...	<1%
62	Internet	www.iapjournals.ac.cn	<1%
63	Publication	Nalaka Geekiyana, M.H.J.P. Gunarathna, Manjula Ranagalage, Guttula Yuganth...	<1%
64	Publication	Nimmakanti Mahendra, Jasti Sriranga Chowdary, Patekar Darshana, Pilli Sunitha,...	<1%
65	Publication	Saswata Nandi, Sabyasachi Swain. "Analysis of heatwave characteristics under cli...	<1%
66	Internet	edoc.ub.uni-muenchen.de	<1%

67	Internet	iwaponline.com	<1%
68	Internet	mobt3ath.com	<1%
69	Internet	pure-oai.bham.ac.uk	<1%
70	Internet	swat.tamu.edu	<1%